ELECTRICITY GENERATION FROM WASTEWATER USING MICROBIAL FUEL CELLS: A STUDY OF ELECTRODE AND MEMBRANE MATERIALS

Newcastle University

A Thesis submitted for the Degree of Doctor of Philosophy at Newcastle University

by

Beate Christgen

July 2010

School of Chemical Engineering and Advanced Materials

Abstract

The environmental, social and economic challenges facing society make sustainability and resource efficiency a necessity. To overcome these challenges in wastewater treatment, energy conservation and recovery are two central requirements. Microbial fuel cells (MFCs) as an energy producer could provide a sustainable solution to fulfil both objectives.

A challenge for reliable and efficient use of microbial fuel cells is achieving low material costs due to the low power output especially when using wastewater as substrate. Low cost materials for the anode, cathode and membrane in MFCs were studied to increase the knowledge of reactions and interactions between microbiology and materials in a MFC and to try to increase the power performance and coulombic efficiencies when using complex wastewaters as substrate.

Activated carbon cloth, as one of the anode materials tested, showed the greatest potential for high power performances from wastewater. It reached power densities of 67 mW m^{-2} during polarisation in a membrane-less reactor and 29±3.4 mW m^{-2} under 1000 Ω external load using a radiation grafted ion exchange membrane based on ethylene tetrafluoroethylene (ETFE). Coulombic efficiencies (CE) observed reached 92±6% CE for reactors using ETFE radiation grafted membranes and 68±11% CE for membranes-less reactors with an interior biocathode opposite to the anode in the anode chamber. Both reactors used activated carbon cloth as anode material and carbon black as cathode catalyst.

The low conductivity of the wastewater (1-2 mS cm^{-1}) limited the power density achieved as it created high ohmic losses because of a high internal resistance in the reactors using 4 cm electrode spacing. Reducing the electrode distance to 2 mm decreased the internal resistance by a factor of ten. A simultaneous reduction in anode potential of 100 mV lead to lower power densities presumably due to oxygen diffusing into the anode chamber.

With the exception of carbon cloth, the anode materials investigated showed low overpotential losses and charge transfer resistivities. The cathode was the more limiting influence in the system when a low costs separator (Rhinohide) was used as membrane. However when an ion exchange membrane (Nafion or a radiation grafted membrane based on ETFE) or membrane-less (carbon paper with an internal cathode) was used lower overpotential losses were observed on the carbon black cathode than the anode. The different membranes and separators tested showed a greater influence on the system than previously anticipated.

Although durability studies of the activated carbon cloth as anode material and the different cathode materials over three and two month respectively showed a concerning decline in power performance, the coulombic efficiencies increased over time. So the high coulombic efficiencies achieved and a capability for high power densities using inexpensive materials give hope for the use of microbial fuel cell systems for economical energy generation from wastewater.

DECLARATION

I hereby certify that this work is my own, except where otherwise acknowledged, and that it has not been submitted previously for fulfilment of a degree at this, or any other University.

Beate Christgen

ACKNOWLEDGEMENTS

CONTENT

LIST OF FIGURES

LIST OF TABLES

GLOSSARY OF TERMS, ABBREVIATIONS AND ACRONYMS

ANOVA	Analysis of Variance
AEM	Anion exchange membrane
C/HNO$_3$	Nitric acid activated carbon black
C/PANI	Carbon black modified with polyaniline
CAC	Activated carbon cloth
CB	Carbon black
CC	Carbon cloth
CE	Coulombic efficiency
CEM	Cation exchange membrane
CNT	Carbon nanotubes
COD	Chemical oxygen demand
CP	Carbon paper
D.O.G.	Degree of grafting
DAPI	4',6 diamindino-2-phenylindole
DGGE	Denaturing gradient gel electrophoresis
DNA	Deoxyribonucleic acid
DO	Dissolved oxygen
ESA	Electrochemical surface area
ETFE	Ethylene tetrafluoroethylene
FePc	Iron(II)phthalocyanine
FePc+Mn	Iron(II)phthalocyanine mixed with manganese oxide
FP	Flat plate
HDPE	High-density polyethylene
HRT	Hydraulic retention time
iR	Internal resistance
LSV	Linear sweep voltammetry
MDS	Multidimensional scaling
NHE	Normal hydrogen electrode
OCP	Open circuit potential

ORR	Oxygen reduction reaction
PBS	Phosphate buffer solution
PCR	Polymerase chain reaction
PE	Polyethylene
PFSA	Perfluoro sulfonic acid polymer
PP	Polypropylene
Pt/C	Platinum on carbon
PTFE	Polytetrafluoroethylene
PVA	Polyvinyl alcohol
PVDF	Polyvinylidene fluoride
RH	Rhinohide®
SS	Suspended solids
TAC	Total anode compartment
UHMWPE	Ultra-high-molecular-weight polyethylene
VSS	Volatile suspended solids

ACRONYMS

Dm^{-3}	l^{-1}
1 atm	101325 Pa

1 INTRODUCTION

1.1 BACKGROUND TO THE STUDY

To overcome the challenges of climate change, ever increasing world energy consumption and a growing scarcity of fossil fuels, the sustainable use of our resources is essential.

Sustainability as a concept is based on the observation that economy, environment and society are not separate, but parts in one system interacting and influencing each other and are influenced by changes in other systems (Balkema *et al.*, 2002). Sustainability challenges us to look at 'the whole picture' instead of just finding solutions to, usually man-made problems. "…we can no longer afford to consider the environment as a collection of discrete sub-systems in any one of which we can make adjustments without affecting other sub-systems." (Isaac, 1978, p499) In view of the challenges facing us understanding the whole system (how nature deals with waste and gains from it) and mechanisms underlying it is even more important.

Traditional wastewater treatment is an intensive and expensive process with high energy usage and in many cases not the most sustainable option for economic reasons alone. Even though moving towards sustainability, the UK water industry utilized 8,650 GWh energy in water supply and wastewater treatment in 2008/2009 (Sustainability Indicators for the UK Water Industry) while only producing 8.6 % (742 GWh) of the energy used. As energy prices and the landfill tax in the UK rise year on year, wastewater treatment is becoming more expensive and even less sustainable. Traditional wastewater treatment faces a number of problems (Metcalf & Eddy. et al., 2003; Rittmann and McCarty, 2001; Kiely, 1997; Peavy et al., 1985):

- Energy costs are high as aeration and recirculation (pumps are the single greatest energy consumer in wastewater treatment plants) require extensive amounts of electricity;
- Different treatment units necessitate large surface areas thus increasing the footprint and costs;

- Not only does wastewater have to be treated to acceptable standards but also large amounts of sludge, which are formed during the treatment stages, especially during aerobic biological treatment. This increases overall expenditure as sludge treatment is difficult, time-intensive and costly;

- Nutrient removal units have difficulties in achieving adequate and reliable removal efficiencies on influents containing distorted COD/N/P ratios;

- As wastewater characteristics change over time new process strategies have to be found for new contaminants (such as pharmaceutical hormones).

Technologies addressing these challenges and leading wastewater treatment towards sustainability should include the reduction of cost, energy use, land area and waste production (sludge) while increasing the production of clean water, biogas, biomass, fertilisers and compost (Balkema A. J., 2002). Because of the large energy consumption of traditional wastewater treatment methods (Stenstrom and Rosso, 2007; Metcalf & Eddy. et al., 2003; Rittmann and McCarty, 2001; Kiely, 1997) two central requirements are:

- Energy conservation;

- Energy recovery or recovery of valuable products.

Thus recognising wastewater as a resource and wastewater treatment plants as potential (ideally net) producers of energy and/or other valuable products is a way to achieve sustainability and resource efficiency in wastewater treatment.

Fuel cells are electrochemical devices that continuously convert chemical energy to electrical energy as long as fuel and oxidants are supplied (Oniciu, 1976). In a microbial fuel cell a range of biodegradable substrates (ie in wastewater) is directly converted into electricity. Thus MFCs are one technology with potential for furthering self-sustainability and resource efficiency in wastewater treatment (Rabaey and Verstraete, 2005; Angenent et al., 2004; Bennetto et al., 1983).

A microbial fuel cell (MFC) is a biological system, in which microorganisms act as biocatalysts for the anaerobic oxidation of organic compounds in for example wastewater and transfer the produced electrons to the anode thereby generating electricity (Logan et al., 2006).

Bacteria play a dual role in MFCs, to degrade the organic compounds in wastewater and simultaneously generate electricity. Using microorganisms in biological fuel cells permits a wide range of substrates as a fuel source including the complex and changeable mixture of organic substrates found in wastewater. This offers opportunities to economically treat wastewater with the added benefit of recovering a proportion of the energy required for wastewater treatment as electricity.

Anaerobic digestion (AD) is a mature and commercially viable energy producing treatment process for methane production from, mostly, high strength wastewaters, sludges and the organic fraction of solid wastes. However microbial fuel cells potentially have a much wider scope and possibility of efficient energy generation than AD in the future. But poor understanding of the microbial community and the interactions between materials and microorganisms make in depth investigations of microbial fuel cells essential to try to achieve efficient energy production from waste resources. A better understanding of the microbial consortia in the biofilm and their interactions with each other and reactor materials could possibly lead to a wide range of different sustainable ways to exploit waste resources efficiently.

1.2   RESEARCH PROBLEM AND AIMS OF THE STUDY

Efficient exploitation of wastes for energy generation depends on understanding the underlying biological processes. The complex and changing composition of wastes and the multitude of microorganisms involved present major challenges for the understanding of underlying processes. In microbial fuel cells simplified experiments using a known composition or pure cultures are often used to understand underlying processes. However the complexity of wastes and microbial consortia often means that knowledge learned from single substrates and micro-organisms does not give a realistic insights into actual behaviour.

Expensive cathode catalysts such as platinum and membranes, such as Nafion, that are often used in MFC studies mean the capital costs of microbial fuel cell technology would be at least one order of magnitude higher compared to conventional wastewater treatment systems

(Rozendal et al., 2008). Since microbial fuel cells show low power output, reducing their costs is essential. Thus to be economically viable for the treatment of wastes, microbial fuel cells have to be cost effective.

The aims of this research were to:

- reduce the capital cost of microbial fuel cells by investigating the influence of potentially cost effective materials for the anode, cathode and membrane on power performance and wastewater treatment efficiency of microbial fuel cell for wastewater treatment;
- gain understanding of interactions between electrochemistry and microbiology in wastewater fed microbial fuel cells.

1.3   OUTLINE OF THE THESIS

Chapter 1 Introduces the subject and research aim of the thesis.

Chapter 2 Review of microbial fuel cell technology.

Chapter 3 Materials and Methods used are discussed.

Chapter 4 Studies of anode materials and supports.

Chapter 5 Study of the durability of cathode materials.

Chapter 6 Different membranes are characterised and studied in MFCs.

Chapter 7 Four continuous flow reactors with different reactor architecture are investigated.

Chapter 8 The main results of the different studies are summarised in an overall conclusion and future work is discussed.

2 MICROBIAL FUEL CELLS

2.1 OVERVIEW

Fuel cells are electrochemical devices that directly convert the chemical energy in a fuel into electrical energy. As intermediate steps such as heat and mechanical work are avoided fuel cells show promise for highly efficient power generation with a low environmental impact (Williams, 2004).

In a microbial fuel cell (MFC) microorganisms act as biocatalysts for the anaerobic oxidation of biodegradable substrates present in a wide range of wastewaters. Produced electrons are transferred to the anode while protons are released into the anodic compartment and pass through a semi permeable membrane into the cathode chamber. Electricity is obtained if the electrons pass through an external circuit between anode and cathode (Scott et al., 2007; Shukla et al., 2004).

MFCs exploit processes used for millions of years by different groups of anaerobic microorganisms to break down complex organic matter ie proteins, carbohydrates (cellulose) and lipids (Figure 2.1). Anaerobic bacteria are a hugely diverse group of microorganisms and were some of the earliest organism formed on Earth. Commonly they are defined as three types (Levett, 1990, Prescott *et al.* 2005)

- *Obligate anaerobes* cannot grow in the presence of atmospheric oxygen;
- *Facultative anaerobes* do not require oxygen for growth but will use aerobic respiration in the presence of oxygen;
- *Aerotolerant anaerobes* ignore oxygen and grow equally good under both aerobic and anaerobic conditions.

Electron transfer plays a central role in biological energy conversion. In anaerobic environments organic compounds are degraded through fermentation or anaerobic respiration. During fermentation the substrate is both the electron donor and electron acceptor (Madigan and Brock 2009). In respiration, aerobic or anaerobic, external electron acceptors are present to

receive the electrons. Microorganisms using anaerobic respiration have the ability to use various alternative electron acceptors intra- or extracellular (Stams et al., 2006). In the anaerobic degradation of organic substrates (Figure 2.1) this creates an opportunity to transfer electrons to an electrode, instead of other naturally occurring electron acceptors, which is exploited in a microbial fuel cell.
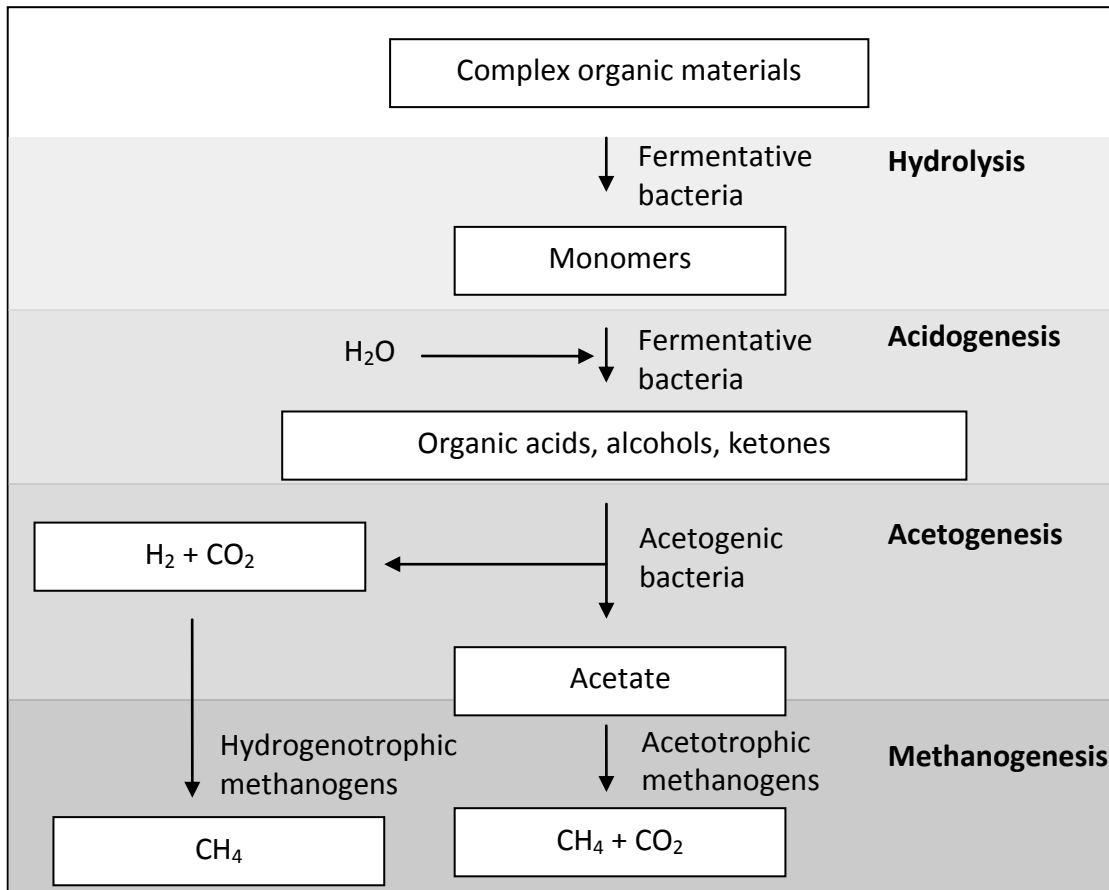
Figure 2.1: Anaerobic digestion of complex organics (Bitton and Ebooks Corporation., 2005; Levett, 1990; Stafford et al., 1980)

Energetically microorganisms gain the most energy using aerobic respiration and therefore oxygen as terminal electron acceptor (Zehnder 1988). High energy gains are also reached by denitrification and nitrate reduction as anaerobic respiration processes. In anaerobic environments with a limited supply of inorganic electron acceptors, such as lake sediments and sewage, methanogenesis is the terminal process (Figure 2.1). Complex organics, sugars, etc. are converted by fermentative bacteria to organic acids, alcohols and ketones. These products are then converted by acetogenic bacteria to acetate and also to hydrogen and carbon dioxide. In methanogenesis acetate as substrate is converted to methane and carbon dioxide by

acetotrophic methanogens and hydrogen and carbon dioxide is converted to methane by hydrogenotrophic methanogens. The anaerobic digestion of complex organics is a synthrophic process, due to the absence of terminal electron acceptors, as the primary fermentation products are converted by syntrophs to key products for methanogens, acetogens and other hydrogen consumers. In microbial fuel cells the anode presents a terminal electron acceptor which cuts into the syntrophic relationship. Thus in a working MFC methane should not be produced as long as the anode is energetically favourable as terminal electron acceptor.

Anaerobic microorganisms play a dual role in MFCs; they generate electricity and simultaneously degrade the organic compounds in wastewater. This is potentially important in the field of waste treatment and wastewater engineering as they may help to minimize operation costs and to recover valuable resources such as water, energy or nutrients (Logan et al., 2006). MFC performance can be influenced by various parameters including reactor design, anode and cathode materials, the membrane and the microbial community that compromises the anodic biofilm.

2.2   PRINCIPLE OF BIOCATALYTIC ENERGY GENERATION AND ELECTRON TRANSFER MECHANISMS

Bioelectrocatalysis is the biological catalysis of electrochemical processes. The biocatalyst can be an enzyme or whole microorganisms. The living cell metabolises energy-rich substances, i.e. glucose, and gains energy from coupled oxidation and reduction reactions (Equation 2.1 and 2.2). Enzymes in the cell reduce the activation energy in the cell to help metabolise the substrate.

$C_{16}H_{12}O6 + 6\ H_2O \rightarrow 6\ CO_2 + 24\ H^+ + 24\ e^-$ $E^0 = 0.014$ V   **(2.1)**

$6\ O_2 + 24\ H^+ + 24\ e^- \rightarrow 12\ H_2O$ $E^0 = 1.23$ V   **(2.2)**

7
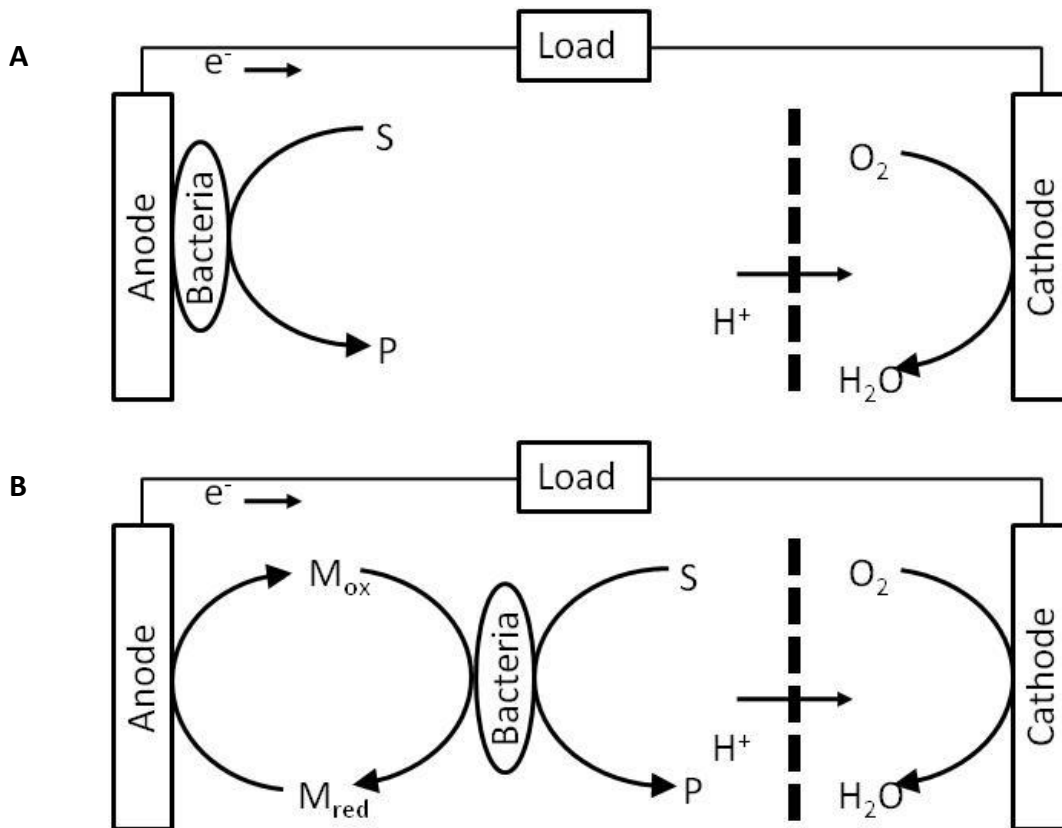
Figure 2.2: Principle of microbial fuel cell showing the mediated (B) and direct (A) electron transfer. M_{ox}: oxidised mediator; M_{red}: reduced mediator; S: substrate; P: product.

Figure 2.2 shows the microbial fuel cell principle for mediated and direct electron transfer from the microorganism to the anode. The electrons produced in Equation 2.1 are transferred to the anode as a terminal electron acceptor. They then pass through an external circuit to the cathode where they react with oxygen and protons passing through the membrane to form water.

Efficient electron transfer to the anode is an important issue in microbial fuel cells. Proposed electron pathways from microorganism to anode are either through conduction (direct) or mediated (Figure 2.2) (Torres et al., 2010).

Electron transfer through conduction can be facilitated by redox enzymes (e.g. cytochromes) in the outer membrane of the microorganisms. Strains of yeast, Geobacter and Shewanella have been shown to use this mechanism (Prasad et al., 2007; Bond and Lovley, 2003; Myers and Myers, 1992). Other pathways include the use of a conductive polymeric matrix and conductive

nanowires for direct contact to the anode (Marcus et al., 2007; Gorby et al., 2006; Laspidou, 2005; Reguera et al., 2005).

Mediated electron transfer is achieved through mobile redox shuttles (e.g. phenazine, pyocyanin, humic acids, quinones, flavins) that are produced by the microorganisms or that naturally occur in the substrate (von Canstein et al., 2008; Rabaey et al., 2005a; Hernandez et al., 2004; Rabaey et al., 2004; Newman and Kolter, 2000). The reduced form of the mediator diffuses to the anode where it is oxidised and diffuses back to the microorganism.

Marcus *et al* (2007) hypothesised that a conductive biofilm polymer matrix (EPS) would be the most probable pathway for high current production from a biofilm. Since direct electron transfer using redox enzymes would be limiting due to the need for direct contact which would only leave one layer of microorganisms able to transfer electrons to the anode if redox enzymes are used. And likewise a large number of mediators would have to be present to account for high current production.

MFCs inoculated with electrochemically active pure cultures are able to illustrate the complete oxidation of specific organic substrates. Together with the availability of complete genome sequences and genetic systems for these bacteria strains detailed investigations into electron transfer mechanism of pure cultures are possible and could enhance the understanding of the basic workings, ecology and physiology of a MFC (Lovley, 2006; Bramucci et al., 2003). Pure culture studies of MFCs operating with fuels such as glucose or starch, where mechanism by which bacteria metabolise the feed are known, could lead to a detailed characterisation of the basic mechanisms influencing electricity production. But will not aid in explaining complex interactions of substrate and microbiology in more complex systems.

However research into biofilm formation showed biofilms to be a well-regulated, highly structured and complex community of organisms (Stoodley et al., 2002; O'Toole et al., 2000). In methanogenic and sulphate reducing environments interspecies electron transfer in syntrophic anaerobic communities is an important process. It is used to digest complex compounds and overcome energy barriers (Stams and Plugge, 2009; Stams et al., 2006). As it is unknown which proposed pathways are dominant under certain conditions (e.g. mixed consortia using

wastewater as substrate), it is probable that these pathways and to date unknown electron transfer mechanisms are used in mixed anaerobic biofilms. Higher current production observed using mixed culture biofilms could presumably be an indicator for syntrophic behaviour in electroactive consortia. This could be the case as mediators and substrates produced by one microorganism using anaerobic respiration improve the growth and electron transfer capabilities of other microorganisms growing nearby. Different microorganisms would also take advantage of different electron transfer mechanisms being used at the same time (Park and Zeikus, 2002). Thus microorganisms which do not produce redox mediators could be able to use mediators produced by another microbial species thereby increasing the electron transfer rate and the power output of mixed strain community microbial fuel cells (Rabaey et al., 2005a).

2.3   MATERIALS

Capital costs of full scale bioelectrochemical systems are estimated to be at least a magnitude higher than the capital costs of conventional wastewater treatment systems assuming a produced current density of 1000 A m^{-3}(Rozendal et al., 2008). With the cathode and membrane making up the largest proportion of the overall cost (an estimated 47 % and 38 % respectively) due to the use of expensive cathode catalysts (platinum) and expensive ion exchange membranes (Nafion). While a few studies reported high power densities up to 1010 W m^{-3}, none of these used wastewater as a substrate (You et al., 2008; Fan et al., 2007). Accordingly it is essential to investigate cost-effective materials for anode, cathode and membrane which increase the power performance and coulombic efficiency using wastewater as substrate.

2.3.1   Anode materials

The anode material in a microbial fuel cell provides a surface for the biocatalyst to attach to and react with the substrate. Consequently the anode material has to be biocompatible, conductive and allow extensive contact between the biocatalyst and substrate.

The anode can be improved by either biological or material means. One way to realise biological enhancement is the immobilisation of electroactive microorganisms in a gel on the anode surface (Karube et al., 1977). But entrapping microorganism can be impractical as only a thin layer of entrapped bacteria is able to act as biocatalysts and the microbial community might not be able to reproduce and grow. A more sustainable way to improve the microbial community on the anode is the enrichment of electroactive microorganisms through natural selection influenced by the anode material and the system conditions (Rabaey et al., 2004).

The most commonly used anode materials are a range of carbon materials especially carbon paper, carbon cloth and graphite due to their high conductivity and specific surface area, biocompatibility, versatility and low cost (Pham et al., 2009; Logan, 2008; Logan et al., 2006). Studies of improvement in anode performance through materials have focused on increasing the specific anode surface area using three dimensional or porous anode materials to increase the surface area relative to the cathode surface area and thus increase electricity generation. Carbon or graphite granules, as three dimensional and porous materials, were reported to achieve high power densities in up-flow continuous reactor designs presumably due to the large surface area available to microorganisms (Aelterman et al., 2008; You et al., 2008; You et al., 2007; Rabaey et al., 2005b). However an increased internal resistance was observed, probably because the carbon granules are not directly connected to each other. A carbon fibre brush anode solved the conductivity problem and comparably high power densities were reported for reactors using a carbon fibre brush in a laboratory setting (Logan et al., 2007). Using these or similar porous and three dimensional carbon materials vastly increases the surface area microorganisms are able to attach to. But electrochemically only protons produced on the surface area opposite to membrane and cathode are able to easily transfer to the cathode. This would mean the large surface area inside the three dimensional structure, or near the core for the carbon fibre brush, is not electrochemically active and scaling up would only increase the inactive surface area. When investigating the scalability of graphite granules through extended layering of the anode a lower increase in power densities was observed than expected with rising anode bed size (Di Lorenzo et al., 2010).
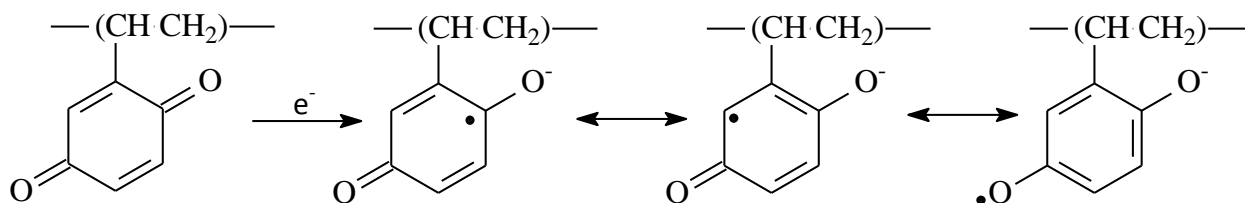
Figure 2.3: Coupling reaction between neighbouring quinone groups (Funt and Hoang 1983).

Besides enhancement of the surface area the addition of redox mediators on the anode surface (Figure 2.3 and 2.4) can lead to more efficient electron transport from the microorganisms to the anode. Modification of graphite electrodes with neutral red doubled the current produced using E.coli as biocatalyst (Park et al., 2000). Carbon activation to introduce quinone groups (Figure 2.3, Figure 2.4) and modification with polyaniline to add quinoide groups on the carbon surface, which both act as mediators under anaerobic conditions, tripled power densities compared to the base material (Scott et al., 2007).
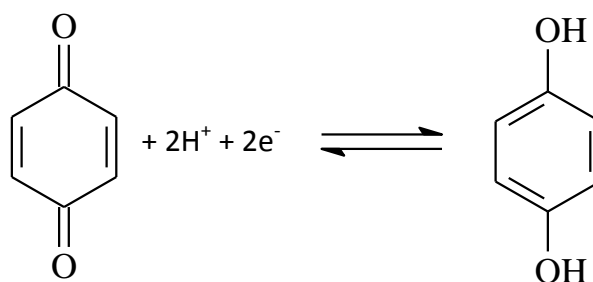
Figure 2.4: Reversible redox schemata of quinone to hydroquinone.

Addition of a positive charge (i.e. through ion oxides) can increase the adhesion of negatively charged microorganisms (Li and Logan, 2004; Johnson and Logan, 1996). Thus addition of Mn^{2+} and Ni^{2+} or Fe_3O_4 and Ni^{2+} on graphite showed a 1.5 to 2.2 times greater activity than plain graphite (Lowy et al., 2006). Ammonia treatment of carbon cloth and the carbon fibre brush exploited the same microbial behaviour by increasing the positive charge on the anode surface by introducing a high density of pyridinic-type nitrogen groups which improved the power production up to 48 % (Feng et al., 2010b; Cheng and Logan, 2007; Boudou, 2003).

Carbon nanotubes (CNTs) have shown promise as catalyst support in fuel cells due to their high conductivity and unique structure (Liu et al., 2006). But CNTs have only been used modified (e.g. with polyaniline or polypyrole) as anodes in microbial fuel cells as they are reported to

show cellular toxicity (Zou et al., 2008; Qiao et al., 2007; Magrez et al., 2006). Direct comparisons of power densities achieved are difficult in this case, as a known carbon material was not investigated as an anode material at the same time.

Chemical modification of carbon materials shows great potential for high power generation as an anode material in microbial fuel cells. But a better understanding of the interaction of bacteria and the carbon surface could lead to even more efficient electron transfer and therefore higher current production.

2.3.2 Cathode materials

In an air-cathode system platinum is the most commonly used cathode material due to its high catalytic activity towards the oxygen reduction reaction (ORR). But the price of platinum makes it uneconomical in microbial fuel cells treating wastewater.

Alternative catalysts based on transition metal porphyrin and phthalocyanine have been long known to show good electrochemical activity towards the oxygen reduction reaction (Jasinski, 1964). In half cell tests similar reduction currents were obtained for iron(II) phthalocyanine (FePc) and cobalt tetramethoxyphenylporphyrin (CoTMPP) when compared to commercial platinum on carbon (HaoYu et al., 2007; Zhao et al., 2006). HaoYu et al. (2007) reported higher power densities using FePc on carbon black in MFC tests than power densities achieved using platinum cathodes, while CoTMPP reached slightly lower power densities than platinum as a cathode catalyst (Cheng et al., 2006b). Other alternative cathode catalysts which showed promising activity towards ORR in half cell tests at neutral pH and reached power densities similar to platinum cathodes include manganese oxides (MnO_x) (Li et al., 2010b; Roche and Scott, 2009) and activated carbon black (nitric acid activated VulcanXc-72R) (Duteanu et al., 2010).

In an MFC gas diffusion cathodes are dependent on the anode to produce electrons and protons and transfer those through an external circuit and a proton exchange membrane to the cathode. Therefore a badly performing anode, low anolyte conductivity and the membrane can

severely decrease the activity of the cathode (Zhao et al., 2006). Additionally the use of complex substrate (i.e. wastewater) could lead to inhibition or deactivation of the catalyst if other substances besides protons are transported through the membrane which could lead to precipitation (e.g carbonate salts) on the cathode side (Franz et al., 2002). The presence of sulphides been shown to inhibit the electrocatalysis of platinum and FePc (Harnisch et al., 2009b).

Microbial biocathodes were proposed as an inexpensive and sustainable alternative to abiotic cathode catalysts (Rabaey and Keller, 2008). Advantages of mixed microbial cathodes would be resistance to poisoning by substances in the wastewater and the ability to replenish themselves. But the lower power densities obtained to date make an improved understanding of oxygen transport and reaction mechanisms in biocathodes essential (Freguia et al., 2010; Rabaey and Keller, 2008; He and Angenent, 2006; Barton, 2005).

2.3.3   Membrane materials

The function of the membrane is to separate the anode and cathode reaction in an electrochemical system while permitting selective transport of protons from the anode to the cathode and preventing transport of oxygen into the anode chamber. While a porous separator also serves as a barrier separating the anode and cathode reaction any ions can be transported from the anode chamber to the cathode through diffusion processes.

Nafion is an expensive ion exchange membrane commonly used in fuel cell systems for proton transport from the anode to the cathode. Due to its good transport characteristics and selectivity it is often used as a membrane in MFCs. Although it is frequently described as a proton exchange membrane Nafion also selectively transports other cation species (e.g. Na^+, K^+, NH^{4+}, Ca^{2+}, Mg^{2+}) found in the anolyte in MFCs to maintain charge balance in the system (Mauritz and Moore, 2004; Okada et al., 1998). Using wastewater, concentrations of other cations can be 10^5 times higher than the proton concentration in the anolyte which can lead to preferred transfer of other ions through the membrane and salt precipitation on the cathode inhibiting the cathode catalyst (Rozendal et al., 2006; Zhao et al., 2006; Franz et al., 2002). High

permeability to oxygen and substrate (acetate) of Nafion is also a challenge to the realisation of high power densities (Chae et al., 2008). Strategies to reduce the cost and overcome these limitations included the use of inexpensive ion and ultrafiltration membranes or separators in a membrane-less MFC design.

Kim *et al.* (2007) reported higher power densities and coulombic efficiencies using an anion exchange membrane (AEM) compared to the use of Nafion or an inexpensive cation exchange membrane (CEM). It was suggested that the better performance of the AEM was due to the use of phosphate or carbonate as proton carriers which would also contribute to a better pH balance in the anode and cathode chamber (Li, 2010; Kim et al., 2007). Similarly microfiltration membranes have been shown to achieve higher or similar power densities as CEM in MFC tests (Sun et al., 2009). An in depth characterisation of the membranes used could provide solutions to the pH gradient observed in many studies (Harnisch et al., 2009a).

Membrane-less MFCs describe MFCs use either an inexpensive separator as a membrane or the electrolyte itself as barrier between anode and cathode. The most important characteristics of materials used as separators are low costs, durability and high mechanical strength. Materials investigated in MFC tests as separators included battery separators, carbon paper and various other materials. Proton conduction occurs in separators through diffusion processes balancing charge and pH from the anode to the cathode. But as the separators are not selective, any substance in the substrate can be transferred to the cathode and higher oxygen diffusion into the anode chamber was observed. Therefore membrane-less reactors showed high power densities compared to reactors using a proton exchange membrane, but achieved lower coulombic efficiencies as the substrate was digested aerobically (Du et al., 2008; Liu and Logan, 2004). Membrane-less MFCs are the most cost-effective solution if the challenge of low coulombic efficiencies can be overcome. Addition of a material layer (J-cloth or carbon fibres) in front of the separator increased the coulombic efficiencies achieved by further reducing oxygen diffusion into the anode chamber, presumably through either lower oxygen permeability of the material or formation of an aerobic biofilm (Zhang et al., 2009b; Fan et al., 2007). Though higher coulombic efficiencies were reached aerobic degradation still occurs in this configuration.

2.4 REACTOR DESIGN AND OPERATION

For high power production and coulombic efficiencies the reactor design of a MFC has to overcome the limitations presented by the materials (anode, cathode and membrane) and the substrate. Challenges for MFCs used in wastewater treatment are the

- Low power densities;
- Low coulombic efficiencies;
- Capital costs of the materials used.

The low conductivity of wastewater (1-2 mS cm^{-1} for domestic wastewater) increases the internal resistance in the reactor which leads to high ohmic losses in the system and therefore less energy production (Rozendal et al., 2008). Other ohmic losses reducing the power generation can be ohmic losses on the electrodes due to low activity of the catalyst or for the cathode catalyst inhibition and deactivation due to substances in the wastewater.

Anaerobic respiration is the main electron donor for electrogenesis. Low coulombic efficiencies observed for wastewater are thought to be mainly due to the degradation of substrates by competitive processes such as fermentation as electrons are transported to terminal electron acceptors produced during the fermentation process instead of the anode.

Research must provide solutions to the problem of cost as many studies investigate the reduction of costs for anode, cathode and membrane while increasing the material activity and efficiency. At the same time the design and operational parameters can provide solutions to the low power densities and coulombic efficiencies observed. Reducing the electrode distance from 4 to 2 cm lead to a slight decrease in internal resistance (79 Ω to 71 Ω) while nearly doubling the power density (720 mW m^{-2} to 1210 mW m^{-2}) (Liu et al., 2005). Against expectations further reduction of the electrode distance showed a decrease in power density, coulombic efficiency and internal resistance, possibly due to oxygen diffusion into the anode chamber (Cheng et al., 2006a). Advective flow through a porous anode improved the power production as it aided the diffusion of substrate to the anode and protons to the cathode (Cheng et al., 2006a). Similarly the sequential flow from the anode to the cathode improve coulombic efficiencies, the pH balance and the effluent quality (Freguia et al., 2008).

If the reactor design and operation can be matched to the application high power densities at high coulombic efficiencies can hopefully be achieved.

To optimise and enhance power generation, wastewater treatment and coulombic efficiencies it is important to know the factors influencing these and optimising them. Thus to seek better understanding of the physiology and ecology of MFCs and electrochemical engineering limitations such as materials and physical design. Cathodic and anodic electron transfer mechanisms have to be understood in depth, including detailed characterisation of the interfacial electron transfer rates, biocatalytic rate constants, cell resistance, COD and nutrient removal mechanisms and the knowledge about which steps are rate-limiting. With a better understanding of these mechanisms, design limitations can be challenged and material costs, as well as operating costs, reduced until MFC systems are economically feasible and applicable

3 MATERIALS AND METHODS

This chapter explains and describes the experimental methods and materials used in the MFC research reported in this thesis. An overview of the different materials for anode, cathode and membrane and the substrate used are given in Table 3.1.

3.1 MATERIALS

3.1.1 *Single Chamber Microbial Fuel Cell configuration and operation*

Figure 3.1 shows the different MFC configurations used during the experiments. The single chamber MFCs for operation under anaerobic conditions, were made from polyacrylate. Reactor configuration (A) was used in most batch experiments and had a total working volume of 50 cm^3 (ml) (internal length 4 cm; internal diameter, 12.5 cm^2). The anode was fixed to the back of the reactor in the wastewater filled chamber. Configuration (B) was used to study the influence of the electrode distance on the power performance in Chapter 4.5.

Configuration (C) to (F) were used as continuous flow reactors. (C), (D) and (E) were used in the experiment studying the influence of external load and electrode spacing on the performance in an experimental design. Reactor (F) was used as a flat plate continuous flow reactor with an electrode spacing of 0.5 cm, an electrode area of 100 cm^2 and a working volume of 50 cm^3.

The air cathode (cross sectional area 12.5 cm^2) was located at the opposite end of the reactor. A gas diffusion electrode directly supported on the surface of a membrane and exposed to air was used as cathode in all studies. The catalysts layer, prepared from catalyst ink with 10 wt% PTFE, to keep the cathode dry, and 15 wt% PVA as binder, was deposited directly onto the membrane at a load of 1 mg cm^{-2}.

Anode catalysts, prepared from a catalyst ink with 10 wt% PVA, were deposited directly onto a support with a load of 1 mg cm^2. The system was designed for proton conduction by transfer of

the ions present in the wastewater present in the porous separator. Titanium wires connected the electrodes to the external circuit.
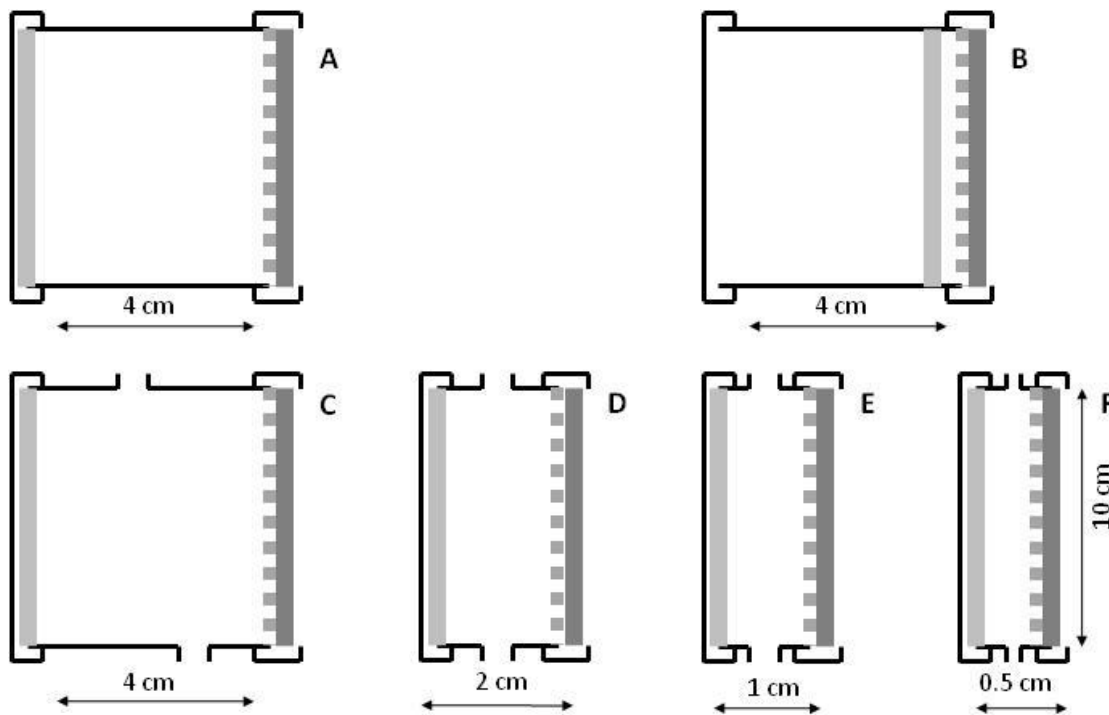
Figure 3.1: Single chamber microbial fuel cell reactor with the anode (light grey line), membrane (grey dotted line) and the cathode (dark grey). Reactor (A) and (B) were used in fed-batch experiments and the reactor has an internal length of 4 cm and a working volume of 50 cm³. Reactor configurations (C) to (E) were used in a factorial designed experiment to study the electrode spacing in a flow through system and configuration (F) was designed as a flat plate reactor with an internal spacing of 0.5 cm and a working volume of 50 ml.

During acclimatisation and enrichment the reactors were operated without polarisation under a stable load (5000 Ω, 1000 Ω, 500 Ω, or 50 Ω depending on the experiment) or at OCP to allow time for the formation of a biofilm on the anode.

Reactors under fed batch mode were operated at room temperature and substrate (wastewater) was added when the voltage started to decrease. To replace the substrate, effluent was pumped out and the MFC was immediately refilled with nitrogen purged substrate (wastewater) without disturbing the anode biofilm. Stabilisation of the voltage generation in

the reactors showed acclimatisation of the anodic community and consequent adaptation of system.

Reactors under continuous flow mode were fed with substrate at a constant flow rate until the voltage output stabilised.

Once the reactors were assumed to be acclimatised with a mature electroactive biofilm covering the anodes surface and electrochemical (polarisations, linear sweep voltammetry) as well as analytical measurements (COD, pH, Conductivity) were made.

Raw domestic wastewater was collected from the influent at a local municipal sewage treatment works (Cramlington Sewage Treatment Works, Northumbrian Water, Cramlington, UK) and brewery wastewater was provided by the Federation Brewery (Newcastle upon Tyne, UK). The same wastewaters were used throughout each study and wastewaters were stored at 4 ^{o}C in order to arrest physicochemical changes in wastewater and minimise biological activity.

Table 3.1: Description of anode, cathode, membrane and substrate used in the different experiments.

Experiment	Anode	Cathode	Membrane	Substrate
Anode Studies				
Modified Anode Materials	Carbon cloth[a] Carbon black[b] C/HNO3[c] C/PANI[d]	Carbon black[a]	Rhinohide[e]	Domestic wastewater[f] with 0.5 % brewery wastewater[g]
Activated Carbon Cloth[h]	FM30k H[h] FM30k[h] FM70[h]	Carbon black[a]	Rhinohide[e]	Domestic wastewater[f]
Anode Support Materials	C/HNO$_3$ on titanium mesh[i] C/HNO$_3$ on stainless steel mesh[i] C/HNO$_3$ on aluminium mesh[i] FM30k[h]	Carbon black[a]	Rhinohide[e]	Domestic wastewater[f]
Cathode Studies				
Cathode materials and their durability	FM30k[h]	Pt/C[j] Carbon black[a] C/HNO$_3$[c] FePc[k] FePc+Mn[k]	Rhinohide[e]	Domestic wastewater[f]

Membrane Studies	FM30k[h]	Carbon black[a]	Membrane separators are described in detail in Chapter 6	Domestic wastewater[f]
Reactor Studies				
Flat plate reactor	C/HNO$_3$[c]	FePc[k]	Rhinohide[e]	Domestic wastewater[f]
Factorial design	FM30k[h]		Rhinohide[e]	Domestic wastewater[f]

[a]designation A, supplied by E-Tek, UK.

[b]Ketjen Black EC 300J, Akzo Nobel, Netherland.

[c]Nitric acid activated carbon black (Ketjen Black EC 300J, Akzo Nobel, Netherland).

[d]Polyaniline modified carbon black (Ketjen Black EC 300J, Akzo Nobel, Netherland).

[e]Micropouros battery separator supplied by Entek International, UK.

[f]Influent collected at a local municipal sewage treatment works (Cramlington Sewage Treatment Works, Northumbrian Water, Cramlington, UK.

[g]Provided by the Federation Brewery (Newcastle upon Tyne, UK).

[h]Provided by Chemviron Carbon Cloth Division, UK.

[i]Provided by Dexmet Corporation, UK.

[j]Commercial platinum on carbon supplied by E-Tek, UK.

[k]Details of the materials are supplied under cathode materials in Chapter 5.

3.2 METHODS

3.2.1 Electrochemical Measurement

After samples were taken during one batch under load, the reactors were refilled under OCP. Once the voltage stabilised, the reactors were polarised. During polarisation the change in cell current and voltage, as well as the anode and cathode behaviour under polarisation against a Ag/AgCl reference electrode, was recorded continuously as a function of time using a data acquisition system (ADC 16, Pico Technology Ltd, UK) connected to a personal computer via a BS 232 Pico high resolution analogue cable. Polarization curves were recorded under open circuit potential (OCP) using a potentiostat (GillAC, ACM Instruments, UK) at a scan rate of 1 mV s^{-1}.

Anode and cathode potentials were monitored during cell polarisation using an Ag/AgCl reference electrode (Thermo Scientific, UK) placed in the anode chamber through a capillary using phosphate buffer (100 mM; pH 6.5) as electrolyte. No additional electrolyte was added to the substrate, during the measurement of anode potentials, as it was established that ionic conduction was supported by the presence of ions naturally occurring in the wastewater. The cathode potential were internal resistance (iR) corrected as the cathode potential had to be measured through the membrane.

Since the polarisation results indicate possible capabilities of the reactors only the peak power achieved with the best performing reactors out of the duplicates is shown in graphs and discussed in the appropriate results and discussion of the chapter. To indicate the variation between duplicates during polarisation the average performance is included with calculated standard error in the results of the chapter or where appropriate in the appendix.

The internal resistance was measured by electrochemical impedance spectroscopy using a potentiostat (Gillac, ACM Instruments). Impedance measurements were conducted at OCP over a frequency range of 30000 to 0.1 Hz with a sinusoidal perturbation of 10 mV amplitude.

3.2.2   Wastewater Characteristics

Standard chemical analyses were carried out according to the Standard Methods for the Examination of Water and Wastewater (Eaton et al., 1998) to measure

- Suspended solids (SS)
- Volatile suspended solids (VSS)
- Chemical oxygen Demand (COD)

Sulphate, phosphate, chloride and nitrate concentrations in the feed were estimated by ion-chromatography (DX-100, Dionex International, UK).

The ionic conductivity of the feed substrate was measured using a handheld conductivity meter pIONeer 30 (Radiometer Analytical, France).

The pH was measured using a portable 3310 pH Meter (Jenway, UK) and the dissolved oxygen (DO) was measured using a portable 9500 DO_2 Meter (Jenway, UK)

The chemical oxygen demand (COD) is the amount of oxygen needed to degrade a sample chemically and is used to describe the amount of organic substrate in a wastewater. The COD in mg COD/l is calculated using the Standard Methods for the Examination of Water and Wastewater (Eaton et al., 1998).

The coulombic efficiency (CE) directly shows the number of electrons used for electricity production and therefore is an indicator for the efficient use of the substrate as power producer. For batch experiments the coulombic efficiency was calculated using:

$$\epsilon_{CE} = \frac{M \int_0^t I dt}{F b V_{Anode} \Delta COD} \tag{3.1}$$

Where M is the molecular weight of oxygen, F is faraday's constant in coulomb, I the current in ampere, b = 4 is the number of electrons exchanged per mole of oxygen, V_{Anode} is the liquid volume of the anode, and ΔCOD is the change in COD over time.

For continuous flow systems the COD consumption rate ($COD_{consumed}$) was measured once steady state was reached using

$$COD_{consumed} = Q \cdot (COD_{IN} - COD_{OUT}) \qquad \textbf{(3.2)}$$

Where Q is the volumetric flowrate (m^3 T^{-1}) and the COD (mg/l) of the influent and effluent is described as COD_{IN} and COD_{OUT}.

The coulombic efficiencies of the continuous reactors was calculated using

$$\epsilon_{CE} = \frac{MI}{FbQ\Delta COD} \qquad \textbf{(3.3)}$$

Where F is Faraday's constant in coulomb, M the molecular weight of oxygen, I the current in ampere at steady state, b the number of electrons exchanged per mole of oxygen and ΔCOD the difference between influence and effluent COD.

The hydraulic retention time τ in T, as a measurement of how long the substrate stayed in the reactor, is defined as (Metcalf & Eddy. et al., 2003):

$$\tau = \frac{V}{Q} \qquad \textbf{(3.4)}$$

Where V is the reactor volume in m^3 and Q the volumetric flowrate in m^3 T^{-1}.

3.3 MICROBIOLOGY

3.3.1 Bacterial sampling

For microbial community analysis, the anodic biofilms formed at the end of the experiments, were transferred along with the entire anode separately into sterile centrifuge tubes containing 20 ml of sterile phosphate buffer (PBS) and 20 ml of absolute ethanol (1:1 ratio [v/v]). Then the biofilm was extracted from the anode by shaking and finally stored at --20°C until analysis. In the case of the feed, uniformly mixed liquid samples were placed in ethanol at a 1:1 volumetric ratio.

3.3.2 DNA extraction and PCR amplification of 16S rRNA genes

Total DNA was extracted from 250µl of the ethanol fixed samples, using a Fast DNA Spin Kit (BIO 101, Q-BioGene, UK). Extracted DNA was found to be suitable for PCR amplification without any further purification. The 16S rRNA gene fragments were amplified from the extracted total DNA using VrVf primers i.e. Vf GC clump forward (5′-CGC CCG CCG CGC GCG GCG GGC GGG GCG GGG GCA CGG GGG GCC TAC GGG AGG CAG CAG-3′) and Vr reverse (5′-ATT CAC GCG GCT GCT GG-3′). Amplification was achieved with a 50 µl reaction volume containing 47µl of PCR mega mix blue, i.e. PCR reaction mix with loading buffer, supplied by BIO 101, Q-BioGene, UK, 1 µl of pA primer, 1 µl of pH reverse primer and 1 µl of DNA. PCR amplification was performed in an automated thermal cycle (Hybaid, Omn-E) with an initial denaturation (95 °C for 3 min) followed, for the first-round amplification, by 24 cycles of denaturation (95°C for 1 min), annealing for 1 min (starting at 65°C and decreased by 1°C every second cycle) and extension (72°C for 1 min) and a single final extension (72°C for 10 min). The detailed steps were described clearly in Table 3.2.

PCR products were visually analysed by electrophoresis on a 1% (w/v) agarose gel (NuSieve; FMC Bioproducts) in 1×TAE buffer (2 M Tris-Acetate, 0.05 M EDTA, pH 8.3, Eppendorf Scientific Inc., New York, USA) for 50 min at 100 V and gel images were recorded using a FluorS gel documentation System (Bio-Rad) after staining with ethidium bromide.

Table 3.2: Summary of VfGC clamp/Vr (nested) PCR program.

No	Step	Temperature (^{0}C)	Time (min)	Cycles
1	Denaturation	95	3	1
2	Denaturation	95	1	
3	Annealing	65	1 (reduced 1°C for every 2nd cycle)	
4	Extension	72	1	24
5	Denaturation	95	1	
6	Annealing	53	1	15
7	Extension	72	1	
8	Final Extension	72	10	1

3.3.2.1 Denaturing gradient gel electrophoresis (DGGE)

Community profiles of the anodic biofilms analysed were obtained using DGGE analysis. PCR product (11 µl) was mixed in equal volumes with loading buffer (0.25% bromophenol blue, 0.25% xylene cyanol FF, 15% Ficoll in water) and run on a polyacrylamide gel (acrylamide–N,N'-methylenebisacrylamide ratio, 37.5:1) in 1 x TAE buffer (40 mM Tris, 20 mM acetic acid, 1 mM EDTA, pH 8.0) over a chemical denaturing gradient of urea and formamide; equivalent to 30–55% denaturant (100% denaturant is 7M urea and 40% (v/v) formamide). Electrophoresis was performed using the D-Gene system (Bio-Rad, Hercules, CA, USA) at 200 V constant current at 60 °C, for 4.5 hours. The separated DNA was stained for 30 min with SYBR green I (Sigma, Poole, UK; diluted 1/10,000 in 1 X TAE). Stained gels were viewed and documented using a Fluor-S Multilmager (Bio-Rad, Hercules, CA, USA).

3.3.2.2 Numerical and statistical analysis of DGGE banding patterns

Scanned DGGE gel was processed through the Bionumerics software (version 3.5, Applied Maths, USA) to analyze the intensity and position of all bands within a single lane in relation to the positions and intensity of the bands in all other lanes. To correct for variations across the gel, a marker sample was run on either side of samples. During the first step of gel processing, all lanes/strips are defined on the gel and aligned and a densitometric curve was calculated for each gel track. In the following normalization step, one reference sample (marker lane) was defined as the "standard" pattern (external reference pattern) and bands were assigned. Then remaining reference patterns (remaining marker lanes) on DGGE gel were aligned to this external reference pattern and the band assignments were checked manually. The banding patterns of the samples were aligned gradually according to the alignment information provided by the closest neighbouring standard patterns. By aligning the bands of all references and sample tracks from gel to the external reference pattern, it became possible to compare band patterns from different samples with each other. DGGE fingerprints were automatically scored through software, by the presence or absence of co-migrating bands without consideration of the band intensity. Then the patterns were analyzed in two ways:

- Similarities between anodic communities were analysed based on the Bray Curtis similarity index (Murguia and Villasenor, 2003) through cluster and non metric MDS methods.

- Comparison of band patterns between all samples by band matching.

Similarities were displayed graphically as dendogram and ordination using an un-weighted pair group method with arithmetic averages (UPGMA) clustering algorithm.

4 ANODE MATERIALS AND DESIGN

ABSTRACT

The materials investigated for the anode were carbon black, carbon black modified with polyaniline (C/PANI) and nitric acid (C/HNO$_3$) using domestic wastewater with 0.5% brewery wastewater as substrate under three external loads (500 Ω, 1 kΩ and 5 kΩ). During polarisation C/PANI reached power densities of 18±0.4 mW m^{-2} while C/HNO$_3$ and carbon black achieved 15.7±0.3 mW m^{-2} and 15.6±1.3 mW m^{-2}. Carbon cloth reached a third of this with 5.6±0.4 mW m^{-2}. Very low power densities, on average, 6 mW m^{-2} under 5 kΩ, 5 mW m^{-2} under 1 kΩ and 3 mW m^{-2} under 500 Ω),and coulombic efficiencies, with 3-9% with decreasing external load, were obtained. Additionally three activated carbon cloths were studied as anode materials with domestic wastewater as substrate. These materials showed greater potential for high power densities reaching on average 40 mW m^{-2} during polarisation and 20 mW m^{-2} under 1000 Ω external resistance. The influence of the external resistance on power performance and coulombic efficiency was statistically significant while differences between the different materials were insignificant.

The high internal resistance observed due to the low conductivity of wastewater (1-2 mS cm^{-1}) was the main influence limiting the power densities achieved through high ohmic losses in the reactors using 4 cm electrode spacing. Reducing the electrode distance to 2 mm and the use of titanium, stainless steel and aluminium meshes and, comparatively, activated carbon cloth as anode support decreased in the internal resistance by a factor of ten. A simultaneous decrease in anode potential using 2 mm electrode spacing, presumably due to oxygen diffusing into the anode chamber, lead to comparably lower power densities reaching up to 22 mW m^{-2} during polarisation and 15 mW m^{-2} under 1000 Ω. Although covered with a protective catalyst layer aluminium meshes were quickly degraded by microorganisms and are therefore not recommended for use in MFCs.

4.1 INTRODUCTION

Microorganisms on the anodic side of a MFC act as biocatalysts for the anaerobic oxidation of a range of organic compounds present in a fuel. Transferring the electrons produced to the anode yields energy for microorganism due to the potential difference. The complex interactions between different microorganisms in a mixed microbial community and their interactions with their support (usually a carbon material) are poorly understood making it difficult to reliably determine or discover efficient anode materials.

The function of anode materials is to provide a surface for the electrochemical and biological reactions taking place. Porous anode materials can supply a large surface area for microorganisms to adhere to and allow extensive contact between biocatalyst (microorganisms), substrate and the conducting electrode materials. Other functions of the anode material in microbial fuel cells are (Williams, 2004):

- to conduct electrons
- add connections to other MFCs and the load
- ensure that sufficient substrate reaches the biofilm
- allow effective release of anode reaction products (e.g. protons)

To fulfil these functions anodes are typically porous, biocompatible and electrically conductive (Logan et al., 2006; Williams, 2004). However to be viable anode materials should also demonstrate high chemical, electrochemical and biological stability, be resistant to poisoning, show high electrocatalytic activity and be inexpensive.

In this study the performance and long-term durability of alternative anode materials in a MFC, the influence of the anode position (distance from the cathode) and the anode support material on internal resistance and the power performance were investigated. These aspects were studied in a single chamber MFC using a carbon black based air-cathode and an inexpensive hydrophilic battery separator as membrane.

4.2   ANODE SURFACE AREA AND ACTIVITY

The electrochemical or specific surface area (ESA) of a material describes the number of electro-active sites on the material and is therefore an important parameter to determine the catalyst activity (Bard and Faulkner, 2001; Rodriguez et al., 2000). The mechanism of electrocatalysis is based on the electrode and electroactive species charge transfer at the electrode surface. The reaction rate is proportional to the electrochemical electrode surface area and electric current (Rodriguez et al., 2000).

The ESA of a material is most commonly evaluated using the BET method (Brunauer, Emmett and Teller, 1938) of gas adsorption on the electrode surface i.e. hydrogen adsorption (Pozio et al., 2002; Rodriguez et al., 2000; Ralph et al., 1997; Ho and Piron, 1995). But BET methods, as other adsorption methods, require the adsorbents to bind reversibly to the electrochemical active sites. As different gases are absorbed differently depending on surface species (Watt-Smith et al., 2008) and electrode morphology, especially the pore size (Shi, 1996) of carbon materials (Stoeckli and Centeno, 2005; Pozio et al., 2002), estimated surface areas can vary by up to 100% (Watt-Smith et al., 2008). Especially for carbon materials the relationship between high surface area (capacity), surface chemistry (kinetics) and pore size (kinetics) raises questions about the validity of the gas adsorption models commonly used to estimate porous electrode surface areas and pore size distribution (Salitra et al., 2000; Sing, 1994). For activated carbon materials with their different morphologies and surface chemistry this means that "the real surface area cannot be determined in a reliable way from the enthalpy of immersion and a specific heat of wetting alone", as Stoeckli *et al* conluded in 2005.

The anode material in microbial fuel cells is not so much a catalyst for the reaction but a holding area for the anodic biofilm consortia. Thus high surface area, biocompatibility and conductivity of any anode material are essential for the formation of an electroactive biofilm. Furthermore, as microorganisms are around micrometers in size, the BET surface area of a porous material with small pores (less than a few µm) is probably irrelevant, as only pores bigger than the organisms can be colonised. Thus for this investigation the geometric surface

area (in cm^2) of the materials was used in calculations, whilst the specific surface area of a material was reported, whenever known.

Anode activity is defined through appropriate reaction kinetics. Generally the oxidised form (O) of the reactant reacts with a number (n) of electrons (e⁻) to form the reduced form (R)

$$O + ne^- \underset{k_O}{\overset{k_R}{\rightleftharpoons}} R$$

(4.1)
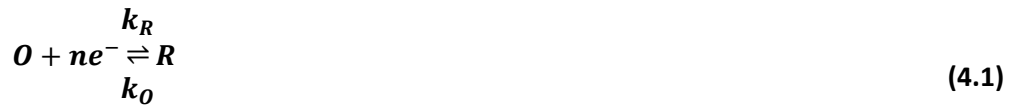
The rate of the reaction is determined by the rate constant for reduction k_R and oxidation k_O.

The equilibrium for this reaction is characterised by the Nernst equation(Bard and Faulkner, 2001):

$$E_{eq} = E^{0'} + \frac{RT}{nF} \ln \frac{c_O^*}{c_R^*}$$

(4.2)

where $E^{0'}$ is the formal potential, E_{eq} is the equilibrium potential, R is the gas constant, T the temperature, n the stoichiometric number of electrons involved in the electrode reation, F is Faraday constant and c_O^* and c_R^* are the bulk concentrations of form O and R.

$$\Delta E = 0 \qquad \Rightarrow \qquad i = 0$$

(4.3)

Although a net current (flow of electrons) does not flow at the equilibrium, a dynamic equilibrium exists on the electrode surface.

$$O + ne^- \rightarrow R$$
$$R - ne^- \rightarrow O$$

(4.4)

As both processes occur at equal rates the solution composition of the substrate does not change. Expressed as exchange current i_0, which is equal in size to the cathodic component current i_C or the anodic component current i_A this is (Bard and Faulkner, 2001)

$$i_0 = FAk^0 c_O^{*(1-\alpha)} c_R^{*\alpha}$$

(4.5)

where α is the transfer coefficient, A the area and k^0 is the standard heterogeneous rate constant.

Therefore the exchange current density i_0 is a measure of the electron transfer activity at equilibrium (Bard and Faulkner, 2001). A large i_0 describes fast reaction kinetics, while a small i_0 describes slow reaction kinetics.

The overpotential η is the deviation of the cell or electrode potential from the equilibrium potential.

$$\eta = E^{0\prime} - E_{eq} \qquad\qquad (4.6)$$

In a well mixed solution the electron transfer reaction on the electrode are slow, thus no mass-transfer effects occur, the bulk and surface concentrations are equal and therefore the relationship between current density and electrode overpotential is given by the Butler Volmer equation (Bard and Faulkner, 2001).

$$i = i_0 \left[e^{\left(\frac{-\alpha \cdot F}{RT}\eta\right)} - e^{\left(\frac{(1-\alpha) \cdot F}{RT}\eta\right)} \right] \qquad\qquad (4.7)$$

(4.7 describes the dependence of the electrical current on the electrode to the electrode potential while cathodic and anodic reactions occur on the same electrode.

The Butler-Volmer equation has two limiting cases. At low overpotentials η the current varies linearly with η near E_{eq}.

$$i = -i_0 \frac{F}{RT}\eta \qquad\qquad (4.8)$$

For large η, both negative and positive, the Butler-Volmer equation can be expressed for the anodic current as

$$i = i_0 e^{\frac{(1-\alpha)F\eta}{RT}} \qquad\qquad (4.9)$$

Or

$$\eta = \frac{RT}{(1-\alpha)F} \ln i_0 + \frac{RT}{(1-\alpha)F} \ln i \qquad\qquad (4.10)$$

These equations are the anodic form of the Tafel equation which relates the rate of an electrochemical reaction i to the overpotential η. The Tafel equation is often expressed as

$$\eta = a + b \log i \qquad\qquad (4.11)$$

Tafel relationships can be observed in systems with irreversible electrode kinetics and no mass-transfer effects. Good Tafel relationships can be seen when electrode kinetics and a high activation overpotential is required (Bard and Faulkner, 2001). The slopes of a Tafel curve are usually indicative of pathways underlying electrode reactions. The intercept can be used to calculate the exchange current density i_0 which gives information about the reaction kinetics.
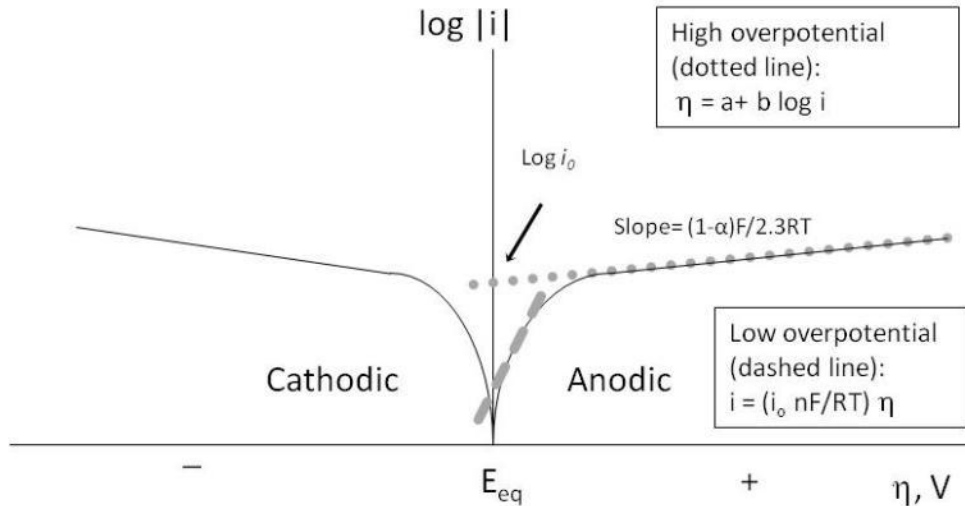
Figure 4.1: Tafel behaviour at high and low overpotential. (Bard and Faulkner, 2001)

The reaction kinetics in fuel cells depend on the chemical reaction mechanism involved, whereas in microbial fuel cells, as microorganisms act as biocatalysts, the reaction rate is controlled by the metabolisms of electroactive microorganisms, which can be very slow in comparison with chemical mechanisms of electron transfer.

When anodes show (near) linear behaviour in the low overpotential range (<40mV), the relative activity of the anodes can be compared using the linear approximation of the Butler-Volmer equation (Figure 4.1) (Scott et al., 2008; Lowy et al., 2006). (Equation (4.12) and (4.13)

$$i = \left(i_0 \frac{nF}{RT}\right) \eta \tag{4.12}$$

$$i = \frac{2Ai_0 c^* \alpha nF\eta}{RT} = \frac{2Ai_0 c^* \eta}{b} \tag{4.13}$$

Where i_0 is the exchange current density, α is the transfer coefficient, A is the active area per unit cross sectional area of the electrode and depends on the particular material used, c* is the bulk concentration of active species and b = RT/αnF

In Equation (4.13) the charge transfer resistivity (Ω cm^2) is given as the slope (b/Ac*i_0 in Ω cm^2) when plotting the overpotential against the current density (i/2). The charge transfer resistivity is a measure on the relative anode activity with a lower resistivity describing higher activity (Scott et al., 2008).

4.3   MODIFIED CARBON AS ANODE MATERIALS

4.3.1 Introduction

Carbon black is an industrially manufactured carbon material composed of spheres and their fused aggregates with a range size of 10 to 1000 nm (Lahaye and Ehrburgerdolle, 1994). It consists of spheroidal particles with a distinct ordering of the carbon layer (graphene layer). The layers are wrapped around a disordered nucleus and preferentially orientate themselves parallel to the particle surface (Boehm, 1994). Carbon black materials are very versatile and used in a wide range of different applications.

Depending on manufacture processes carbon materials and their properties vary widely with respect to the particle size, aggregate size, morphology of the aggregates and its microstructure, surface area characteristics (structural organisation, porosity, surface area). The surface chemistry is dictated by factors such as oxygen complexes chemisorbed on the carbon surface in varying degrees (Seredych et al., 2008; Bleda-Martinez et al., 2006; Bleda-Martinez et al., 2005; Boehm, 1994; Donnet et al., 1993; Jankowska et al., 1981). These surface functional groups influence and change the chemical, physical and electrical properties of the material. Thus differently manufactured carbon blacks differ in surface potential, electrochemical activity and conductivity (Bleda-Martinez et al., 2006; Loutfy, 1986).

Four carbon materials were studied as anode materials in this experiment

- Carbon cloth (designation A from E-Tek, UK) as support material (CC);

- Carbon cloth covered with carbon black (Ketjen Black EC 300J) (CB);

- Carbon cloth covered with carbon black modified with polyaniline thus integrating quinoide groups on the carbon surface (C/PANI);

- Carbon cloth covered with carbon black activated with nitric acid incorporating quinone groups onto the carbon surface (C/HNO$_3$).

The deposition of unmodified and modified carbon black (load 1 mg cm^{-2}) onto carbon cloth was designed to increase the activity, surface area and electrical conductivity of the carbon cloth anode.

The activated carbon material C/HNO_3, contains redox active quinone groups on the carbon surface which not only improve the wetability of the carbon material and make interaction between surface and water molecules easier (Bleda-Martinez et al., 2006) but also act as local mediators under anaerobic conditions and improve the electron transfer from bacteria to anode (Freguia et al., 2009; Uchimiya and Stone, 2009; Newman and Kolter, 2000; Tarasevich et al., 1987; Nohl et al., 1986).

For C/PANI modification with polyaniline introduces quinoide groups onto the carbon surface which also act as local mediators under anaerobic conditions (Lowy et al., 2006; Niessen et al., 2004; Schroder et al., 2003; Simon et al., 2002). Furthermore the polymer coating of the carbon particles makes C/PANI more conductive, biocompatible and environmentally stable (Ibrahim and Koglin, 2005; Muhammad-Tahir and Alocilja, 2003; Zengin et al., 2002; Misra and Angelucci, 2001).

4.3.2 Hypotheses

The hypotheses in this study were that the anode materials and the external load influence the power and wastewater treatment performance, of an economically designed single chamber MFC, through specific selection of electroactive microorganisms forming the microbial biofilm consortia.

4.3.3 Experimental

The study consisted of four experiments examining the influence of surface chemistry and load with a range of anode materials and three external resistances (1 kΩ, 5 kΩ, 500 Ω) and at open circuit potentials (OCP) on power and wastewater treatment performance and the microbial community. For all experiments four duplicate reactors and a control reactor (feed substrate under anaerobic conditions) were operated at the same time and all results reported are the average of the two duplicate reactors.

The anode modifications used in this work were based on the enhancement of active surface area, biocompatibility, electrical conductivity and the addition of quinone or quinoide groups to

the surface of the carbon black used. These groups act as mediators under anaerobic conditions. The modifications were achieved by depositing carbon black and carbon black modified with quinoide groups and activated with quinone groups, as a catalyst ink with 15 wt% PVA, with a load of 1 mg cm^{-2} on the carbon cloth support. None of the modifications involved the addition of a catalyst.

The carbon/polyaniline composite (C/PANI) was made according to the literature (Scott et al., 2007; Zhang and Wan, 2002). For this 1.7 g aniline sulphate and 0.7 g D-camforsulphonic acid were dissolved in 30 ml deionised water. The solution was added in drops to 1.5 g Ketjen Black EC 300J powder and the mixture was sonicated for 30 min. Then 15 ml ammonium peroxydisulphate solution (24.7 g l^{-1}) were added to the mixture which was again sonicated for 30 min. The mixture was polymerised for 20 h at RT.

The HNO$_3$ treatment of the carbon support was performed according to Scott et al, 2007. 1 g of Ketjen Black EC 300J was refluxed in 300 ml 70% HNO$_3$ for 7 hours. Then the suspension was centrifuged for 20 min to collect the precipitate and washed thoroughly with deionised water and methanol. The obtained precipitate was oven dried at 105 ^{o}C and ground to a fine powder. The nitric acid treated carbon is labelled as C/HNO$_3$ in this study.

The modified carbon materials were produced and supplied by G.A. Rimbu from the National Research Institute for Electrical Engineering (INCDIE ICPE-CA) in Bucharest, Romania.

For the preparation of the modified anodes, Ketjen Black EC 300J was used as the basis material. Thus the influence of Ketjen Black as anode material on bacterial electron transfer was also studied. Carbon cloth was coated with 1 mg cm^{-2} carbon black by spraying an ultrasonically mixed ink containing the carbon black, isopropanol, and polyvinyl alcohol as binder.

For all anodes, carbon cloth was used as a support material, thus experiments were also carried out with carbon cloth as the anode material.

The reactors consisted of the anode, a carbon black air cathode (1 mg cm^{-2}) and used a microporous battery separator (Rhinohide from Entek International) as membrane. Domestic

wastewater with 0.5% brewery wastewater was used as fuel source. The addition of brewery wastewater increased the organic substrate (COD) in the wastewater. Brewery wastewater has a high carbohydrate content and, as it is a food processing wastewater, has a low concentration of inhibitory substances, such as ammonia, which makes is especially suitable for electricity generation (Pant et al., 2010; Wen et al., 2009; Feng et al., 2008; Wang et al., 2008b). The detailed characteristics of the feed are provided in **Table 4.1**.

Table 4.1: Physiochemical characteristics of the substrate (domestic wastewater with 0.5% brewery wastewater) used throughout the present study.

Parameter	500Ω	1000Ω	5000 Ω	OCP
sCOD /mg l^{-1}	816	756	688	912
SS / mg l^{-1}	378.8	461.9	197.8	235.4
VSS / %SS	33.5	28.9	53.9	32.7
Sulphate / ppm	86.58	50.70	115.11	202.53
Chloride /ppm	141.77	173.38	129.93	719.52
Phosphate /ppm	14.28	7.09	Not detected	8.55
Fluoride /ppm	5.52	21.99	6.17	13.53
Conductivity / mS cm^{-1} at RT	1.295	1.483	1.347	1.304

The reactors were operated continuously for 20 to 30 days for each experiment in fed batch mode. During the start up period the reactors were refilled with new substrate whenever the decrease in cell potential suggested that the substrate was digested. Once voltage production stabilised COD measurements were taken daily over one batch and the MFC reactors refilled at OCP and polarised.

4.3.4 Results and discussion

4.3.4.1 Power performance

4.3.4.1.1 Variations in voltage evolution

The variation in voltage over time is used as an indicator for the acclimatisation of the microbial consortia forming the biofilm. Figure 4.2 shows the evolution of cell potential under 500 Ω; 1 kΩ, 5 kΩ and OCP. Depending on the external resistance used the period to acclimatise the reactors to the outside conditions varied slightly. Under OCP acclimatisation was fast, as similar potentials were achieved for the different materials from the second batch. Under 1 kΩ and 5 kΩ batches started to show similar voltage profiles after the third batch. Acclimatisation took longest under 500 Ω with similar batches being observed from the 4th batch until an increasing shift during the 6th batch in power performance was apparent for C/PANI reactors from the worst performing to the best performing material. A reason for this shift could be an even slower acclimatisation of C/PANI compared to the other materials or otherwise a change in the microbial community which forms the anodic biofilm. This change could not be observed as the microbial community was only studied at the end of the experiment.

In fed-batch mode the increase in cell potential indicated the development of a mature biofilm; as it increased over the first two to four batches, depending on the external load used, and then stabilised.

Figure 10.1 (Appendix) shows the voltage evolution and acclimatisation of the different materials under different external resistance and OCP. Under 500 Ω the voltage stabilised from the 5th batch on. Slighly shorter acclimatisation was observed under 1 kΩ and 5 kΩ with 3 to 4 batches while acclimatisation was nearly instantaneous near OCP as all reactions are at equilibrium and current does not flow. The higher the external resistance the smaller the current demand on the anode leading to rapid culture growth and acclimatisation.
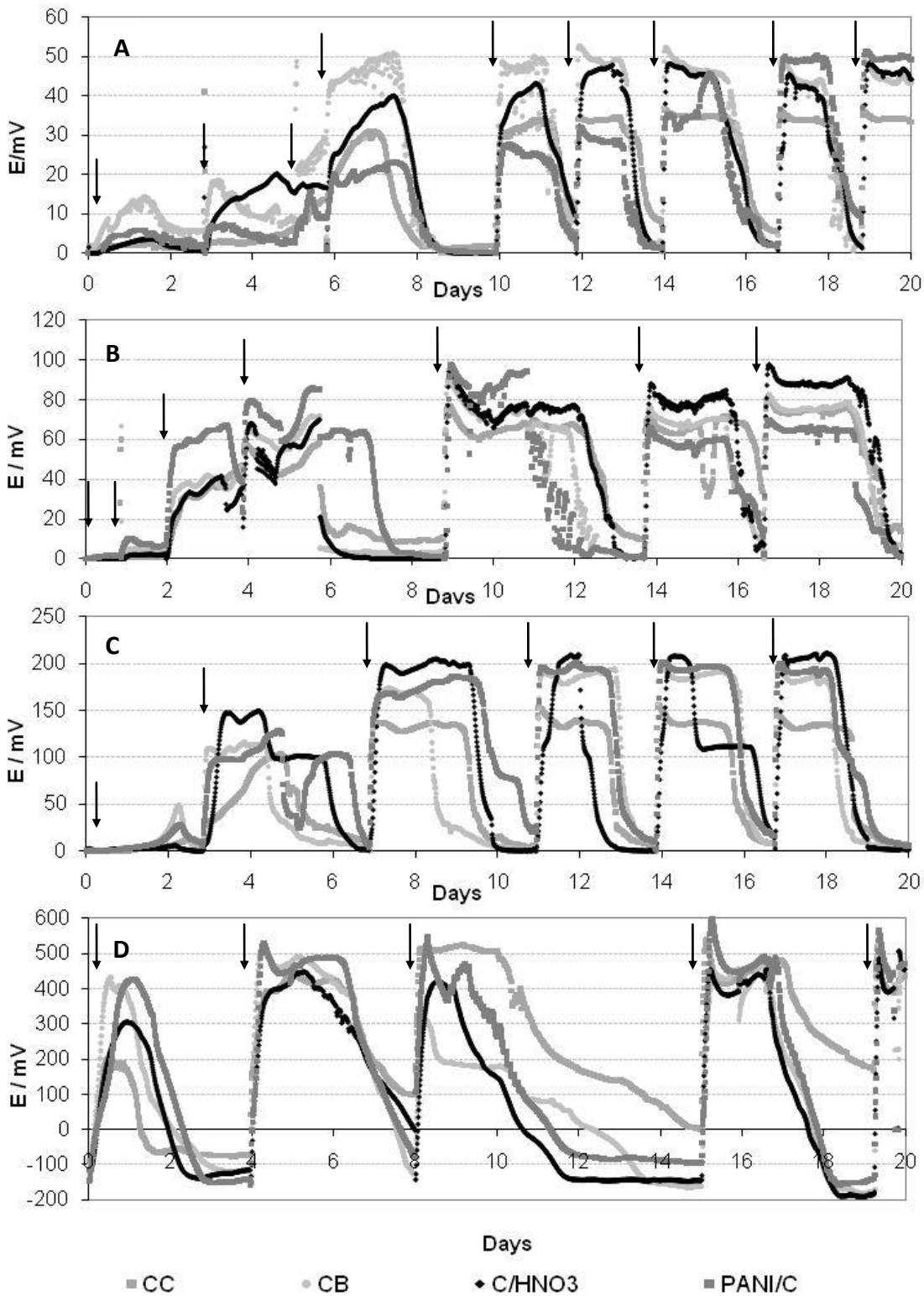
Figure 4.2: Voltage evolution for the different anode materials under 500 Ω (A), 1 kΩ (B), 5 k Ω (C) and OCP (D). Arrows indicate refilling of the reactors.

The internal resistance of the reactors was measured under 1 kΩ and OCP at the end of the experiment (Table 4.2) and a distinct difference between both conditions was observed. The

40

internal resistance for each anode material used was 200-300 Ω lower under 1 kΩ although still high for electricity production. This suggests that more electroactive bacteria grew under load and the biofilm acclimatises.

Table 4.2: Average standard deviation of the internal resistance of the reactors under OCP and 1 kΩ.

	CC / Ω	CB / Ω	C/HNO₃ / Ω	C/PANI / Ω
Under Load (1kΩ)	843±68	693±8	720±100	825±100
OCP	1042±325	1082±175	1166±50	994±180

4.3.4.1.2 Variations in voltage, current and power density under constant load

Figure 4.3 shows the voltage, current and power density reached under OCP and with different external loads. Under OCP the reactors reached on average 475 mV with only very minor variations between the different materials. As all other conditions of operation were the same, the influence of the different materials on the equilibrium potential under these conditions was negligible. Under steady load the potential increased for all materials under an external load from an average potential of 44 mV under 500 Ω to 76 mV under 1 kΩ and 185 mV under 5 kΩ (Figure 4.3).
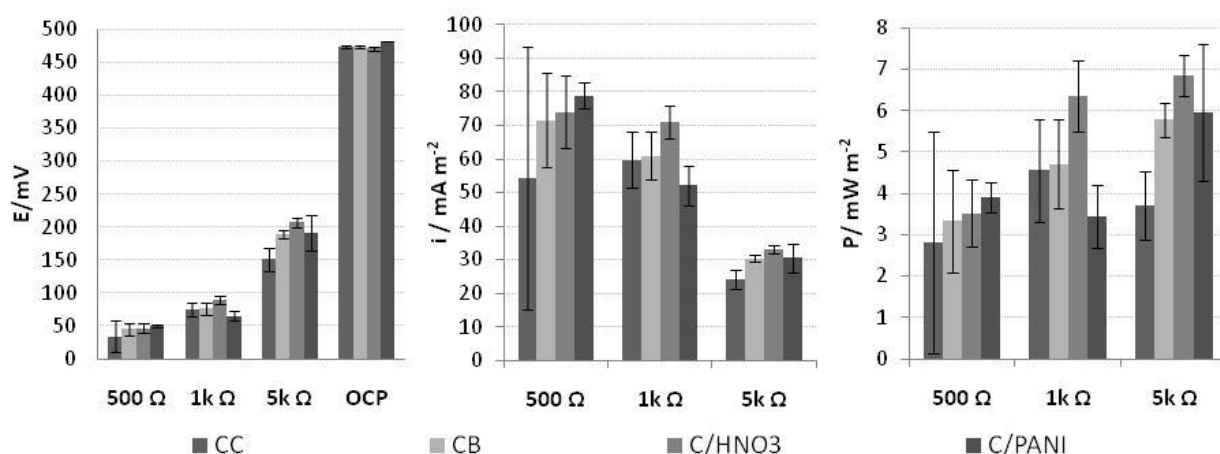
Figure 4.3: Voltage, current and power density for the different anode materials with biofilms formed under OCP and load.

Accordingly the highest current densities for all materials were observed under 500 Ω with on average 70 mA m^{-2} followed by an average of 61 mA m^{-2} under 1 kΩ and 31 mA m^{-2} under 5 kΩ.

The highest power densities were reached under 5 kΩ with on average 6 mW m^{-2} followed by 5 mW m^{-2} under 1 kΩ and 3 mW m^{-2} under 500 Ω.

Statistical analysis (fully nested ANOVA) of the duplicate reactors under OCP and load showed that the variation in potential under OCP and steady load is statistically significant (p=0.000) for the potential whereas the slight variations in the potential between the different materials is not (p=0.224). This indicated that the reactor design, external load and substrate used overpower any effect of the materials used in this study. Current density (p=0.00 for different loads, p=0.477 for materials) and power density (p=0.044 for different loads, p=0.280 for materials) graphs reinforce the conclusion that the external load is the significant factor overwhelming the influence of the materials used.

The statistical analysis of the power densities, current densities and potential showed that higher load correlated to higher power density; with a peak performance at different loads depending on the material used.

Table 4.3 shows the voltage, current and power density achieved with the different materials. These variations were not statistically significant.

Table 4.3: Peak voltage, current density and power density (average of the duplicate reactors) of the different reactors observed over one batch.

	E / mV				i / mA m^{-2}			P / mW m^{-2}		
	500 Ω	1 kΩ	5 kΩ	OCP	500 Ω	1 kΩ	5 kΩ	500 Ω	1 kΩ	5 kΩ
CC	34±24	75±10	151±17	474±2.4	54±39	60±8.2	24±2.8	2.8±2.7	4.6±1.2	3.7±0.8
CB	45±8.7	76±8.9	190±6.5	473±2.2	72±14	61±7.1	30±1.0	3.3±1.2	4.7±1.2	5.8±0.4
C/HNO$_3$	46±6.8	89±6.0	207±7.6	470±3.3	74±11	71±4.8	33±1.2	3.5±0.8	6.3±0.9	6.8±0.5
C/PANI	49±2.4	65±7.2	191±27	482±0.4	79±3.8	52±5.8	31±4.3	3.9±0.4	3.4±0.8	6.0±1.7

The smaller increase in average power density achieved under 1 kΩ and 5 kΩ from 5 mW m^{-2} to 6 mW m^{-2} (average of all reactors) suggested that in the system used the power performance is limited by reactor architecture and/or the substrate used. This hypothesis is supported by results from a similar study (Scott et al., 2007) which achieved steady state power densities of 20 mW m^{-2} under 10 kΩ for 20 hours using the same modifications to enhance power production. In contrast to this study Scott *et al* (2007) acclimatised their reactors at OCP which

implies that electroactive bacteria are not advantaged during acclimatisation of the biofilm, and steady state power densities, measured under high external load of 10 kΩ and 300 kΩ over 60-80 hours, might not be consistent over longer time. This is supported by Lyon *et al* (2010) who reported that their reactors reached higher power densities for a few days when switched from 10 kΩ external resistance to 470 Ω. In contrast to high power densities achieved under lower load recorded by Lyon *et al* (2010) and Scott *et al* (2007) the highest power densities in this study were achieved under higher load which could also be a sign for an inhibition on the system through the design and/or substrate.

Observed variability between duplicate was high, as errors bars in Table 4.3 and Figure 4.3 show, especially for reactors using carbon cloth as anode materials. The reactors using carbon black and modified carbon black as anode material also show variations in steady state power performance. This supports the 'intrinsic lack of reproducibility' observed by Larrosa *et al* (2009) in two chamber experiments, using mixed cultures and wastewater as substrate.

4.3.4.1.3 Anode activity

Since the electrochemical activity of carbon is influenced by the surface chemistry (Wang et al., 2008a; Silva et al., 1999) a difference between the carbon black, C/PANI and C/HNO$_3$ in power performance and therefore onset potential and activity was expected.
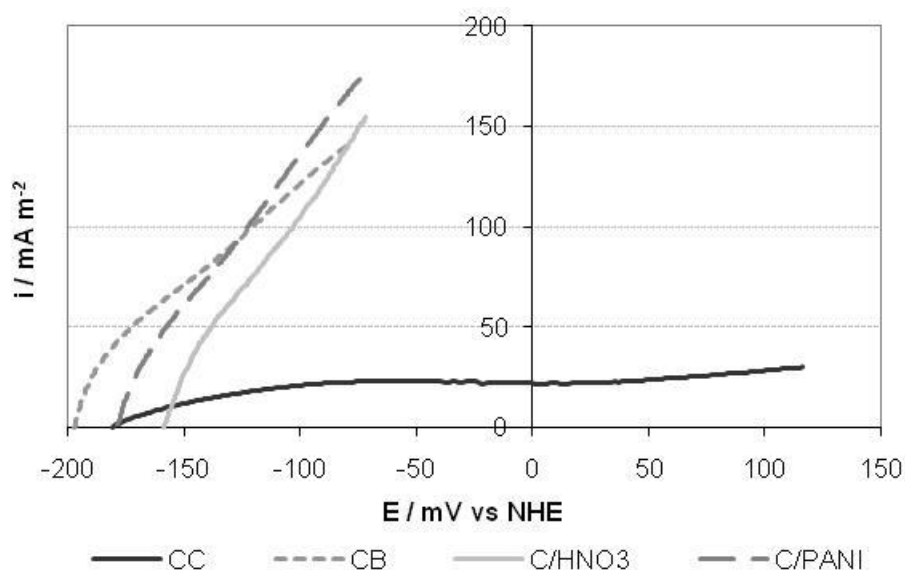
Figure 4.4: Linear sweep voltammograms of carbon cloth (black), carbon black (grey) showing the anode behaviour at a scan rate of 1 mV s^{-1}.

Figure 4.4 shows the linear sweep voltammograms of the different anode materials. The onset potential varied between the different materials with C/HNO_3 showing the lowest onset potential at 158 mV, followed in ascending order by carbon black, carbon cloth and C/PANI with an onset potential of 178 mV, 180 mV and 197 mV respectively (Table 4.4, Figure 4.4). The linear sweep of carbon cloth showed an initial linear increase in current density from a potential of 180 mV seemingly reaching a limiting current density of 30 mA m^{-2}. The linear sweep of the other three materials increased rapidly after an initial gentle curve to current densities of 168 mA m^{-2}, 147 mA m^{-2} and 137 mA m^{-2} for C/PANI, C/HNO_3 and carbon black respectively. Table 4.4 shows that C/PANI achieved on average the highest peak power density of 18±0.4 mW m^{-2} followed by carbon black and C/HNO_3 with peak power densities of 15.6±1.3 mW m^{-2} and 15.7±0.3 mW m^{-2} respectively. Carbon cloth achieved one third of the peak power density of C/PANI with 5.6±0.4 mW m^{-2}.

Table 4.4: Average peak power density, anode charge transfer resistivity and onset potential of the anode for the four different anode materials.

	Peak power density / mW m^{-2}	Anode charge transfer resistivity / Ω cm^2	Onset potential / mV
CC	5.6±0.4	11.3±1.3	-182±1
CB	15.6±1.3	2.38±0.4	-180±17
C/HNO$_3$	15.7±0.3	1.02±0.3	-158±1
C/PANI	18.0±0.4	1.2±0.1	-186±8

The charge transfer resistivity is a measure of the relative activity of the anodes (Scott et al., 2008) and was calculated at the lower potential range of 10-100 mV. The highest charge transfer resistivity was calculated for carbon cloth with 11.3±1.3 Ω cm^2. Carbon black, C/HNO_3 and C/PANI revealed one fifth the charge transfer resistivity of carbon cloth with 2.38±0.4 Ω cm^2, 1.02±0.3 Ω cm^2 and 1.2±0.1 Ω cm^2 respectively. Thus these materials were much more conductive than carbon cloth.

The anode charge resistivity showed that although reaching higher power densities the charge transfer resistivity was slightly higher for C/PANI than for C/HNO_3. Thus C/HNO_3 showed the

greatest electrochemical activity as anode material although C/PANI, due to the higher onset potential, reached higher peak power densities. Carbon cloth showed poor electrochemical activity together with the biofilm which was mainly due to the large overpotential (Table 4.4).

Compared with Scott *et al.* (2008) study of anode activity in marine fuel cells the anode activity of carbon black and both modified materials was similar to carbon sponge with a charge resistivity of 1.0 Ω cm^2. Other studies investigated the charge transfer resistance using impedance spectroscopy. Use of impedance spectroscopy can be problematic in systems using complex feed substrates, such as wastewater, as the substrate can produce interference during the measurement. He *et al.* (2006) He *et al.* (2006) studied the charge transfer resistance of activated carbon granules with much higher resistances of 7.05 Ω than resistances observed in this study. Higher charge transfer resistances were also seen for materials such as the graphite fibre brush with 28.62 Ω (Zhang et al., 2008) and over 1000 Ω for graphite felt (Ha et al., 2010).

4.3.4.1.4 Polarisation studies

The peak voltage, current density data achieved with carbon cloth, carbon black, C/HNO$_3$ and C/PANI during polarisation is shown in Figure 4.5. The current range was varied with carbon black and the two modified anode materials reaching current densities between 140 mA m^{-2} and 170 mA m^{-2} whereas carbon cloth reached current densities of only 28 mA m^{-2}. Interestingly the current/voltage plots for all MFC reactors ended in the resistance region with no visible mass transport limitations. This suggests that the reaction kinetics of microbial fuel cells were very slow so that mass transport limitations were not reached during polarisation.

The power density plots (Figure 4.5) showed that the worst performing material was carbon cloth reaching 6 mW m^{-2} at 20.3 mA m^{-2} current density and a potential of 145 mV whereas the deposition of carbon black, C/HNO$_3$ and C/PANI on carbon cloth tripled the amount of power generated to 16.8 mW m^{-2} (at 57.6 mA m^{-2}and 279.5 mV), 16.3 mW m^{-2} (at 63.3 mA m^{-2} and 257.5 mV) and 18.4 mW m^{-2} (at 67.4 mA m^{-2} and 272.9 mV) respectively. Surprisingly plain carbon black as well as both modified carbon blacks, C/HNO$_3$ and C/PANI achieved peak power densities in the same region as C/PANI.
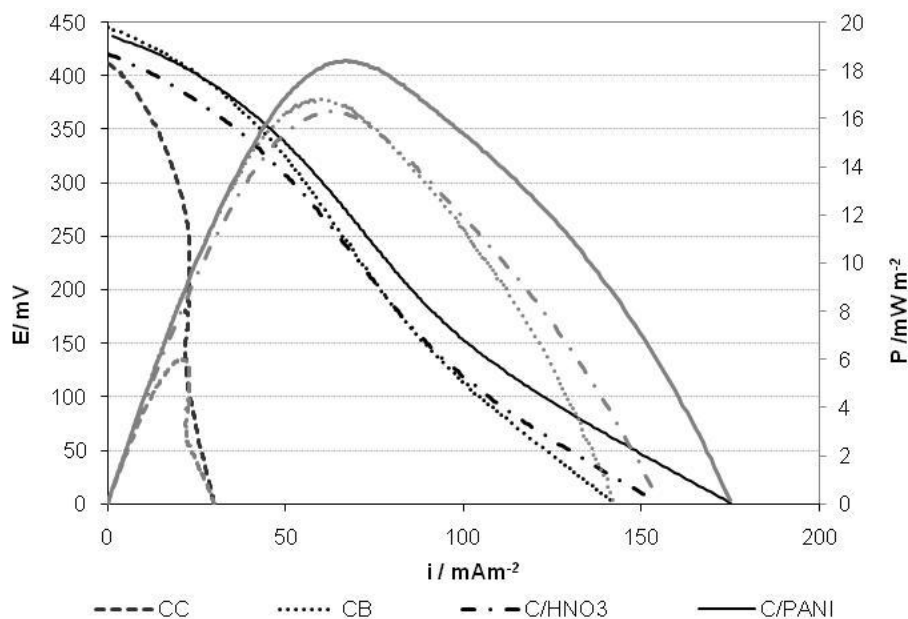
Figure 4.5: Linear sweep voltammograms for the cell potential (black) and power density (grey) during polarisation of the different anode materials at a scan rate of 1 mV s^{-1}.

The power density plots of the different materials were iR corrected to show the possible power densities reactors could reach without internal resistance limitations (Figure 4.6). Carbon black, C/HNO$_3$ and C/PANI doubled their power density under these circumstances to 30 mW m^{-2}, 40 mW m^{-2} and 42 mW m^{-2} respectively whereas only a minor increase in power density was estimated for carbon cloth with 6.6 mW m^{-2}. C/PANI showed the greatest possible capabilities for higher power production followed by C/HNO$_3$ and carbon black.
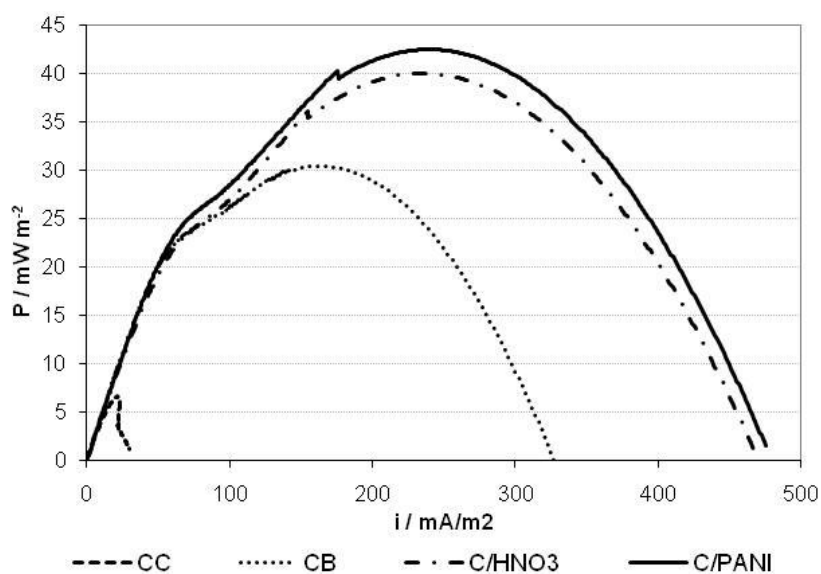
Figure 4.6: iR corrected power density plots of the different anode materials during polarisation at a scan rate of 1 mV s^{-1} showing the possible power densities achievable.

46

C/PANI gave the greatest power density with 18.4 mW m^{-2} of the four materials. These results were slightly lower (10 mW m^{-2} lower) than power performances reported by (Scott et al., 2007) of 28.44 mW m^{-2} and 26.5 mW m^{-2} for C/HNO$_3$ and C/PANI in a similar system using similar materials and substrates in a different design. Other studies which used similar modification in very different systems achieved very high power densities (more than 1000 mW m^{-2} in each case) with anodes quinone and quinoide modifications (Feng et al., 2010a; Qiao et al., 2008) which confirmed the great potential of quinone and quinoide modified anodes in MFC systems.

Plots of the anode and cathode behaviour (Figure 4.7) during polarisation indicated limitations in the system. iR correcting the cathode potential showed the cell performance to be resistance limited, which could also be seen in the linear sweep voltammograms of the cell potential. The anode and cathode behaviour during polarisation showed that in reactors using carbon black and the modified anode materials, the cathode limited power production. Figure 4.7 A showed that there was a loss of 300 mV or more potential on the cathode over the polarisation while the anode potential loss ranges around 100 mV. The MFCs using unmodified carbon cloth as anode are anode limited as the potential loss is higher on the anode than on the cathode (Figure 4.7).
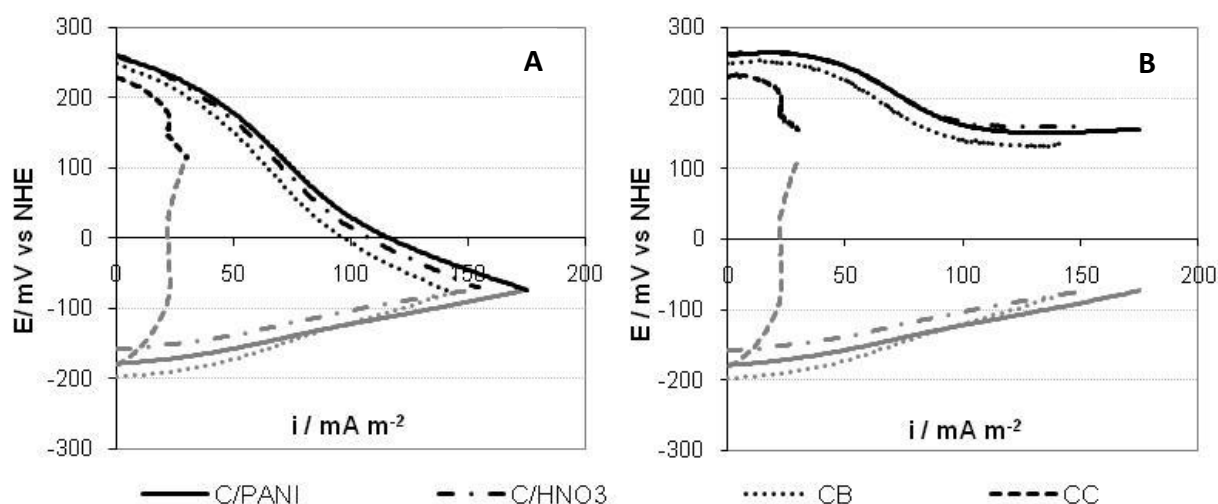
Figure 4.7: Linear sweep voltammograms of the anode (grey) and cathode (black) measured (A) and iR corrected (B) during polarisation at a scan rate of 1 mV s^{-1}.

The cathode potential was obtained by iR correcting the cell voltage and adding the measured anode potential (Figure 4.7 B). With the exception of carbon cloth, the iR corrected graph showed an overpotential loss of 100 mV at both anode and cathode for reactors using carbon black, C/HNO_3 and C/PANI suggesting that the internal resistance (mostly through the electrolyte resistance and electrode distance) is the greatest limitation in the reactors using carbon black, C/HNO_3 and C/PANI as anode materials.

4.3.4.2 Wastewater treatment and coulombic efficiencies

The COD removal was measured daily during different batches under the different loads. The duration of a batch increased with an increase in external load with values of 2 days, 2-3 days, 3-4 days and 6-7 days per batch for 500 Ω, 1 kΩ, 5 kΩ and OCP respectively. As the shortest batches took just 2 days the COD removal was studied at the second day of a batch and results are given in Table 4.5.

Table 4.5: Percentage COD removal two days into the batch as an average of the duplicate reactors.

	COD removed / %				
	CC	**CB**	**C/HNO$_3$**	**C/PANI**	**Control**
OCP	65±8	79±4	73±8	68±4	70±1
5k Ω	80±3	80±8	82±5	79±11	n/a
1k Ω	82±11	86±8	83±1	87±1	n/a
500 Ω	86±7	87±6	85±0	89±1	n/a

The lowest COD removal was achieved under OCP with 79±4%, 73±8%, 70±1%, 68±4% and 65±8% COD removed for carbon black, C/HNO_3, the control reactor, C/PANI and carbon cloth respectively. An increase in COD removed was observed for all materials with smaller external load. C/HNO_3 reached a COD removal of 82±5% under 5 kΩ, 83±1% under 1 kΩ and 85±0% under 500 Ω. Carbon cloth achieved 80±3% under 5 kΩ, 82±11% under 1 kΩ and 86±7% under 500 Ω. Slightly higher COD removal was observed for carbon black with 80±8% under 5 kΩ, 86±8% under 1k Ω and 87±6% under 500 Ω and C/PANI with 79±11% under 5 kΩ, 87±1% under 1k Ω and 89±1% under 500 Ω.

As expected the COD removal rate increased when a smaller external resistance was used. The lower external resistance on the system increased the current demand on the anode forcing the microorganisms to transfer more electrons to the anode and therefore metabolise the substrate faster which was apparent in an increasing percentage of COD removed after two days under 5 kΩ, 1k Ω and 500 Ω (Table 4.5). The lowest COD removal took place under OCP and varied between 64% and 78%. The control reactor, which degraded the substrates under anaerobic conditions, showed modest performance of 70% removal comparable to the MFC reactors under OCP. Reactors under steady state conditions demonstrate that a lower external resistance made the anode more advantageous as terminal electron acceptor so that microorganisms transfer more electrons to the anode under low external resistance and metabolise the substrate at a faster rate.

Table 4.6: Coulombic efficiencies two days into the batch as an average of the duplicate reactors.

	CE / %			
	CC	**CB**	**C/HNO$_3$**	**C/PANI**
500Ω	7.6±5.2	7.4±2.0	8.8±3.5	9.7±0.1
1kΩ	4.1±0.9	3.8±0.7	4.6±0.2	3.3±0.1
5kΩ	2.3±0.2	2.3±0.1	2.7±0.3	2.6±0.1

Table 4.6 shows the coulombic efficiencies achieved under load for the different materials. The highest coulombic efficiencies, like the highest COD removals, were achieved with the greatest current density (under 500 Ω external load) with 9.7±0.1% CE for C/PANI, 8.8±3.5% for C/HNO$_3$, 7.6±5.2% for carbon cloth and 7.4±2.0% for carbon black. Under 1 kΩ and 5 kΩ loads coulombic efficiencies were on average 4% and 2.5%. The reactors were very inefficient with respect to energy generation under these conditions and most of the substrate was digested using other processes.

Statistical analysis of COD and CE for the different materials under load showed that the only statistically significant influence on the COD removal and CE was the external load applied ($p < 0.001$ for COD removal and CE). The use of different materials did not statistically influence COD removal and CE. A probable explanation for the negligible influence of the materials is their similarity to each other and possibly the effect of bacteria suspended in the solution.

Figure 4.8 shows that high COD removal and high current densities correlate to high coulombic efficiencies. The more active role of the electroactive biofilm suggested by higher coulombic efficiencies could be responsible for higher COD removal efficiencies under lower load. But with coulombic efficiencies of 2% to 9.7%, most of the substrates were degraded using other processes thus making the reactors very inefficient at energy generation.
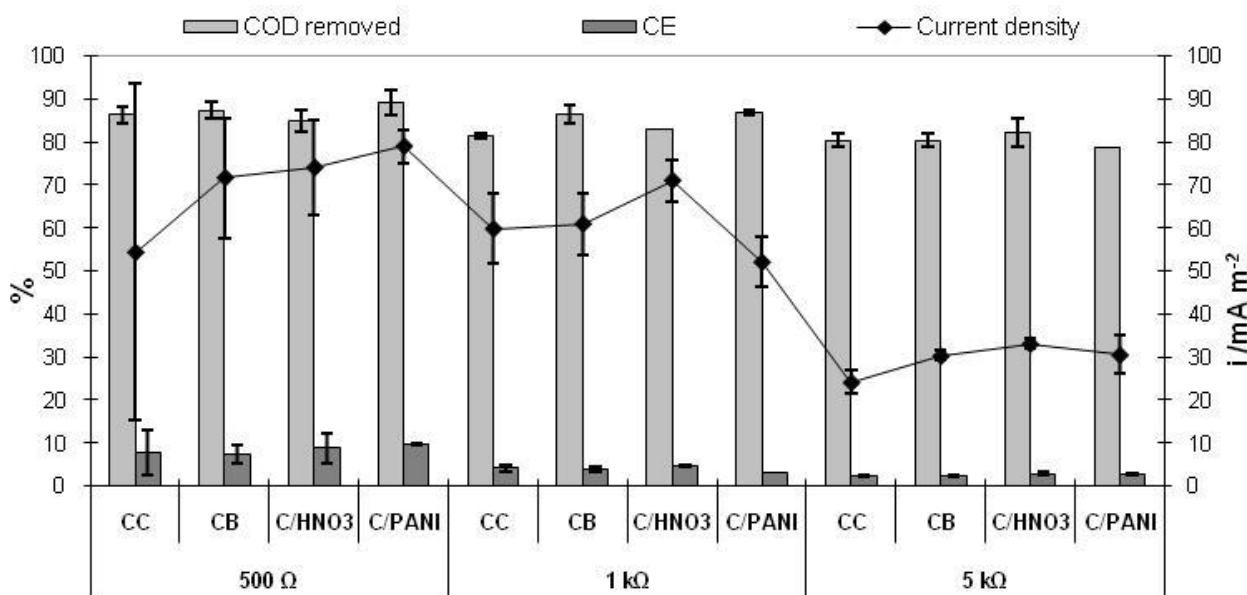
Figure 4.8: Percentage COD removal, coulombic efficiency and current density of the different anode materials under load.

Feng *et al.* (2008) reported coulombic efficiencies of 10% at 30°C under 1 kΩ external load using brewery wastewater as substrate in a reactor with a carbon cloth as anode and a platinum cathode. Even higher coulombic efficiencies of 31% when the brewery wastewater was diluted with phosphate buffer (Wang et al., 2008b). Similar coulombic efficiencies to this study were reported with 7.61% CE when continuous flow reactors were used (Wen et al., 2010). Wen *et al.* (2010) also reported that addition of phosphate buffer increased the coulombic efficiency of the continuous flow reactors due a lower internal resistance of the reactor and a higher conductivity of the substrate.

The reported lower power performances and coulombic efficiencies using brewery wastewater compared with domestic wastewater were presumably due to the fermentable substrates in the brewery wastewater being more easily degraded by fermentation than for electricity

production (Feng et al., 2008). Similarly Min and Logan (2004) reported lower coloumbic efficiencies for fermentable than for non-fermentable substrates.

4.3.4.3 Microbial community analysis

The anodic biofilm developed at the anode was collected at the end of each experiment for community analysis by DGGE of the hyper variable V3 region of the 16S rRNA gene. Analysis of the DGGE fingerprint using the Dice coefficient revealed that distinct consortia were supported at each anode.

Cluster analysis (dendogram) revealed that similarity indices were higher for consortia acclimatised at lower external load and although the number of bands varied slightly between the different anode materials used the external load and the MFC system are the obvious influences on the anodic consortia (Figure 4.9). Und OCP and 5 kΩ the anodic consortia also cluster by material but this is not visible any more under 500 Ω and 1 kΩ.

Consortia similarities for anodic communities acclimatised under different external loads ranged from 75% at 500 Ω, 69% at OCP, 68% at 5 kΩ and 64% at 1 kΩ (Figure 4.9). Communities under lower external loads showed higher similarities to each other (52% between 500 Ω and 1 kΩ) than to communities acclimatised under higher loads (59% between 5 kΩ and OCP) with 49% similarity between lower and higher load. The feed substrate for 1 kΩ and OCP was 64% and 77% similar to the acclimatised anodic community under OCP showing very similar starting condition. Overall similarties between substrate/inocula and anodic biofilm were decreasing from 77% under OCP, 56% under 5 kΩ, 49% under 1 kΩ and 34% under 500 Ω.
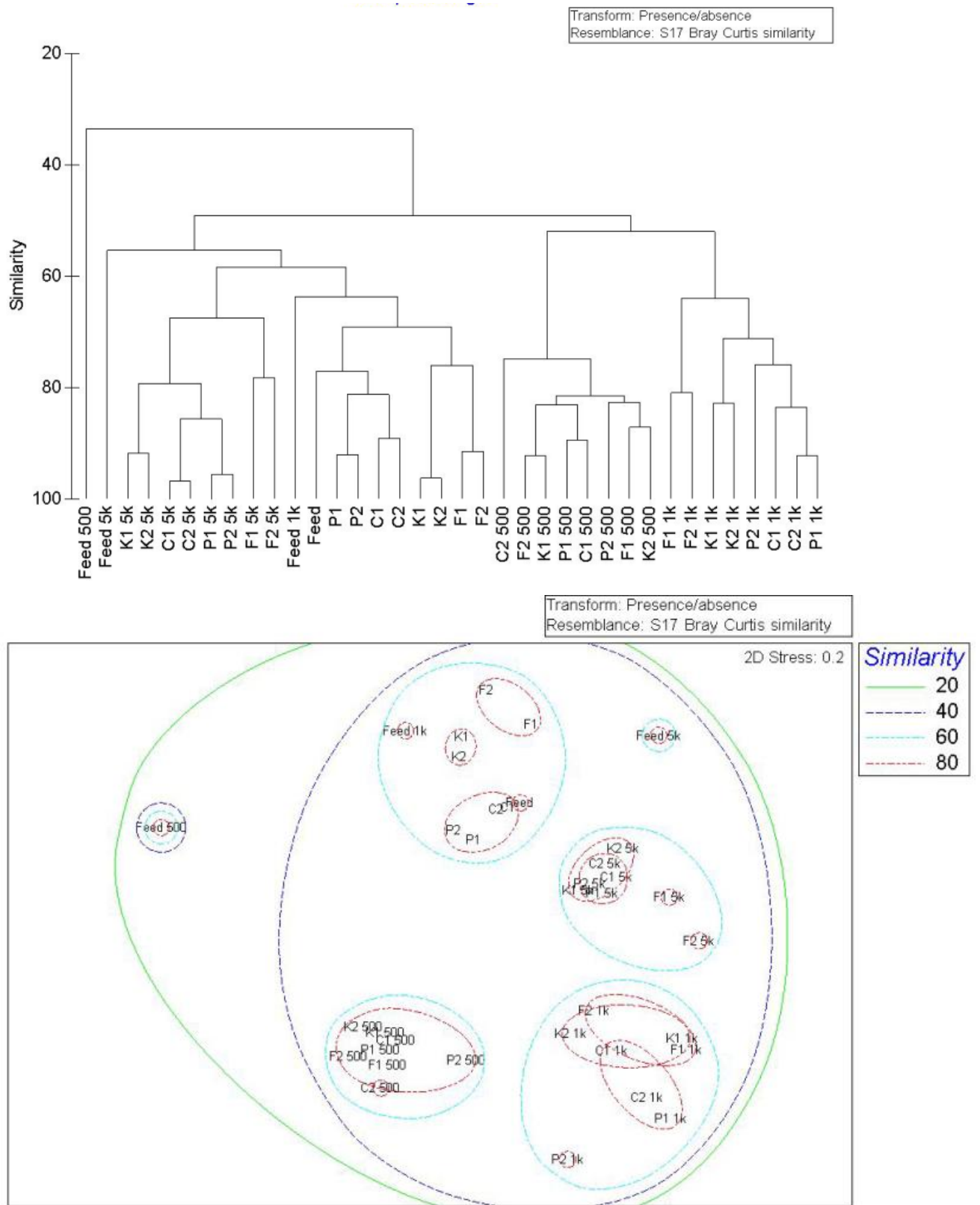
Figure 4.9: Dendrogram and ordination of the communities based on species presence and absence was derived from MDS analysis of Bray–Curtis similarities (stress = 0.2). Samples were named CC: F; CB: K; C/HNO₃: C; C/PANI: P with the duplicate number and external load added to the name and no addition for OCP.

The results of the microbial community analysis were difficult to interpret mainly because the low coulombic efficiencies showed that energy generation was not the predominant degradation process which made a primarily electroactive biofilm questionable. The clear influence of the external load and less evident influence of the anode materials on the selection of the microbial consortia implied that either at least a part of the community is electroactive and therefore advantaged by the MFC system or a number of microorganisms is able to use a range of terminal electron acceptors with the preferably the anode in a MFC environment. This would suggest that a range of microorganisms gain a higher energy yield by using the anode as terminal electron acceptor than other anaerobic processes. Logan and Regan (2006) came to a similar conclusion in their review about microbial communities in MFCs. This would explain why diversity seems to be a vital ingredient for high power production (Logan, 2009) and makes understanding the processes and interactions underlying mixed biofilm consortia essential for further system improvements.

4.3.5 Conclusion

Power, wastewater treatment and microbiological analysis all emphasise the significant influence of the external load on the MFC system. The different materials used only showed a minor influence which is not statistically significant during steady state operation of the reactors, but fairly obvious during polarisation of the cells and the anode activity. Thus the materials show potential for higher power production, but to achieve this, the system, i.e. reactor design and external load, has to be improved through better understanding of the underlying microbial processes and interaction of microorganisms with each other, the anode surface and the feed substrate (i.e. wastewater).

The external resistance had a statistically significant influence on power performance, wastewater treatment efficiency and the microbial community. These results concur with Lyon *et al.* (2010) showing that the external resistance is a major influence on the MFC system irrespectively of reactor design.

The low CE of 3-9% at different external loads makes it obvious that electricity production was not the predominant process digesting substrate in the system. This makes it difficult to draw conclusions on the effect of materials, reactor design and substrate on the system. And any direct influence of the materials on the microbial biofilm and therefore power performance could be hidden beneath other processes taking place.

4.4   ACTIVATED CARBON CLOTH AS ANODE MATERIAL

4.4.1   Introduction

Activated carbons are highly porous materials produced by chemical or physical activation processes from a carbon-rich material, which can be manufactured as fine powders, granules, or in the form of cloth, felt or a consolidate membrane (Setton et al., 2002; Rouquerol et al., 1999). Due to the high specific surface area and porosity activated carbon shows strong adsorption behaviour and is widely used as an all-purpose adsorbent (Rouquerol et al., 1999). In wastewater treatment activated carbon as a powder or granulated is added to physical or biological treatment steps. Carbon adsorption is principally used for the removal of refractory organic compounds and residual amounts of inorganic compounds such as nitrogen, sulphides and heavy metals (Metcalf & Eddy. et al., 2003) in the wastewater. However studies have been undertaken on the effect of added activated carbon on COD removal (El-Naas et al., 2010; Mohan et al., 2008; Hami et al., 2007).
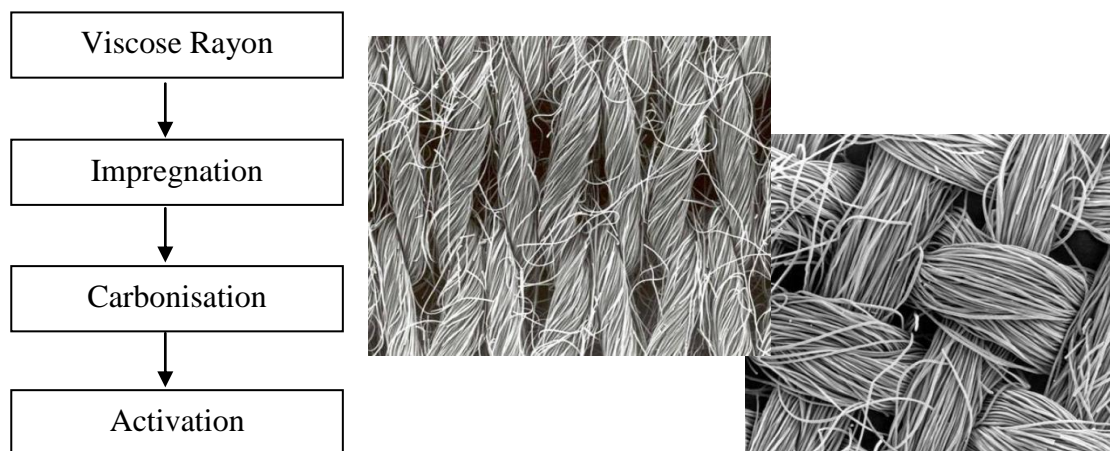
Figure 4.10: Manufacturing process of Zorflex® activated carbon cloth and SEM pictures with a magnification of 500 of the knitted and woven fabric.

Activated carbon cloth (CAC) also known as 'charcoal cloth' was developed by Bailey and Maggs in 1972 (Rouquerol et al., 1999). The process used viscose rayon cloth as precursor to produce flexible knitted and woven cloth. Activated carbon cloth is widely used for protection against noxious gases, odour removal, water filtration and medical dressing. The properties of activated carbon cloth can be specified by changing the impregnation or activation process (Rouquerol et al., 1999).

In MFCs activated carbon cloth appears to be an ideal anode material as it has a high specific surface area which gives the microbial consortia a large surface to adhere to, is conductive and hydrophilic. While the specific surface area of carbon black in powder form is comparable to the specific surface area of activated carbon cloth ($800\ m^2\ g^{-1}$, E-Tek, UK), carbon black has to be deposited onto a support, such as carbon cloth, which will block part of the pores and the hydrophobic character of carbon black makes wetting into the smallest pores impossible.

Zorflex® is a flexible activated carbon cloth (produced by Chemviron Carbon) which is hydrophilic, conductive and antimicrobial with a high specific surface area (BET surface area measured for activated carbon cloth: $800\text{-}1200\ m^2\ g^{-1}$, Chemviron Carbon Cloth Division, UK), which is predominantly microporous. Zorflex® is used in wastewater treatment, air cleaning, and as antibacterial material in wound dressing. The cloth is electrically conductive, shows high adsorption properties for chemical compounds and bacteria. The Zorflex® materials used as anode materials were

Table 4.7: Characteristics of the activated carbon cloth used as provided by Chemviron Carbon Cloth Division, UK.

	FM30k H	FM30k	FM70
Weave	double jersey/knitted	double jersey/knitted	Compound/ woven
Surface density / g m^{-2}	110	110	160
Thickness / mm	0.4	0.4	0.6
Tensile strength, Warp / N	6	6	15
Conductivity	highly conductive	conductive	conductive
BET surface area / m^2 g^{-1}	800-1200	800-1200	800-1200

4.4.2 Hypothesis

Hydrophilic activated carbon cloth can produce high power and wastewater treatment efficiencies due to its large surface area, conductivity and durability during long-term use in MFC systems.

4.4.3 Experimental

Six MFC reactors with the three activated carbon cloth materials as anode were operated under 1 kΩ external resistance. Three "dummy" reactors (each activated carbon cloth in feed substrate) and a control reactor (feed under anaerobic conditions) were operated as controls. After initial acclimatisation of the reactors COD samples were taken over one batch after 40 days and the reactors were polarised (1st sampling/40 days). After a three week break the procedure was repeated after another 35 days (2nd sampling/75 days) to gain knowledge of the durability of the anode materials and deterioration over time (80 days). Domestic wastewater was used as fuel source and the detailed characteristics of the feed substrate before sampling are provided in **Table 4.8**.

Table 4.8: Physiochemical characteristics of substrate (domestic wastewater) used in the present study.

Parameter	1st sampling	2nd sampling
pH	7.36	7.9
COD /mg l^{-1}	256	272
SS / mg l^{-1}	177.8	193.3
VSS / %SS	31.3	37.9
Sulphate / ppm	93.58	117.27
Chloride /ppm	181.31	261.98
Phosphate /ppm	Not detected	Not detected
Fluoride /ppm	Not detected	Not detected
Conductivity / mS cm^{-1} at RT	1.578	1.613

At the end of the experiment the anodic biofilm and a biofilm grown on the membrane inside the anode chamber were collected for microbial community analysis. Duplicate reactors were used in the experiment to ensure validity of the experimental observations and all results shown are the average of the two duplicate reactors.

4.4.4 Results and discussion

4.4.4.1 Power performance

4.4.4.1.1 Variations in Voltage Evolution

Figure 4.11 shows the variation in voltage evolution for different activated carbon cloth materials under 1 kΩ external load and OCP. At first the reactors did not seem to acclimatise. For this reason at arrows 1-6 wastewater was taken from the wastewater treatment plant, which was thereafter stored at 4 °C to arrest biological and chemical characteristics and used for the following batches. At the pointed arrow (NaAc) the reactors were fed with acetate, for one batch only, to investigate if the slight changes in the wastewater, happening even at 4°C, were inhibiting acclimatisation or the anode materials. At the dashed arrow the reactors were restarted after a three week break during which they were kept in the fridge at 4 °C. Polarisations were done at OCP.
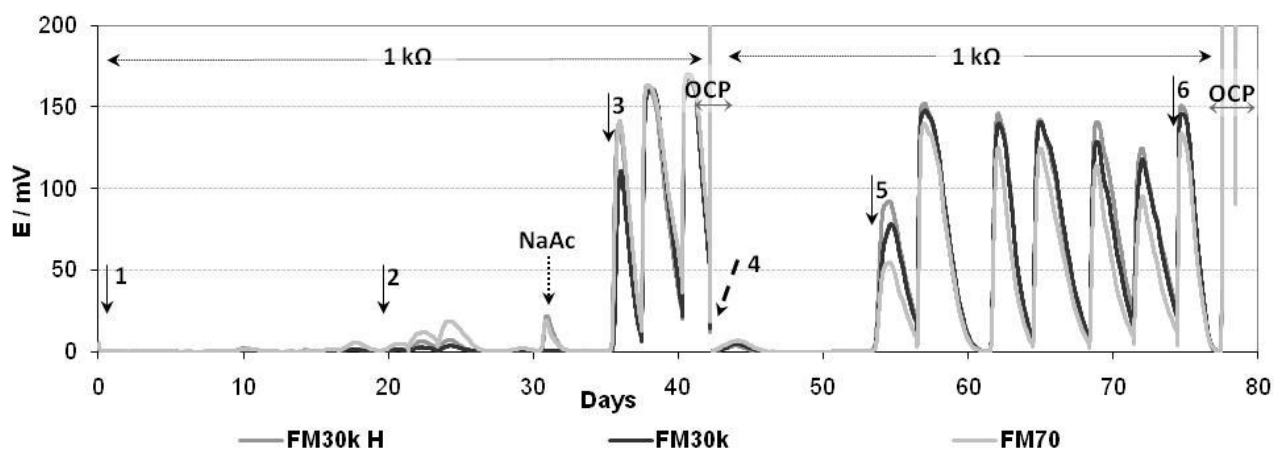
Figure 4.11: Average variation in cell voltage of the duplicate reactors using activated carbon cloths as anodes under 1k load.

Under external load the first 20 days very small amounts (0 to 6 mV) of voltage were produced by all reactors and voltage production was perceptibly influenced by the chemical composition of the wastewater. After 30 days the reactors were refilled once with acetate and as the voltage production improved it was assumed that the electroactive biofilm was inhibited by sulphides gradually accumulating during storage at 4°C.

58

As the activated carbon cloths have antibacterial characteristics the first few batches were expected to produce little or no voltage. Acclimatisation took much longer than expected. This could be on the one hand due to even stronger adsorption behaviour of the carbon cloth, (which was obvious as refilling of the reactors lead to perceptibly cleaner water being pumped out) or on the other hand due to the inhibition of the electroactive community when the feed wastewater changed over time. Once this was established feed substrate was collected more frequently at the wastewater treatment plant. Once the cloth was saturated and the reactors fed with wastewater (arrow 3) voltage production rapidly stabilised (Figure 4.11). Acclimatisation was much quicker after the break, because the biofilm already covered the carbon cloth and new feed substrate (arrow 5 and arrow 6) clearly lead to higher voltage production. The different chemical composition of the feed also noticeably lead to a decrease in voltage production for each batch between 60 and 75 days until new wastewater was used as feed substrate. Before the first sampling little variation between the three materials was visible but all three showed a noticeable decline at the second two sampling points and slight differences in voltage generation are visible at the second sampling.

The internal resistance increased from on average 205 Ω, 225 Ω and 220 Ω at the 1st sampling to 208 Ω, 247 Ω and 246 Ω at the second sampling for FM30kH, FM30k and FM70 respectively showing a loss in power performance during the second sampling under steady state condition (1 kΩ external load) (Table 4.9) compared with the first sampling.

Table 4.9: Internal resistance for the activated clarbon cloth anodes at 1st and 2nd sampling.

	FM30k H / Ω	FM30k / Ω	FM70 / Ω
1st sampling	205±5	225.5±1.5	219±9
2nd sampling	207.5±12.5	247.5±7.5	246±3

4.4.4.1.2 Voltage, current and power density under constant load

Figure 4.12 shows the voltage, current and power densities for the batch starting on the 40th and 75th day under an external load of 1 kΩ. All three CAC materials reached similarly high

power densities up to 22 mW m^{-2} at current densities of 133 mA m^{-2} and a potential around 166 mV for during the first sampling. The steady state power output decreased over time as results from the second sampling show and differences between the materials became visible. Reactors using FM30kH as anode material reached 18 mW m^{-2} (at 119 mA m^{-2} and 149 mV), followed by FM70 reaching 17 mW m^{-2} (at 115 mA m^{-2} and 144 mV). FM30k showed the greatest decline achieving 15 mW m^{-2} (at 109 mA m^{-2} and 136 mV).

The best performing reactors used FM30kH as anode materials reaching power densities of 18±1.5 mW m^{-2} (at 119±4.9 mA m^{-2} and 149±6.2 mV), followed by reactors using FM70 as anode material with 17±0.1 mW m^{-2} (at 115±0.5 mA m^{-2} and 144±0.6 mV). Reactors using FM30k as anode materials showed the worst power performance achieving 15±1.1 mW m^{-2} (at 109±4.2 mA m^{-2} and 136±5.2 mV) (Figure 4.12, Table 4.10).
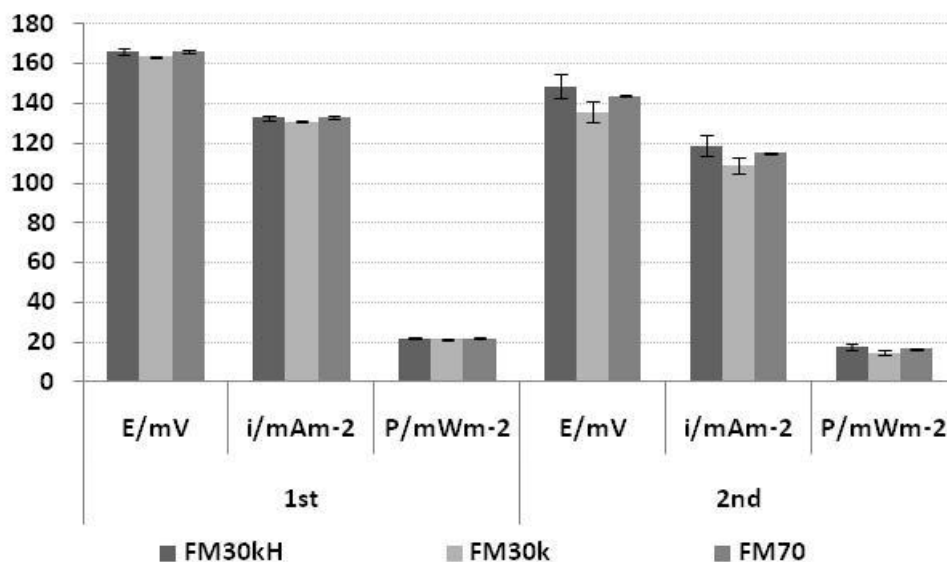
Figure 4.12: Voltage, current and power densities of the different anode materials after 40 (1st) and 75 (2nd) days.

While the differences between the materials are not statistically significant, the decrease in power density, current density and voltage over time is statistically significant (p=0.0). The decline in power performance over time can be partly explained through the increasing internal resistance of the reactors. As the internal resistance increases over time more current is lost per voltage generated.

Table 4.10: Voltage, current and power production for all three materials at 1 kΩ.

		E / mV	i / mA m^{-2}	P / mW m^{-2}
1st	**FM30k H**	166±1.3	133±1.1	22±0.4
	FM30k	164±0.4	131±0.4	21±0.1
	FM70	166±0.8	133±0.7	22±0.2
2nd	**FM30k H**	149±6.2	119±4.9	18±1.5
	FM30k	136±5.2	109±4.2	15±1.1
	FM70	144±0.6	115±0.5	17±0.1

Voltage, current and power densities were two to three times the amount produced by reactors using modified anode materials which could be due the materials used but might also be an influence of the change in wastewater used.

Activated carbon granules have been used frequently (Di Lorenzo et al., 2010; Jiang and Li, 2009; Aelterman et al., 2008; You et al., 2007; He et al., 2006; Rabaey et al., 2005b; Rabaey et al., 2005c) as anode materials in MFCs but their different dimensions make direct comparisons difficult as activated carbon granules have to be used in packed bed type reactors to assure enough contact between granules for high conductivity in the anode material. The difference means that usually a different design is used for MFC reactors using carbon granules as anodes material. Activated carbon cloth has not been used often as anode material in MFCs. Zhao *et al.* (2008) reported the use of CAC for sulphate removal and as CAC has been used in wastewater treatment for exactly this the study showed great removal success. Using a different design, artificial wastewater as substrate, two pure cultures as biocatalysts, Nafion-115 as membrane and platinum at the cathode side Zhao *et al.* achieved peak power densities of 5000 mW m^{-2}. This is a lot higher than the potential output using wastewater as substrate and carbon black but as usual the differences in different studies are so great that direct comparisons are futile.

4.4.4.1.3 Anode activity

Table 4.11 shows the averaged peak power densities, anode charge transfer resistivities and onset potentials after 40 (1st sampling) and 75 days (2nd sampling). The onset potential for the

different carbon cloth materials varied little after 40 days with an average onset potential between duplicates of -203±3 mV for FM30k, -203±2 mV for FM70 and -193±4.5 mV for FM30kH. After 75 days (2nd sampling) the onset potential decreased to -182±9 for FM30k, -161±1 mV for FM70 and -154±25 mV for FM30kH.

The duplicate reactors using activated carbon cloth materials FM30kH, FM30k and FM70 showed very little variation in onset potential, charge transfer resistivity and peak power density during the first sampling (Table 4.11). The activity (onset potential, charge transfer resistivity and peak power density) decreased for all three materials with the high conductivity material FM30kH showing the greatest reduction followed by FM70. The least decline was observed for FM30k. Over the 80 days recorded the activity of the materials was reduced and the materials were visibly degrading in the MFC environment. The FM70 anode fell apart when taken out of the reactors after about 80 days in operation. Within a longer study it would be able to observe if the decline goes on or reaches a limit and stabilises.

Table 4.11: Average of peak power density, charge transfer resistivity and onset potential for the duplicate activated carbon cloth anodes at first (40 days) and second (75 days) sampling.

Sampling		Peak power density /mW m^{-2}	Anode charge transfer resistivity /Ω cm^2	Anode onset potential /mV
1st	**FM30k H**	38±1	0.34±0.005	-193±4.5
	FM30k	37.5±0.5	0.32±0.005	-203±3
	FM70	39.5±0.5	0.30±0.02	-203±2
2nd	**FM30k H**	28.4±3	1.4±1	-154±25
	FM30k	30±2	0.35±0.15	-182±9
	FM70	27.3±2	0.43±0.15	-161±1

Figure 4.13 shows the anode, cathode and cell behaviour during polarisation. The graph shows that the anodes are less limiting than the cathodes with a potential loss of 100 mV for all three anode materials compared to double this with around 200 mV for the cathodes after both 35 and 75 days.
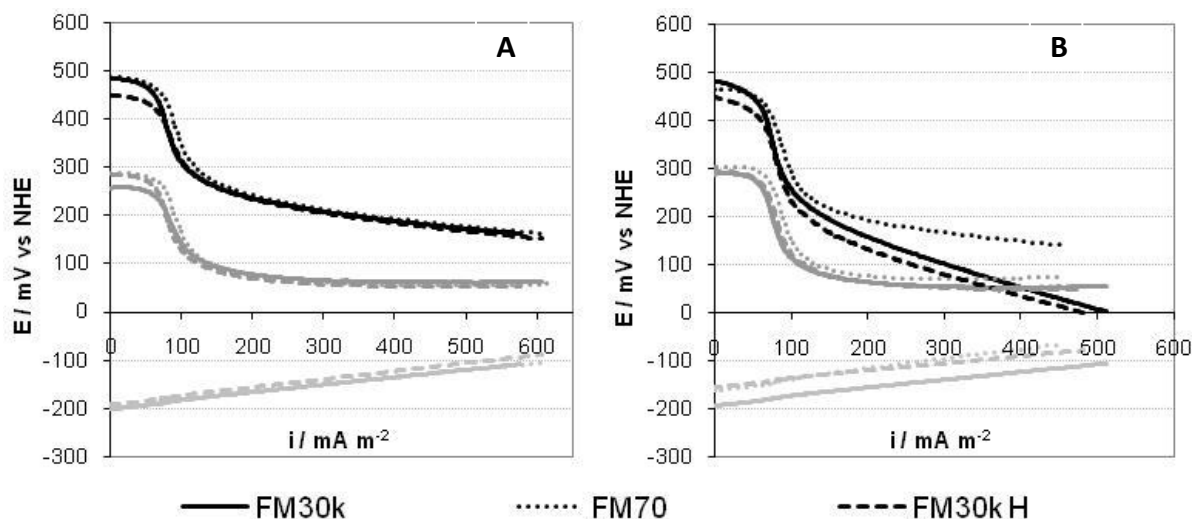
Figure 4.13: Linear sweep voltammograms showing the behaviour of the anode (light grey), iR corrected cathode (grey) and cell potential (black) for the activated carbon cloths during first sampling (A) and second sampling (B) during polarisation at a scan rate of 1 mV s^{-1}.

The cathode potential showed a curious two wave curvature during polarisation. This suggests a change in oxygen reduction mechanisms of the carbon black cathode catalyst. Oxygen reduction mechanisms on most carbon materials tend to follow a 2-electron reduction mechanism to a peroxide reaction product in acidic and alkaline media (Kruusenberg et al., 2009; Vielstich et al., 2003).

$$(In\ acid)O_2 + 2e^- + 2H^+ \rightarrow H_2O_2 \tag{4.14}$$
$$E^0 = 0.67\ V\ vs\ NHE$$

Similar two wave curves to this study were observed for oxygen reduction polarisation curves on carbon in alkaline media (Vielstich et al., 2003; Pirjamali and Kiros, 2002; Appleby and Marie, 1979). When Kruusenberg *et al.* (2009) systematically studied the pH dependence of ORR on carbon nanotube modified glassy carbon electrodes, he reported more distinct two wave profiles at higher pH (pH 12-14) and linked this to an ORR mechanism using quinone groups, which were observed to be more active at lower pH, on the carbon surface as electrocatalyst for the reduction of oxygen to hydrogen peroxide. Similarly the curvature observed in this study could presumably indicate a change in oxygen reduction mechanisms on the carbon black due to the surface structure and surface chemistry of the carbon (Chu et al., 2004).

Similar to the previous study, IR correcting the cathode and cell behaviour showed that the internal resistance through membrane and electrolyte was the greatest limitation to high power densities.

4.4.4.1.4 Polarisation studies

Figure 4.14 shows the peak cell potential and power density for the different activated carbon cloth anodes after 40 and 75 days operation. Polarisation results showed very high peak power densities during the first sampling reaching power densities of 40.3 mW m^{-2} (at 278 mA m^{-2} and 144 mV), 39.2 mW m^{-2} (at 280 mA m^{-2} and 143 mV) and 37.7 mW m^{-2} (at 269 mA m^{-2} and 139 mV) for FM70, FM30kH and FM30k respectively. A slight decrease in cell potential was visible between first and second sampling and peak power densities achieved declined accordingly during the second sampling for FM70 (26.3 mW m^{-2} at 202 mA m^{-2} and 128 mV) and FM30kH (26.3 mW m^{-2} at 205 mA m^{-2} and 126 mV) whereas less reduction/decrease was evident for FM30k achieving 31.9 mW m^{-2} at 238 mA m^{-2} and 134 mV potential. The lower decrease in activity and power production confirmed FM30k as most consistent material out of the three activated carbon cloths.
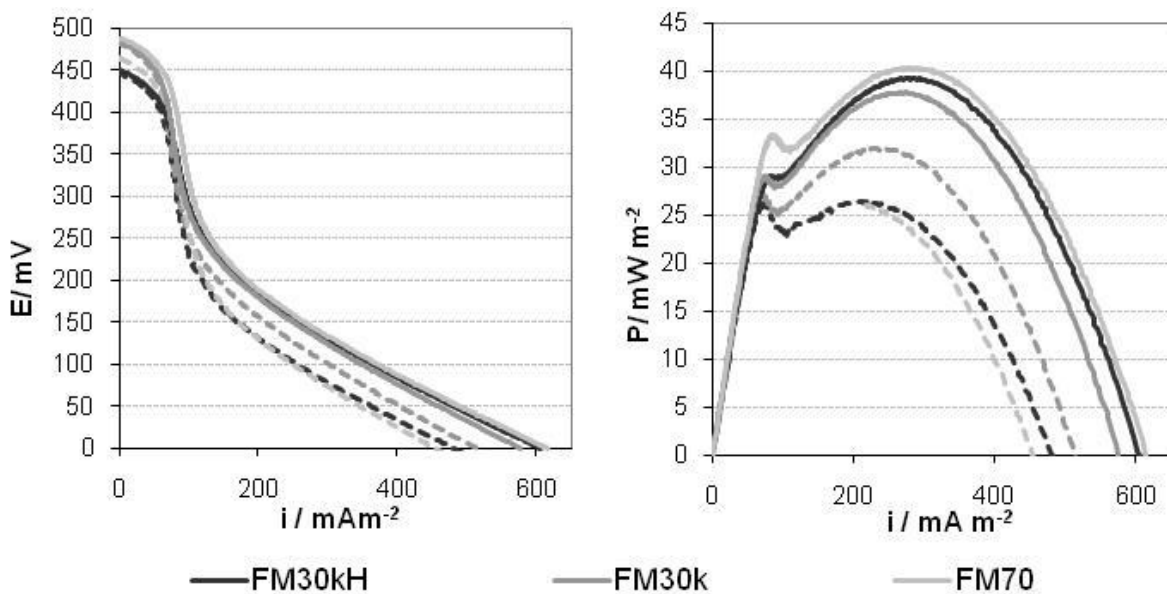
Figure 4.14: Linear sweep voltammograms for the cell potential and power density for FM30k H, FM30k and FM70 at first (full line) and second (dashed line) sampling during polarisation at a scan rate of 1 mV s^{-1}.

The cell potential followed the same curve for all activated materials with a rapid fall due to activation overpotential ending in the ohmic region, which is governed by iR loss. The mass transport region is not visible presumably due to the slow anode kinetics. The cathode potential

affected the cell potential which is visible in a similar two wave profile during polarisation and indicated the cathode to be the more limiting factor in the cell.

4.4.4.2 Wastewater Treatment

4.4.4.2.1 Conductivity and pH

The pH, conductivity and COD of the substrate were measured for MFCs, dummy reactors and the control reactor to help understand reactions taking place between anolyte and biofilm. The pH gives a measure of the protons in the reactor and conductivity indicates all ions in the reactor and how their number changes while microorganisms digest substrate to produce protons and electrons.
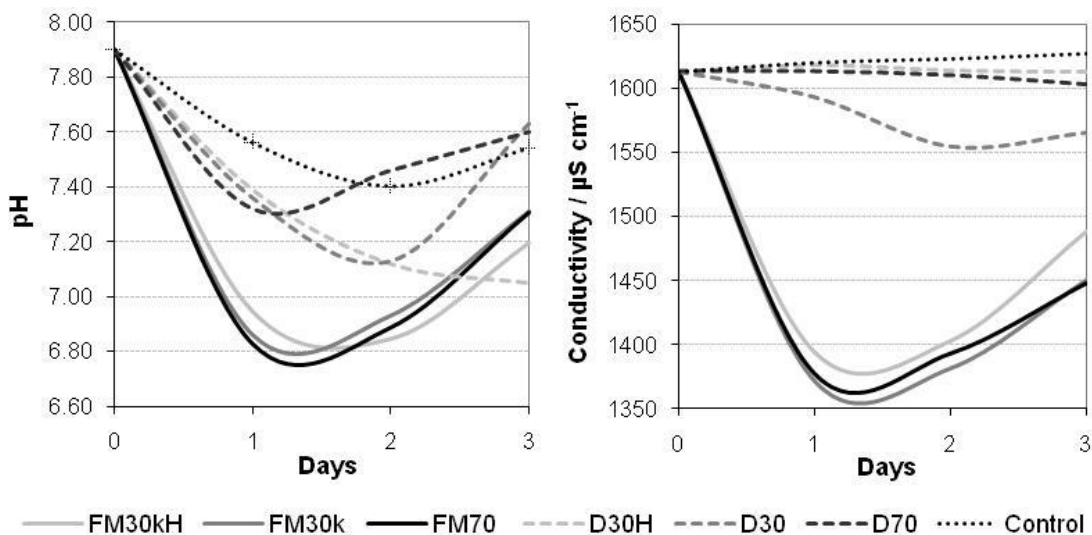
Figure 4.15: Variation in conductivity and pH of MFCs, dummy reactors and the control reactor.

Figure 4.15 shows the variation in pH and conductivity for the different materials, the control reactor and the dummy reactors. The pH decreased during a batch once power production commenced and protons were produced in the anode chamber to be transferred to the cathode. For the MFC reactors using CAC materials as the anode the pH decreased sharply from pH 7.9 to pH 6.8 point while the pH in the dummy reactors decreased less sharply from pH 7.9 to pH 7.3. The control reactor showed the most stable pH with a slight decrease from pH 7.9 to pH 7.4. For all reactors the pH increased slowly again once peak power was reached. The

conductivity followed the same profile as the pH (Figure 4.15) and decreased from 1613 μS cm^{-1} to around 1370 μS cm^{-1} for the MFC reactors over the first day. The conductivity then slowly recovered at the end of the batch, whereas the conductivity of the control reactor and the dummy reactors remained comparatively constant.

A number of studies investigated the influence of the pH on the MFC system showing peak power and/or CE performance around pH 9, pH 8 pH 7 or pH 6 depending on the study and reactor used (Behera and Ghangrekar, 2009; Raghavulu et al., 2009; He et al., 2008; Gil et al., 2003). The pH influence on the system seems to depend on the system used. As domestic wastewater is used as feed substrate slight difference in pH of one pH unit during the power production were not thought to be a major influence on the power production and efficiency of the system as the wide spread peak power performances between pH 9 and pH 6 were observed in literature. The minimum observed for pH and conductivity was possibly linked to most of the substrate being degraded by the second day which lead to less protons being produced and thus an increase in pH and conductivity as also current production started to decline.

An explanation for the different behaviour of pH (more protons in the electrolyte) and conductivity (less ions allover in the electrolyte) was that the minor number or protons present in all reactors did not represent the actual ion movement in the different reactors. As Rozendal et al described the proton concentration at neutral pH (around 7) is with 10^{-4} mM very low whereas other cation concentrations are up to 10^{5} times higher(Rozendal et al., 2006). As the reactors used a microporous membrane as separator in this study any ion would be able to move from the anolyte to the cathode reacting with oxygen to produce salts (e.g. calcium carbonate) on the cathode surface which could affect the cathode performance (Li, 2010; Franz et al., 2002). Different ions contribute differently to the conductivity of water. As wastewater includes a mix of ions contributing the preferential consumption of one type of ions, e.g. sodium ions, while at the same time protons are produced in the system, could explain the drop in pH with a simultaneous drop in conductivity. Also products of competitive processes such as fermentation could act as a weak electrolyte such as acetic acid or carbonic acid and decrease the conductivity even further as other ions are bound into molecules. Thus although

the conductivity describes the total ion movement in the reactor like the pH the measurement has limitations in a wastewater system.

4.4.4.2.2 COD removal and Coulombic Efficiency

Table 4.12 shows the average percentage COD removal using MFC reactors, dummy reactors and the control reactor for the batch starting on the 40th and 75th day. The COD removal in the MFC reactor was satisfactory with 68.7% for FM30kH and FM70 and 65.6% for FM30k during the first sampling rising to 85.3%, 76.5% and 73.5% for FM70, FM30kH and FM30k respectively during the second sampling. During the first sampling the dummy reactors for FM30k H and FM30k showed noticeably higher removal efficiencies with 81% and 75% respectively whereas the dummy reactor for FM70 and the control reactor reached 62.5% (Table 4.12). Removal efficiencies increased for the dummy for FM70 with 82.3% and increased slightly for D30 with 76.5% whereas the COD removal for D30H decreased with 70.5%. The control reactor achieved the lowest COD removal with 70% during the second sampling. It was interesting to note that the COD removal efficiency in all reactors increased while power production dropped showing ongoing acclimatisation of the biofilm consortia but maybe not only of electroactive species.

Table 4.12: Percentage COD removed for the three CAC reactors, dummy reactors and the control.

	FM30k H	FM30k	FM70	D30 H	D30	D70	Control
COD	%	%	%	%	%	%	%
1st	68.7±0	65.6±3	68.7±6	81	75	62.5	62.5
2nd	76.5±0	73.5±3	85.3±3	70.5	76.5	82.3	70.5

Table 4.13 shows the coulombic efficiencies for the MFC reactors using different activated carbon cloths as anode materials. The MFC reactors achieved very similar coulombic efficiencies for 22.6%, 23.2% and 23.8% CE for FM30kH, FM30k and FM70 respectively during the first sampling. This rose to 43% for FM30k H, 42% for FM30k and 38% for FM70 for the second sampling.

Table 4.13: Average coulombic efficiencies of the reactors using CAC materials for batches starting on the 40th (1st) and 75th (2nd) day.

	FM30k H	FM30k	FM70
CE	%	%	%
1st sampling	22.6±0.8	23.2±0.3	23.8±2.9
2nd sampling	42.6±3.6	42.1±6.9	38.0±0.5

Statistical analysis of the reactors for COD and CE showed them to be statistically the same for the materials (p=0.351 for COD and p=0.974 for CE) and the duplicate reactors (p=0.912 for COD and p=0.981 for CE). Presumably the similar behaviour of the three activated carbon cloths is due to similar surface groups and surface area.

Compared with literature a coulombic efficiency of 43% was high for reactors using wastewater as feed substrate. Cheng *et al.* (2006a) reported 27% CE with wastewater as substrate using a continuous flow design with reduced electrode spacing at similar influent COD to this study but a very low flowrate. Di Lorenzo *et al.* (2009b) reported up to 63% CE using a continuous up flow reactor but at very low influent COD (55 mg l^{-1}). As both studies used continuous flow reactors in different ways and used very low influent COD it is difficult to relate the results directly to this study.

4.4.4.3 Microbial Community Analysis

Although high CE of up to 40% was observed in the reactors 60% of the substrate removed is still degraded using other processes (i.e. anaerobic respiration, fermentation or hydrolysis). Another way is aerobic digestion due to oxygen diffusion through the membrane into the reactor chamber. Two biofilms formed in the anode chamber of the reactors used. One on the anode material, the electroactive anodic biofilm, and the other at the surface of the membrane separator, an assumed aerobic biofilm which digests substrate aerobically and thus reduces the coulombic efficiency. Samples of both biofilms were collected at the end of the experiment and the community examined using DGGE. Results were analysed using Bray-Curtis similarities based on cluster and non-metric MDS methods. The cluster analysis and ordinates revealed high similarities with 87% and higher between the anodic biofilm communities. These also showed higher similarity to the feed substrate (73% between feed and anodic biofilm) then the aerobic biofilm consortia (68% between feed and aerobic biofilm). The aerobic biofilm consortia showed 78% and higher similarties between each other (Figure 4.16).

The anodic biofilm acclimatises to the system (reactor under 1 kΩ) which is easily visible as the similarities between influent (feed substrate) and anodic biofilms is lower (73%) than between the anodic biofilm themselves (87% or higher) thus showing a clear influence of the system (external resistance). The aerobic biofilm on the wetted side of the membrane is still very similar to inoculum and electroactive biofilm with 68% which suggests an adaptability of the microbial consortia to environmental conditions making it possible for the microorganisms to switch metabolisms depending on circumstances (Unden, 1998) and use up any oxygen flux into the reactor to degrade substrates aerobically. The reactor is kept anaerobic but at the same time the achievable CE is reduced as substrate is consumed under aerobic conditions with no power produced. Cheng *et al.* (2006a) hypothesised oxygen flux and consequent aerobic degradation as main reason for low CE. As up to 43 % CE were achieved in this study aerobic degradation due to oxygen diffusion into the chamber is probably not the main process reducing the CE.
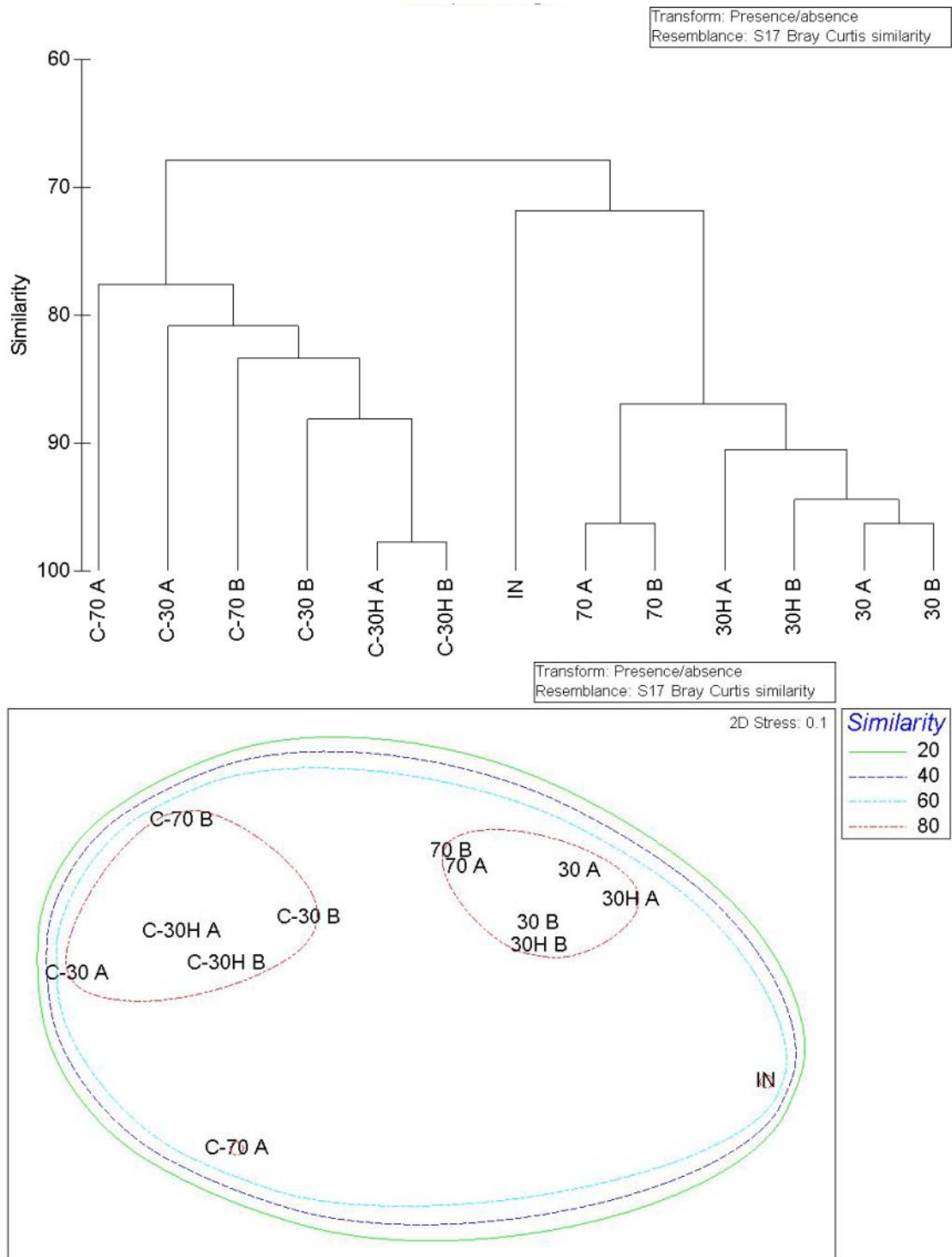
Figure 4.16: Dendrogram and ordination of the communities based on species presence and absence was derived from MDS analysis of Bray–Curtis similarities (stress = 0.1).Samples are named as FM30k H: 30H; FM30k: 30; FM70: 70 with C in front of the name for the aerobic biofilm and no addition for the anodic biofilm.

4.4.5   Conclusion

The activated carbon cloth chosen worked very well as anode material, after a long acclimatisation phase, and showed a high potential for energy generation up to 40 mW m^{-2} during polarisation. Under steady state conditions (1 kΩ external load) with a power density of 20 mW m^{-2} half the potential power realised.

But over the 80 days the reactors were running a decrease in power performance under instantaneous and steady state polarisations was observed. Although FM70 demonstrated the highest power performance at the end of the experiment, followed by FM30k H these two materials showed a greater decline in their power potential under instantaneous conditions meaning that in an improved system FM30k would be able to produce more power over longer time then the other two materials. FM70 also nearly fell apart when taken out of the reactor after 80 days for microbial analysis. Durability of the materials is one of the most important factors for applicability of MFCs in wastewater treatment which made FM70 unsuitable for use as anode material.

The wastewater treatment performance in COD removal and CE increased over time for all three materials and as FM30k H and FM30k showed very similar performances both were established as possible materials for future investigations. In the end FM30k was chosen for the next studies as it showed a higher potential for a stable performance than FM30k H during polarisations.

The activated carbon cloth showed high potential as a biocompatible material. The strong adsorption behaviour attracts particles and microorganisms to the material, and although the antibacterial characteristics increased the acclimatisation time, which meant, once a biofilm formed, a strong connection was formed between material and biology leading to up to 43% CE.

4.5   INFLUENCE OF ANODE SUPPORT MATERIAL

4.5.1   Introduction

The reactor design has been shown to significantly influence the power performance in MFCs (Rozendal et al., 2008; Du et al., 2007; Logan et al., 2006; Angenent et al., 2004) more so, than in many cases, the microbial culture (Logan and Regan, 2006). Thermodynamically the cell voltage is the sum of the theoretical anode and cathode potential (E_A and $E_{C)}$ minus the anodic and cathodic activation overpotential $\eta_{A,act}$ and $\eta_{C,act}$ and the ohmic overpotential η_{ohm}.

$$E_{Cell} = I \cdot R_{ext} = E_C - \eta_{C,act} - \eta_{ohm} - E_A - \eta_{A,act} \qquad \textbf{(4.15)}$$

The ohmic charge transfer resistance in a MFC occurs through resistance to the flow of ions in electrolyte and electrode (Du et al., 2007). The ohmic resistance can be measured through the internal resistance of an MFC. Modifications in the system architecture to reduce the ohmic resistance include the use of highly conductive electrode materials and lower electrolyte resistivity through reduced electrode spacing (Logan and Regan, 2006). Increasing the substrate conductivity is another way to reduce electrolyte resistance but as wastewater is the substrate this is not usually an economically feasible solution.

Domestic wastewater has very low conductivity (around $1 - 2$ mS cm^{-1} at room temperature). Increasing the conductivity is not economical for wastewater treatment, therefore the electrode spacing was reduced to 2 mm and in addition to using activated carbon cloth as an anode material, conductive metal meshes were used to support activated carbon black (C/HNO$_3$) as the anode catalyst.

4.5.2   Hypothesis

Reducing the electrode spacing and the use of metal mesh anode supports will reduce the ohmic resistance in the system and lead to high power generation.

4.5.3 Experimental

In this study three conductive mesh anode supports were coated with activated carbon (C/HNO_3) (1 mg cm^{-2}). The three mesh anodes and one activated carbon cloth anode were used as anode material with a 2 mm distance between anode and the membrane. The meshes used were expanded metal foils made from titanium (Ti), stainless steel (SS) and aluminium (Al). The activated carbon cloth used was FM30k (CAC). Although aluminium is biodegradedable by bacteria, the activated carbon layer would potentially prevent degradation. Table 4.14 shows the surface properties for the anode support materials used.

Table 4.14: Mesh and activated carbon cloth surface properties as supplied by Dexmet Corporation, UK.

Parameter	Ti	SS	Al	CAC
Product	2Ti3.9-031 F&An	2SS(316L)5-077F	2Al6-077F	FM30k
Thickness / mm	0.0508	0.0508	0.0508	0.4
Surface density / g m^{-2}	87	110	45	110

Domestic wastewater was used as feed substrate and inoculum. The detailed characteristics of the feed substrate before sampling are provided in Table 4.15.

Table 4.15: Physiochemical characteristics of substrate (domestic wastewater) used in the present study.

Parameter	Mesh
pH	7.9
COD /mg l^{-1}	368
SS / mg l^{-1}	213.3
VSS / %SS	21.9
Sulphate / ppm	105.65
Chloride /ppm	68.24
Phosphate /ppm	8.84
Fluoride /ppm	6.82
Conductivity / mS cm^{-1} at RT	1.146

Duplicate reactors were used in the experiment and results shown are the average of the duplicate reactors.

4.5.4 Results and discussion

4.5.4.1 Power performance

4.5.4.1.1 Variations in voltage evolution and voltage, current and power density under constant load

Figure 4.17 shows the voltage evolution for the different anode support materials under 1 kΩ external load.
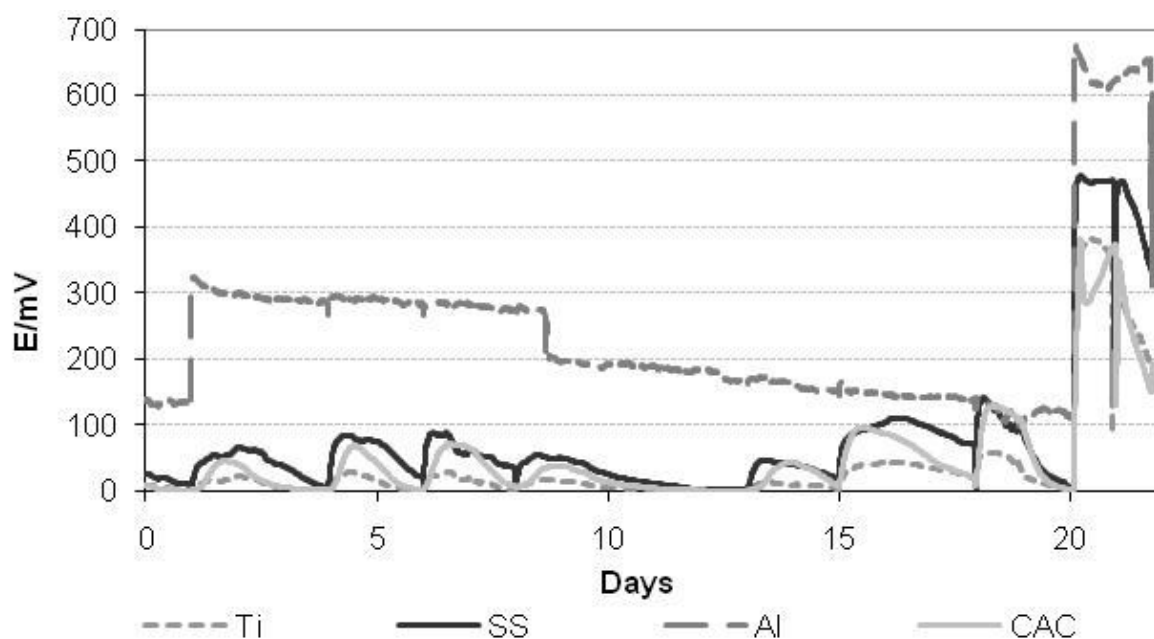
Figure 4.17: Average voltage evolution for the three mesh and acitvated carbon cloth anode supports under 1 kΩ external load.

Reactors using titanium mesh, stainless steel mesh and the activated carbon cloth acclimatised and showed the typical voltage profile for batch-fed reactors with a rapid increase in voltage after refilling, a short plateau of peak voltage and a steady decrease, when the substrate was degraded. The voltage evolution for aluminium mesh reactors showed quickly that the aluminium mesh was rapidly degrading despite the protecting cover of the anode catalyst

74

(C/HNO^3). The high cell potential and therefore power generation under steady state conditions for aluminium supported anodes therefore was presumably produced from the degradation of the aluminium support in those reactors not from the feed substrate.

Reactors using stainless steel and activated carbon supported anodes demonstrated, after a period of acclimatisation, the highest peak power densities at 15±2 mW m^{-2} (at 110±10 mA m^{-2} and 138±12 mV) and 13±3 mW m^{-2} (at 101±11 mA m^{-2} and 127±15 mV) respectively (Figure 4.18). Reactors using titanium supported anodes reached very low power densities with 3±2 mW m^{-2} (at 46±16 mA m^{-2} and 57±20 mV) and showed higher variability between duplicate reactors.
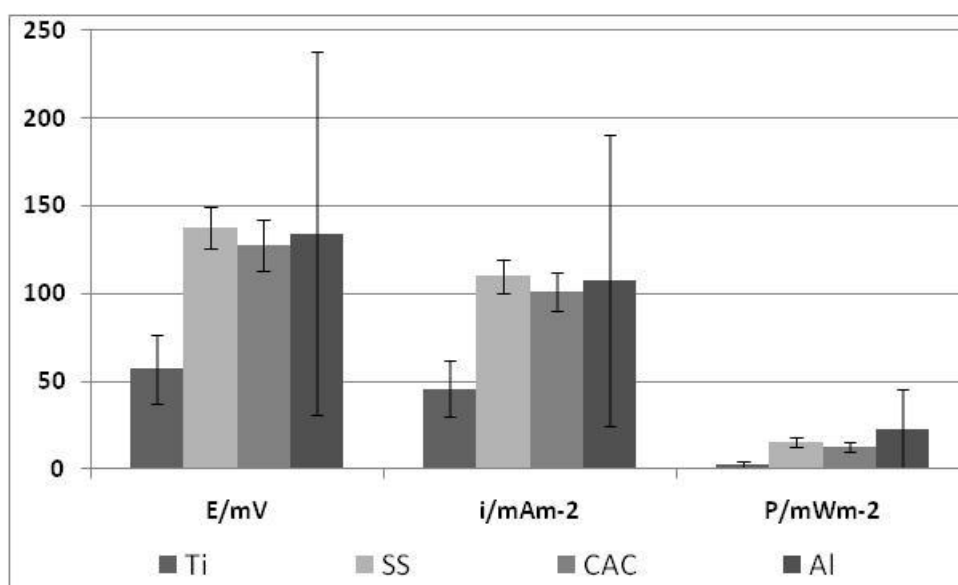
Figure 4.18: Voltage, current and power density under 1kΩ for Ti, SS, CAC and Al anodes.

There is very little literature on the use of meshes as anode support or materials. Only Wang *et al.* (2009) studied the use of a carbon mesh anode at an electrode spacing of 2 cm and found that the material increased the power performance slightly compared to carbon cloth used.

Porous anodes in the form of carbon foam, activated carbon granules or as a carbon fibre brush (Logan et al., 2007) were used in varies studies with flow through the anode or alongside it. These studies showed that the surface area increase in three dimensional anodes did not translate directly into higher power densities but a limiting voltage generation was reached (Di Lorenzo et al., 2010). Electrochemically only the surface area of the anode towards the cathode

is able to react and easily transport reaction products (protons) to the cathode. Therefore mainly the surface directly towards the cathode will be able to react easily in deep three dimensional structured anode materials such as layers of carbon granules or the graphite fibre brush. All carbon anodes are more of less porous and therefore three dimensional structures. A flat sheet anode in a flat plate configuration should achieve maximum power with the least limitations. In this study the influx of oxygen into the anode chamber negated this effect.

4.5.4.1.2 Anode behaviour and activity

Figure 4.19 shows the anode behaviour and activity of the peak performing different mesh supported anodes and the activated carbon cloth anode. Aluminium showed the highest onset potential with -433 mV but the high overpotential in the low current density region showed low activity of the anodes on aluminium meshes. Stainless steel and titanium meshes showed lower onset potentials with -225 mV and -124 mV respectively. Both stainless steel and titanium showed higher activity rapidly reaching higher current densities and lower overpotential losses than aluminium. Activated carbon showed the lowest onset potential with -115 mV but rapidly reached much higher current densities than the mesh supported anodes and had with low overpotential losses the highest activity of the four carbon supports.
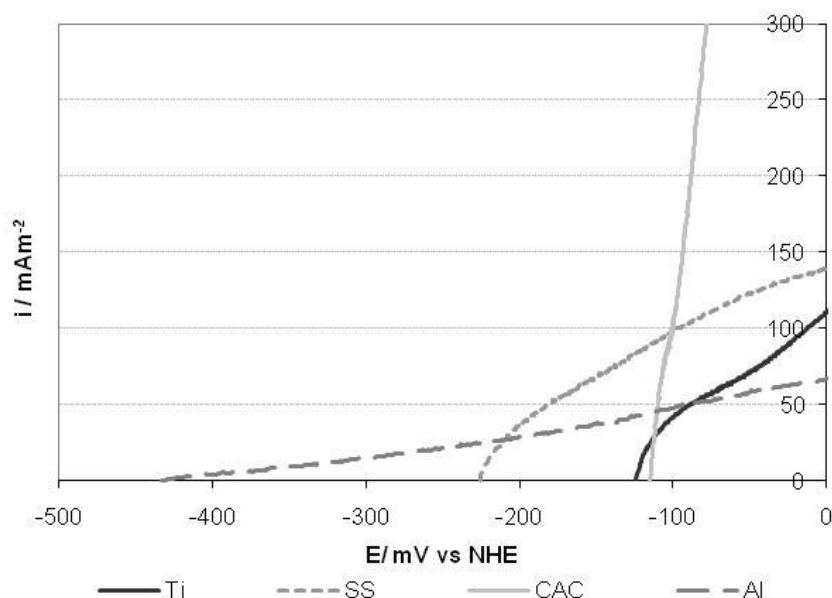
Figure 4.19: Linear sweep voltammograms of the different anodes showing the anode behaviour and activity during polarisation at a scan rate of 1 mV s^{-1}.

Table 4.16 shows the average peak power density, anode charge transfer resistivity, onset potential of the anodes and the internal resistance of the best performing reactors. The lowest charge transfer resistivity and therefore highest activity was observed in reactors using activated carbon cloth (CAC) with 0.22 Ω cm^2, followed by anodes using stainless steel mesh as support with 3.7 Ω cm^2 and titanium mesh at 4.35 Ω cm^2. Reactors using aluminium mesh as anodes support reached the highest average charge transfer resistivity of 3506 Ω cm^2 and showed the highest variability between duplicate reactors.

Table 4.16: Average peak power density, charge transfer resistivity and onset potential of the mesh anodes.

	Peak power density / mW m^{-2}	Charge transfer resistivity / Ω cm^2	Onset potential / mV	Internal resistance / Ω
Ti	12.5±3.5	4.35±1.7	-56±68	7±2
SS	21.3±1.3	3.7±0.1	-226±1	3.5±0.5
CAC	21.8±2.8	0.22±0.005	-104±11	11.5±3.5
Al	5.95±4.6	75.6±63.03	-388±45	3506±3505

Reducing the electrode spacing to 2 mm and the use of metal meshes as anode support reduced the internal resistance of the materials to less than on tenth of the internal resistance measured in earlier experiments using 4 cm electrode spacing, for titanium mesh, stainless steel mesh and activated carbon cloth, showing that the ohmic resistance in the reactor was greatly decreased when changing the reactor architecture.

Figure 4.19 shows the anode, cathode and cell behaviour of activated carbon cloth anodes using 2 mm and 4 cm electrode spacing. The graph shows a distinctive shift in the onset potential of the anode from -200 mV at 4 cm distance to -115 mV with an electrode distance of 2 mm whereas the cathode potential remained consistent. Thus it is apparent that the smaller electrode distance directly influences the anode potential.
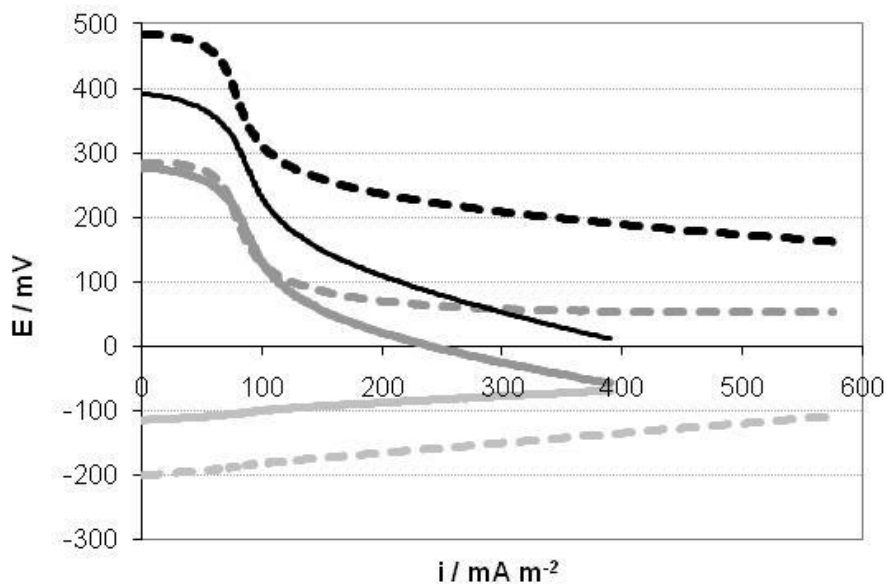
Figure 4.20: Linear sweep voltammograms of the anode (light grey), iR corrected (grey) and cell (black) behaviour during polarisation for 4 cm (dashed) and 2 mm (full line) electrode spacing using activated carbon cloth (CAC) as anode materials and support (Anode and cathode potential vs NHE, scan rate 1 mV s^{-1}).

A possible explanation for the decrease in anode potential, in the 2 mm configuration, was oxygen diffusion into the anode chamber which adversely affected the electroactive biofilm since microorganisms, in a mixed culture, are able to use oxygen as a electron accepter to gain more energy than when using an anaerobic electron acceptor (Rittmann and McCarty, 2001). As oxygen yields more energy as an electron acceptor it is being used preferentially by physiological flexible microorganisms which leads to a decreased anode potential and consequently a decline in cell potential and power produced. Cheng *et al.* (2006a) and Min and Logan (2004) reported similar findings using 1 cm electrode distance and a membrane electrode assembly similar to one used in a fuel cell (no spacing at all) which strongly suggests that the oxygen crossover is generally a serious limitation to the high power generation of MFCs.

Figure 4.21 shows the anode, cathode and cell behaviour during polarisation for the different anode support materials. All mesh supported anodes showed high overpotential losses at low current densities. Reactors using activated carbon cloth as anode materials reached more than two times the current densities of the mesh supported anodes. Although the same anode and cathode catalysts were used the onset potential of anode varied widely using the different

anode supports. Corrosion occurring on the mesh supports could be an explanation for these differences and the difference in surface area using the different meshes and activated carbon cloth anode. The onset potential of the cathode was comparatively similar for reactors using activated carbon cloth, stainless steel and titanium. Reactors using aluminium showed a cathode onset potential that was 140 mV lower than the other three materials which was presumably due to the poor performance of the reactors as aluminium was degraded and limited proton production.
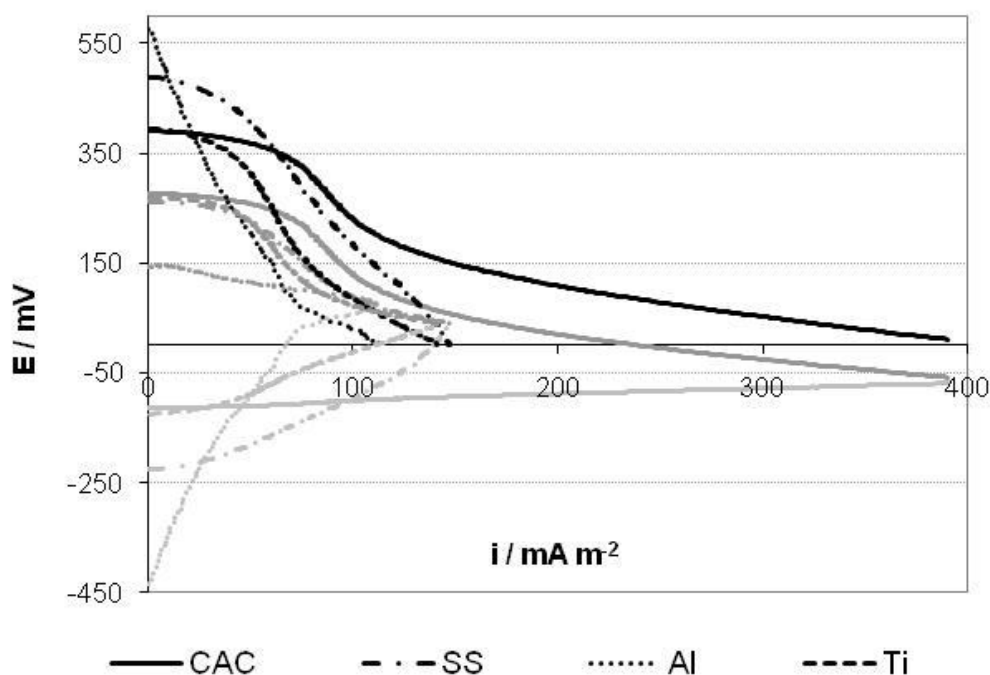
Figure 4.21: Linear sweep voltammogram of the anode (light grey), iR corrected cathode (grey) and cell potential (black) for the different anode support materials during polarisation. (Anode and cathode potentials vs NHE)

Although the lower internal resistance reduced the ohmic resistance in the reactors, as seen in the reduced internal resistance and the shorter ohmic region of the current/voltage plots, the power outputs dropped as the changed reactor configuration directly influences the anode potential.

The comparison of the IR corrected anode, cathode and cell potential for reactors using CAC anodes showed that the reduction in power performance is entirely due to a shift in anode potential of almost 100 mV (Figure 4.20). While the ohmic resistance decreased the cell voltage

showed that the high activation overpotential is necessary to start the reaction. For the different mesh materials the power performance was even more noticeably activation limited. But whereas the cathode is more limiting for reactors using CAC anodes, all three mesh anodes showed a high potential loss during the polarisation similar to the potential loss of the cathodes (Figure 4.21). The mesh anodes were not as active as the activated carbon cloth.

Internal resistance has been reported as a limiting factor in microbial fuel cells (He et al., 2006; Logan et al., 2006; He et al., 2005; Rabaey et al., 2005b) but the use of substrates with a defined composition (such as acetate, glucose, or artificial wastewater with phosphate buffer added to increase the solution conductivity) reduced the internal resistance and masked the importance of the internal resistance in real life applications such as wastewater treatment. The addition of buffer solution to increase conductivity would not be economical (Rozendal et al., 2008). Consequently widely varying results for slight changes (electrode spacing, reactor volume, etc.) in reactor design were observed but rarely explained or quantified. As various research reports have used different reactor designs results are seldom comparable.

4.5.4.1.3 Polarisation studies

Figure 4.22 shows the cell potential and power density curves for the different supported anodes in the 2 mm configuration. CAC reached 24.2 mW cm^{-2} at 328 mA m^{-2} and 73 mV which was also the highest power density achieved in this configuration. Stainless steel supported anodes reached 22.2 mW cm^{-2} (at 327 mA m^{-2} and 67 mV) followed by titanium supported anodes achieving 15.7 mW cm^{-2} (at 286 mA m^{-2} and 49 mV). Aluminium supported anodes reached the lowest peak power densities of 10.3 mW cm^{-2} (at 223 mA m^{-2} and 46 mV).
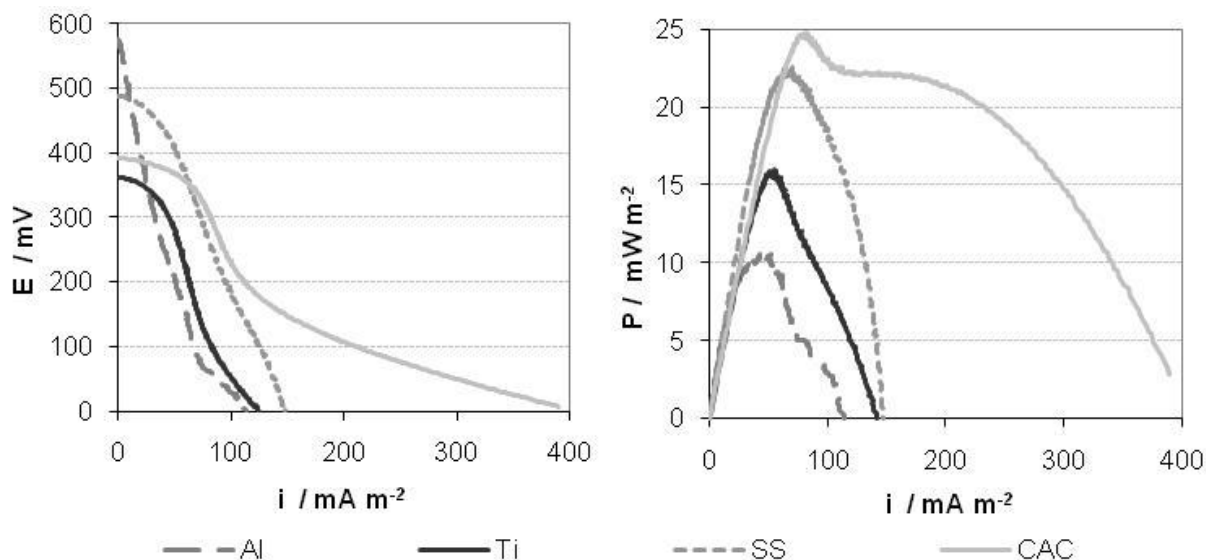
Figure 4.22: Linear sweep voltammogram of the cell potential and power density for the reactors using different mesh and carbon cloth supported anodes.

Although the lower electrode spacing decreased the internal resistance peak power densities achieved for reactors using CAC anodes were 10 mW m^{-2} lower than in the reactors with 4 cm electrode spacing.

Power densities achieved under 1 kΩ were nearly half the amount of power generated under instantaneous conditions and showed a great potential for activated carbon cloth anodes. Reactors using titanium supported anodes performed poorly reaching 3±2 mW m^{-2} (at 46±16 mA m^{-2} and 57±20 mV). Both poor performing reactors showed greater variability between the duplicate reactors. Aluminium showed even wider variability between duplicate reactors (23±22 mW m^{-2} at 107±83 mA m^{-2} and 134±103 mV), due to one of the aluminium meshes degrading faster and showing very poor performance whereas the second one showed the best performance as mainly the aluminium was degraded to produce electrons instead of the substrate.

Research into the influence of electrode spacing on the internal resistance focused on distances of 1 cm to 4 cm (Cheng et al., 2006a; Liu et al., 2005) or even wider distances (Li et al., 2010a; Ghangrekar and Shinde, 2007). Only Rozendal *et al.* (2008) investigated ohmic losses reached by narrower electrode spacing (0 to 1 cm) when using wastewater as substrate. Cheng *et al.* (2006) also reported a decrease in power performance when decreasing the electrode spacing

from 2 cm to 1 cm under fed batch mode which simultaneously reduced the internal resistance. The reduction in power density was also attributed to a decrease in anode potential but a lower electrode spacing was reported to increase the cell performance under continuous flow. This supports the putative influence of dissolved oxygen on the anodic biofilm, although it does not try to explain the phenomenon in detail. But as acetate was used as substrate in Cheng's study the significant influence of the electrolyte resistance on in cell performance, which made oxygen diffusion into the chamber a critical factor and therefore emphasised the importance of the use of a selective membrane, was not deduced.

Flow through the anode was reported to improve the power performance (Sleutels et al., 2009; Cheng et al., 2006a; Rabaey et al., 2005b) and was attributed to a reduction in the influence of mass transport limitations. But as no mass transport limitations were observed in this study this supposition could not be confirmed.

4.5.4.2 Wastewater Treatment Efficiencies and Coulombic Efficiencies

Figure 4.23 shows the percentage COD removal, coulombic efficiencies and current densities produced with the different anode supports. The COD removal was measured daily during the batch under 1 kΩ load and results shown were the COD, CE and current densities 2 days into the batch. The reactors using mesh and carbon cloth supported anodes removed more than 70% of the organic carbon after two days. Titanium supported anodes and activated carbon cloth anodes showed the highest COD removal efficiency at 72±2% and 70±4% removal for stainless steel. However aluminium supported anodes removed 54±11% COD showing high variability between duplicate reactors due to degradation of the support. The control reactor showed slightly better COD removal rates than aluminium with 61% COD removed (Table 4.17).
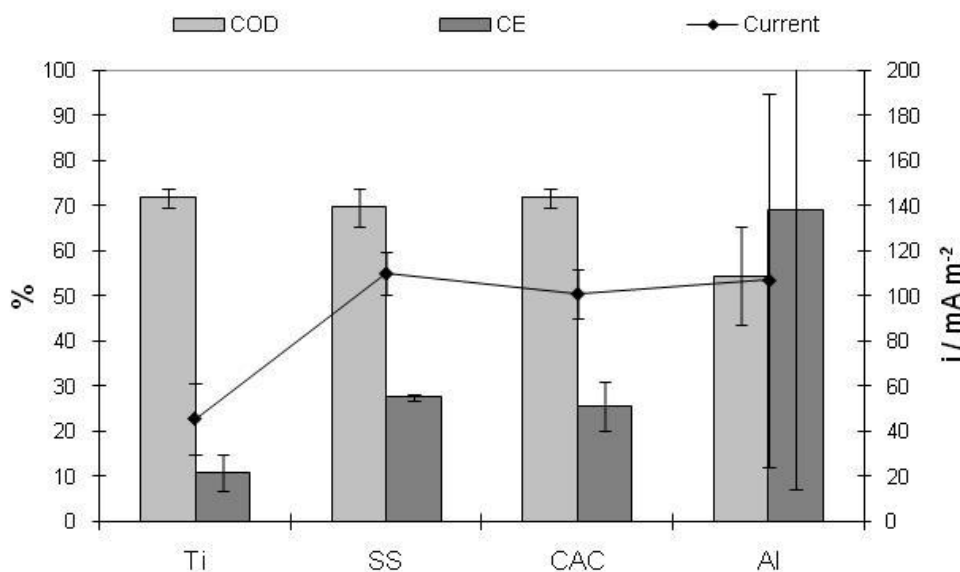
Figure 4.23: COD, CE and current for the carbon cloth and mesh supported anodes.

Peak coulombic efficiencies were 28±1% CE for stainless steel supported anodes. Activated carbon cloth supported anodes gave similar CE at 26±5% whilst titanium supported anodes achieved 11±4% CE. Aluminium supported anodes showed very high COD removal with 69±62% but as the electrons produced came from the aluminium itself as well as the substrate the high CE is not meaningful when looking at the actual MFC performance. As reactors using aluminium showed very rapid degradation of the metal mesh aluminium was a poor choice for an anode support material and is not recommended for use in microbial fuel cell technology.

Table 4.17: COD removal and CE two days into the batch.

	Ti	SS	CAC	Al	Control
COD / %removed	72±2	70±4	72±2	54±11	61
CE / %	11±4	28±1	26±5	69±62	n/a

These results are broadly consistent with the previous study using domestic wastewater as substrate. And like the 'dummy' reactors used in the previous study, the mesh anodes increased COD removal but not always in direct favour of higher energy generation.

4.5.5   Conclusion

The metal meshes used as anode support reduced the internal resistance by half to reductions seen using activated carbon cloth. But less anode activity was observed. Reactors stainless steel mesh supported anodes showed the highest power performance, closely followed by reactors using activated carbon cloth anodes. Titanium supported anodes disappointed with low power densities. Reactors using aluminium supported anodes gave an illusory impression of high power densities due to galvanic corrosion of the support which made them unsuitable as anode support material.

Although the internal resistance was significantly reduced when the 2 mm electrode spacing was used, a lower power performance compared with similar materials used in the previous experiment was unexpectedly observed. As the ohmic resistance is reduced more power should in principle be generated. A decrease in anode potential, due to oxygen diffusion into the anode chamber, negated this effect, leading to less power. Oxygen crossover is a serious limitation to power generation in MFCs as high power densities depend on low ohmic resistances, but oxygen diffuses through most separators or membranes used in MFCs.

Coulombic efficiencies achieved in this configuration for wastewater fed reactors are broadly consistent for stainless steel and activated carbon supported anodes with CE reached using activated carbon cloth anodes in the 4 cm configuration. Activated carbon powder (C/HNO$_3$) supported on stainless steel mesh reached similar coulombic efficiencies to the activated carbon cloth which reflects the similarity in both activated materials. This also suggests that activated carbon cloth is an excellent anode material with probably good interactions between the biocatalyst and the surface area of the material. Moreover the results supported the hypothesis that the brewery wastewater inhibited power generation made in the previous study on modified anode materials.

5   DURABILITY OF CATHODE MATERIALS

ABSTRACT

The durability of different cathode catalysts (platinum, carbon black, activated carbon black (C/HNO$_3$), iron(II)phthalocyanine (FePc) and iron(II)phthalocyanine mixed with manganese oxide (FePc+Mn)) in reactors using wastewater as substrate was investigated over 100 days under a constant resistance of 1000 Ω. The activity of all catalysts tested decreased over the period they were studied. The power performance of all reactors declined rapidly over 60 days using activated carbon powder (C/HNO$_3$) as anodes under constant load. A change in anode material to activated carbon cloth (FM30k) showed an improvement in potential power performance during polarisation but the actual power densities obtained under 1000 Ω external load were very low. Similary, coulombic efficiencies for all reactors decrease rapidly from 20-30% to 11% or lower over 60 days using activated carbon powder as the anode material. Changing the anode material to activated carbon cloth increased the coulombic efficiencies to 55% and 43% for reactors using platinum and carbon black cathodes and to between 17% to 27% for reactors using FePc, activated carbon black and FePc+Mn.

5.1   INTRODUCTION

Oxygen with its high oxidation potential and general abundance is an attractive electron acceptor in electrochemical systems (Kinoshita, 1992). The function of a cathode is to provide a surface for the reaction of oxygen and protons to form water. To accomplish this in a gas diffusion electrode, a "three phase region" has to be formed to interface oxygen in the air, protons through the membrane and electrons through an electrically conducting material. To fabricate this interface a catalyst layer together with a suitable binder (e.g. Nafion solution or polyvinyl alcohol (PVA)) is deposited onto a membrane or a porous separator. On top of the catalyst layer a microporous layer, usually activated carbon black with PTFE, to provide hydrophobicity, is applied followed by the gas diffusion layer, commonly carbon or graphitised paper, which ensures good electrical conductivity and the access of oxygen to the electrocatalytic layer.

The slow kinetics of the oxygen reduction reaction (ORR) can be a limiting factor in the cathode performance of electrochemical systems. In microbial fuel cells the poor kinetics of ORR at neutral pH and low temperatures limit power densities (Roche and Scott, 2009). However in early studies on MFCs sluggish kinetics on the anodic side of microbial fuel cells often meant that limitations on the cathode side were masked and the anode was widely considered to be the limiting factor in MFC systems. So did H. P. Bennetto describe the rate and proportion of electrons transferred as inefficient and searched for solutions using mediators for more rapid electron transfer (Bennetto, Stirling et al. 1983; Roller, Bennetto et al. 1984).

Platinum is the best known and most active catalyst for oxygen reduction in acidic solutions and has tended to dominate in use in early MFC studies. But its ever increasing price makes its use in wastewater treatment uneconomic and makes alternative platinum-free cathode materials an essential research and development requirement.

Numerous studies investigated alternative air breathing cathode catalyst. These included noble metal free catalysts such as pyrolyzed iron(II)phthalocyanine (FePc), cobalt tetramethoxyphenylporphyrin (CoTMPP) based catalysts, manganese oxide (MnO_x) and a

variety of carbon materials which showed good performance in neutral media or MFC test (Deng et al., 2010; Li et al., 2010b; Harnisch et al., 2009b; Roche and Scott, 2009; You et al., 2008; Zuo et al., 2007; Zhao et al., 2005). FePc and activated carbon cathodes even achieved higher performances than platinum cathodes in MFC test (Duteanu N, 2010; Zhang et al., 2009a; HaoYu et al., 2007). However, although good catalyst activity, which is generally measured in half cell tests at neutral pH, is important, long term stability and reliability are even more important for the cost-effective MFC systems used in wastewater treatment systems. None of the catalysts mentioned above were tested specifically for durability in a MFC system using wastewater as substrate.

The durability and therefore long-term reliability of electrode and membrane materials is an essential consideration if microbial fuel cells are to be used for wastewater treatment. Little research has been done on more realistic approaches to microbial fuel use in wastewater treatment and this is, to our knowledge, the first study to examine long term cathode performance in a wastewater fuelled microbial fuel cell using a low cost microporous separator as membrane.

Accordingly the activity and durability of platinum and a range of alternative cathode catalysts in a wastewater fuelled single chamber microbial fuel cell with a microporous separator as membrane were investigated with a view to gaining a better understanding how the system affects the cathode catalyst and its lifetime. The cathode catalysts tested were:

- Platinum on carbon (Pt/C) as a very active catalyst for ORR;
- Carbon black (CB) which is known to demonstrate slower ORR activity (Kinoshita, 1992), but is, as a cheap material, potentially more economical;
- Nitric acid activated carbon black (C/HNO$_3$), which showed good ORR activity in half cell and microbial fuel cell tests presumably due to more active surface groups than observed on unmodified carbon black (Duteanu N, 2010);
- Iron(II)phthalocyanine (FePc) which demonstrated high activity towards ORR in neutral media in half cell and fuel cell tests; (HaoYu, Cheng et al. 2007)
- Iron(II)phthalocyanine mixed with manganese oxide (FePc+Mn). Both materials showed good ORR activity in neutral media and thus may show good or better activity together. (HaoYu, Cheng et al. 2007; Roche and Scott 2009)

5.1.1 Cathode activity

Relative cathode activity is generally compared using the limiting form of the Butler-Volmer equation at high overpotentials (Bard and Faulkner, 2001). This limiting form is the cathodic form of the Tafel equation and can be expressed for large η, both negative and positive, as

$$i = i_0 e^{\frac{-\alpha F \eta}{RT}}$$

(5.1)

Or

$$\eta = \frac{RT}{\alpha F} \ln i_0 - \frac{RT}{\alpha F} \ln i$$

(5.2)

Where η is the overpotential, i_0 the exchange current density, α is the transfer coefficient, R is the gas constant, T is the temperature, i is the current and F is Faraday's constant.

A Tafel plot, log i vs η, was used to calculate the Tafel slope, the transfer coefficient α and the exchange current density i_0. This was used to evaluate the relative cathode activity. Tafel slope measurements in this work were done over 600 mV starting from the cathode OCP (E vs. NHE) using linear sweep voltammetry with a scan rate of 1 mV s^{-1}. The geometric surface area was used in all calculations.

5.2 HYPOTHESIS

Platinum or alternative catalysts for the air cathode are a sustainable and economical solution for high power production from wastewater in single chamber microbial fuel cells.

5.3 EXPERIMENTAL

Five cathode catalysts were studied in a single chamber MFC using activated carbon anodes (nitric acid activated carbon powder on carbon cloth (C/HNO$_3$) and activated carbon cloth

(FM30k) in the subsequent experiment), a microporous battery separator (Rhinohide, supplied by Entek International, UK) as membrane and domestic wastewater as substrate and inoculum.

The cathode catalysts studied were platinum on carbon (Pt/C), carbon black (CB), nitric acid activated carbon black (C/HNO$_3$), pyrolised iron(II)phthalocyanine on carbon (FePc), and pyrolised iron(II)phthalocyanine on carbon mixed with manganese oxide on carbon (FePc+Mn). All catalysts were deposited with a load of 1 mg cm^{-2} directly onto the microporous membrane separator using a catalyst ink with 10 wt% PTFE, to provide hydrophobicity, and 15 wt% PVA as binder.

Pt/C was a commercial catalyst obtained from E-Tek, UK. C/HNO$_3$ was prepared as described in Chapter 4.4 (modified anode materials). Ketjen Black EC 300J was used as carbon black.

FePc was prepared by adding 1.2 g iron(II)phthalocyanine powder (supplied by Alfa Aesar) to 800 mg carbon black (Carbon Monarch 1000). The mixture was then dissolved in 20 ml concentrated H$_2$SO$_4$. After 10 min 100 ml deionised water were added to the solution. The solution was then gently stirred for 16 h after which it was filtered on 8μm pore size filter paper using a vacuum pump. The obtained catalyst was thoroughly washed until reaching pH 6.5. The obtained filtrate was then dried at 100°C for 16 h before being ground into a fine powder. The obtained powder was pyrolised under nitrogen for two hours at 800°C using 300°C ramp rate for heating and cooling.

MnO$_x$ particles were chemically impregnated onto carbon. For this 118.3 mg of MnSO$_4$ (Prolabo) were dissolved in 70 ml deionised water and the solution was heated up to. 4 g of carbon black (Carbon Monarch 1000) were added to the solution and the solutioin was stirred at 80°C for 40 min to allow MnSO$_4$ bonding to carbon surface groups. 1.58 g KMnO$_4$ (Alfa Aesar) was dissolved in 300 ml deionised water and after heating to 80°C drop by drop added to the carbon suspension. The mixture was stirred for 1 h at 80°C and was then filtered. The filter cake was dried at 100°C for 16 h and ground into a fine powder.

FePc+Mn was prepared by mixing FePc and MnO_x in weight ratios of 92.5:7.5 to give molar ratios of 2: 1 FePc to MnOx. This was based on the assumption that the MnOx/C was also ~25% Mn by weight (Roche et al 2007).

The cathode catalysts FePc, MnO_x and FePc+Mn were produced and supplied by R. Burkitt from Newcastle University.

During the start up period the reactors were operated under an external load of 1000 Ω and were refilled with new substrate, whenever there was a decrease in cell potential which suggested that the substrate was digested. This was repeated until stabilisation of the voltage generated in the replicate cells showed acclimatisation of the anodic community.

The experiment was started using activated carbon powder (C/HNO_3) as anode material and after 60 days the anode material was switched to activated carbon cloth to study the influence of the anode materials as a factor on energy production. The physiochemical parameters for the wastewater used are given in Table 5.1.

Table 5.1: Physiochemical characteristics of the feed substrate (domestic wastewater) used in the present study.

Parameter	C/HNO_3 anode	C/HNO_3 anode	FM30k anode
pH	n/a	7.9	7.36
COD /mg l^{-1}	256	288	256
SS / mg l^{-1}	160.0	193.3	202.2
VSS / %SS	31.3	37.9	11.0
Sulphate / ppm	93.58	117.27	105.65
Chloride /ppm	181.31	261.98	68.24
Phosphate /ppm	Not detected	Not detected	Not detected
Fluoride /ppm	Not detected	Not detected	Not detected
Conductivity / mS cm^{-1} at RT	1.578	1.613	1.493

5.4 RESULTS AND DISCUSSION

5.4.1 *Power performance*

5.4.1.1 Voltage Evolution and charge produced under different cathodes

Figure 5.1 shows the voltage evolution of the reactors with different cathode materials using activated carbon powder (C/HNO$_3$) as anode material. The voltage for all the different reactors increased from batch to batch until the 24th day after which the voltage stabilised and subsequent batches were assumed to have acclimatised. The stabilised voltage varied for different cathodes, 190 mV for platinum, 171 mV for carbon black, 141 mV for FePc, 68 mV for C/HNO$_3$ and 56 mV for FePc+Mn. Samples were taken for the batch starting on the 31st day. After this, a steady deterioration in power performance occurred for all MFCs which was due to a reduction in cathode activity. The slowest deterioration in peak voltage over eight batches was observed in reactors using carbon black cathodes from 175 mV to 146 mV whereas an much faster decline was observed for reactors using platinum and FePc cathodes (Figure 5.1); 191 mV to 80 mV and 130 mV to 33 mV respectively.
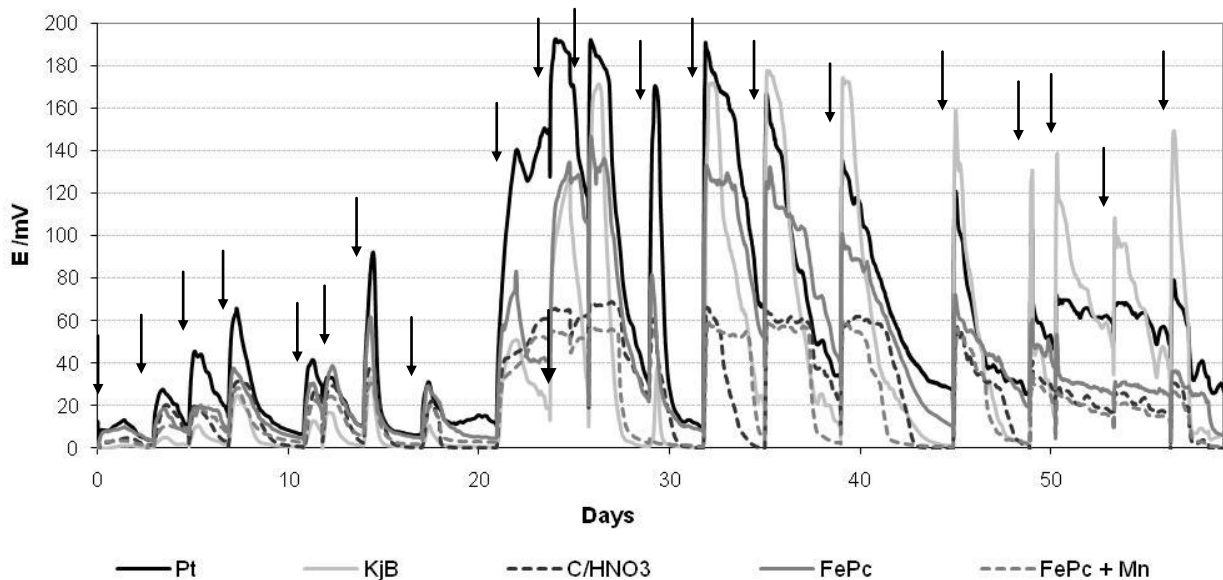
Figure 5.1: Voltage evolution of the reactors using different cathodes with activated carbon powder (C/HNO$_3$) anodes. The arrows indicate when reactors were refilled.

Figure 5.2 shows the voltage evolution of the reactors with different cathodes using activated carbon cloth as anode materials. The fastest acclimatisation, with activated carbon cloth

anodes, was observed for platinum with the reactor reaching a peak voltage of 104 mV after the third batch. A slight decrease of 10 mV in peak voltage achieved was observed in the next batch for platinum. Reactors with FePc, C/HNO$_3$ and FePc+Mn as cathodes were acclimatised after the third batch but achieved lower voltages of 46 mV for FePc, 35 mV for C/HNO3 and 32 mV for FePc+Mn. Carbon black produced the highest voltage; a peak potential of 121 mV at the 4th batch.
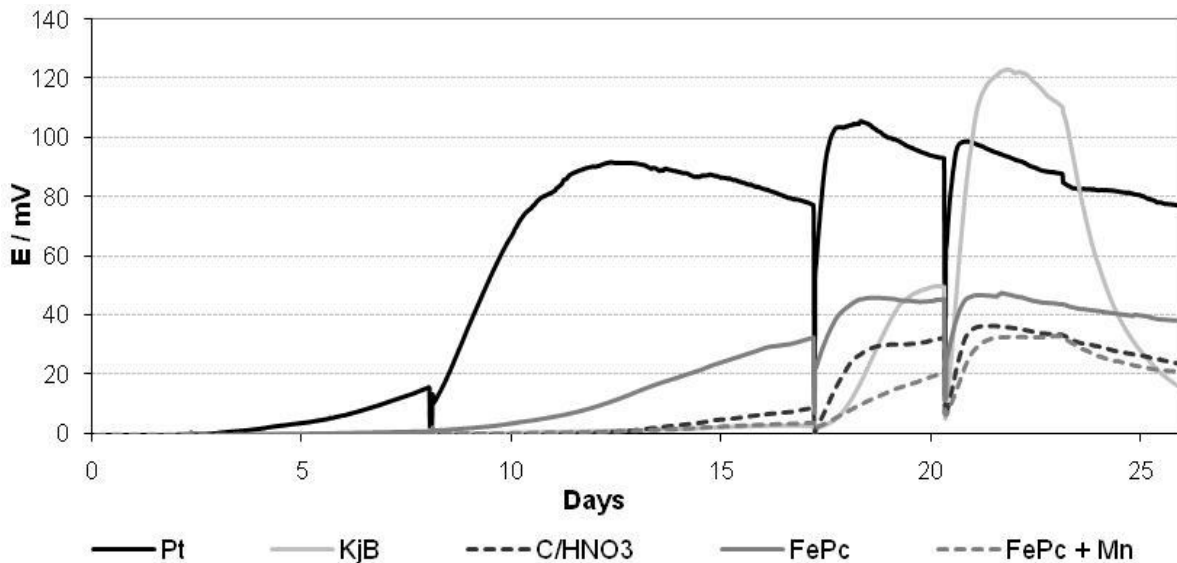
Figure 5.2: Voltage evolution of the reactors using different cathodes with activated carbon cloth (FM30k) anodes.

Figure 5.3 shows the accumulated charge produced by the different cathodes under 1 kΩ external resistance using C/HNO$_3$ and activated carbon cloth as anode. A steeper slope correlates to more current produced thus better energy production. Platinum rapidly reached high voltage after a short acclimatisation period, followed by FePc, C/HNO$_3$, carbon black and FePc+Mn using the C/HNO$_3$ anode. The longer acclimatisation period for carbon black is visible in the slow accumulation until the 24th day, whereby there was a large increase.

Using activated carbon cloth as the anode material, platinum produced the most charge. But whereas the charge produced with FePc showed a steady increase, the charge produced with carbon black increased steeply after 20 days equalling the charge produced by FePc in the last batches (Figure 5.3).
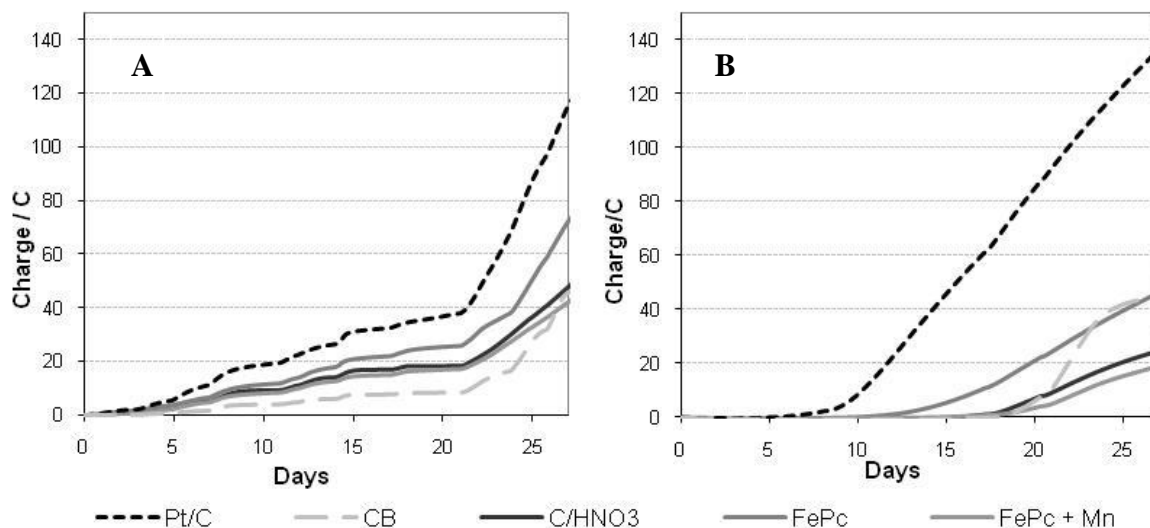
Figure 5.3: Comparison of the accumulated charge for the different cathode catalysts using C/HNO$_3$ (A) and FM30k (B) anodes.

Although platinum was the best performing material and produced the most charge, followed by FePc, carbon black showed a lower decrease in peak voltage obtained over time. Activated carbon black and FePc+Mn produced the least charge and had the highest deterioration in voltage production over time (Figure 5.1).

5.4.1.2 Steady state polarisation results

The polarisation behaviour of the microbial fuel cell reactors under a constant external load of 1000 Ω was studied after 31 days (acclimatisation) and 56 days (decrease in voltage evolution with C/HNO$_3$ anodes). A change in anode material to test the influence of the anode material on the reactor performance meant the polarisation behaviour of the reactors was also tested after 100 days using activated carbon cloth (FM30k) as anode material.

Figure 5.4 shows the average voltage, current and power density achieved over the different batches under 1000 Ω external resistance. The greatest decrease in performance was observed for reactors using platinum and FePc cathodes from 29 mW m^{-2} (at 152 mA m^{-2} and 190 mV) and 16 mW m^{-2} (at 113 mA m^{-2} and 141 mV) on the 31st to 4 mW m^{-2} (at 58 mA m^{-2} and 73 mV) and 1 mW m^{-2} (at 28 mA m^{-2} and 36 mV) on the 56th day respectively. But the power performance of reactors recovered slightly when changing the anode material achieving power

densities of 8 mW m^{-2} (at 78 mA m^{-2} and 98 mV) for platinum and 2 mW m^{-2} (at 37 mA m^{-2} and

47 mV) for FePc. Carbon black achieved the second best performance reaching power densities

of 23 mW m^{-2} (at 137 mA m^{-2} and 171 mV) but declined gradually, even though slower than

platinum, over time. FePc+Mn and activated carbon showed poor performances from the

beginning with 3 mW m^{-2} (at 45 mA m^{-2} and 56 mV) and 4 mW m^{-2} (at 54 mA m^{-2} and 68 mV)

respectively and their performance declined further over time(Figure 5.4). An increase in power

densities was observed for reactors using Pt, FePc, FePc+Mn and C/HNO$_3$ as cathode after the

anode materials switched from activated carbon powder to activated carbon cloth. This

increase was not achieved for carbon black cathodes, which demonstrated a slow decrease

over time with the change in anode material showing no appreciable influence. This suggests

the cathode had a significant influence on the MFC performance.
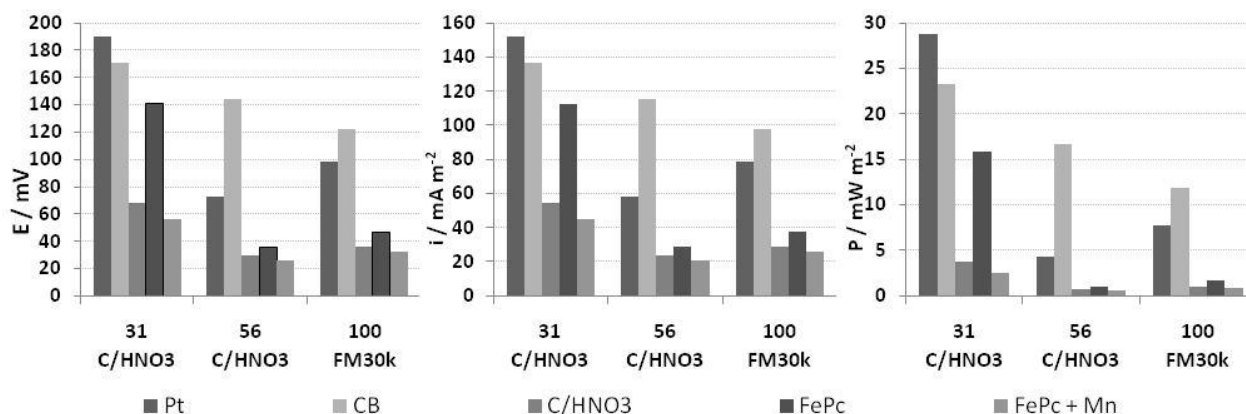
Figure 5.4: Average voltage, current and power density achieved using different cathode materials and C/HNO$_3$ or FM30k anodes for batches at 31, 56 and 100 days operation.

However, as the performance did not recover to previously high power densities this suggests

an irreversible reduction in cathode activity through catalysts deactivation or poisoning. All

materials could conceivably be influenced by the same substances in the wastewater. The poor

activity from the start makes C/HNO$_3$ and FePc+Mn unsuitable as cathode materials in

wastewater fed microbial fuel cells.

HaoYu *et al* (2007) achieved 20 times the power densities reached in this study in glucose fed

reactors using FePc as cathode material. Similarly reported Duteanu *et al* (2010) and Li *et al*

(2010) 20 times higher power densities in acetate fed reactor with activated carbon black as

cathode and wastewater supplemented with acetate fed reactors using manganese dioxide as

cathode catalyst. However the power performance is influenced by the substrate as well as

reactor architecture and the lower power performances were reported using complex substrates (such as a range of wastewaters) (Pant et al., 2010; Scott and Murano, 2007). Both factors make direct comparisons of cathode catalysts in MFC tests difficult. Scott *et al* reported a peak power density of 5 mW m^{-2} using a manure fed microbial fuel cell with carbon cloth anode and cathode. But in contrast to this study little deterioration of the carbon cloth electrodes was reported over three month operation. In addition the use of a selective membrane and biocathodes could be an inexpensive solution to long-term stability with high power densities in microbial fuel cell systems (Rabaey and Keller, 2008; Clauwaert et al., 2007; He and Angenent, 2006).

Table 5.2 shows the internal resistance measured using the different activated carbon materials. For reactors with both the anode material a high internal resistance was recorded. The internal resistance decreased slightly from 257 Ω to 239 Ω for reactors using carbon black cathodes when switching from C/HNO$_3$ to FM30k anodes. For all other cathode materials the internal resistance increased, probably reflecting a further deactivation of the catalyst materials through continuous usage visible in a higher charge transfer resistivity in the cathode (

Table 5.2).

Table 5.2: Internal resistance of the cathode materials using two different anode materials

Anode		Pt	CB	C/HNO$_3$	FePc	FePc+Mn
C/HNO$_3$	/ Ω	575	257	495	496	571
FM30k	/ Ω	905	239	522	520	780

5.4.1.3 Anode and cathode behaviour and activity

The cathode activity was investigated for MFCs using both anodes when the decrease in cell voltage production occured. Figure 5.5 shows the anode and cathode polarisation behaviour. The cathode potential was calculated IR correct cell potential using the measured internal resistance according to $E_{Cathode}=E_{Cell}+E_{Anode}$.

The overpotential was smaller on the anode than the cathode for all reactors using either activated carbon materials as anode (Figure 5.5). The poor performance of the cathodes (MFCs using activated carbon cloth anodes) was apparent through high overpotential losses of 400 mV or more with C/HNO_3 anodes and more than 500 mV overpotential for C/HNO_3, FePc and FePc+Mn. Platinum did not perform much better with overpotential losses of 450 mV and 290 mV for C/HNO_3 and activated carbon cloth anodes respectively. Carbon black showed two time the overpotential losses with 240 mV over a current density of 283 mA m^{-2} using C/HNO_3 anodes and 220 mV over a current density of 522 mA m^{-2} using activated carbon cloth as anode. The only exception to this was platinum where a high overpotential was observed on anode and cathode when using activated carbon cloth anodes (Figure 5.5 B).
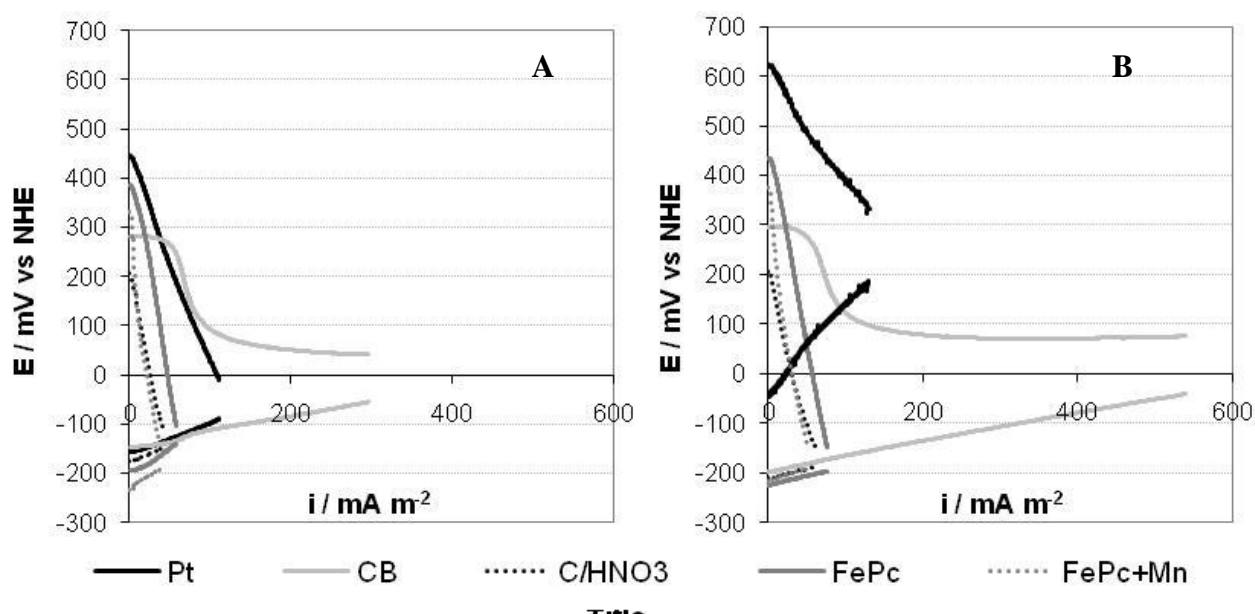
Figure 5.5: Linear sweep voltammogram showing the IR corrected cathode (black) and anode (grey) potential of Pt, CB , C/HNO_3, FePc and FePc+Mn using C/HNO3 (A) and FM30k (B) as anode material.

The carbon black cathode polarisation curve showed a two wave profile for as cathode material. This may indicated a change in oxygen reduction mechanisms corresponding to the oxygen reduction to peroxide, as discussed in Chapter 4.

The onset potential of the C/HNO_3 anodes varied between 20 to 70 mV. The variation in onset potential decreased to 5 mV when using activated carbon cloth anodes with the exception of platinum where the anode showed a 150 mV shift in onset potential. The differences in anode potential of the same anode materials in the different reactors suggest variations in the biofilm

populating the anode materials and for the reactors with C/HNO_3 as anode materials also due to slight differences in the anode fabrication. A significant shift in anodic onset potential from 174 mV to 41 mV was observed for platinum cathodes when changing from C/HNO^3 to FM30k anodes. An explanation for this was not found.

Although platinum showed the best power performance under constant load, the most stable performing reactors used carbon black cathodes. An explanation for this could be the large specific surface area of carbon black and its resistance to poisoning. Freguia *et al.* (2007) came to a similar conclusion, when achieving high power densities using carbon granules as cathode in a continuous two chamber system. Although carbon black showed the lowest losses in this system, the overpotential losses were still higher on the cathode than the anode thus showing that the cathode activity is the greater limitation to high power density in the system.

Tafel plots were used to analyse the relative cathode activity (Appendix, Figure 10.2). Table 5.3 shows the slope, the transfer coefficient α and the exchange current density i_0. The Tafel slope shows the voltage change per decade of current density. Therefore a lower slope shows higher activity towards ORR.

Table 5.3: Average relative activity of the cathodes, calculated using the geometric surface area, measured as the Tafel slope, α and i_0 of η vs log i.

	Slope / mV dec^{-1}	α	i_0 / mA m^{-2}
Pt	-558±54	0.11±0.01	3.15±2.4
CB	-738±94	0.08±0.01	10.4±2
C/HNO$_3$	-463±10	0.13±0.003	0.5±0.001
FePc	-961±36	0.06±0.002	7.4±0.1
FePc+Mn	-442±62	0.13±0.02	0.46±0.3

The cathode catalysts FePc+Mn and C/HNO_3 had the lowest slopes during reactor tests with 442±62 mV dec^{-1} and 463±10 mV dec^{-1} respectively. But the obtained low exchange current density for FePc+Mn and C/HNO_3 showed that both materials reached low current densities and therefore showed poor performance which could also be seen in Figure 5.4. Platinum,

carbon black and FePc showed higher slopes of 558±54 mV dec^{-1}, 738±94 mV dec^{-1} and 961±36 mV dec^{-1} respectively. Corresponding exchange current densities were 10 times higher than for C/HNO$_3$ and FePc+Mn with 10.4±2 mA m^{-2} for carbon black, 7.4±0.1 mA m^{-2} for FePc and 3.15±2.4 mA m^{-2} for platinum.

Although the high slope for carbon black indicated less activity, exchange current densities achieved were higher presumably due to a higher surface are. The low α for all cathode materials indicated that high activation energy is required for the reaction. For platinum the most likely explanation for the low activity is the gradual inhibition and poisoning of the the catalyst material by substances in the wastewater which are transported through the microporous separator to the cathode.

Platinum, FePc, FePc+Mn and C/HNO$_3$ achieved high ORR activity in published half cell and microbial fuel cell tests in literature (Duteanu N, 2010; Harnisch et al., 2009b; Roche and Scott, 2009; HaoYu et al., 2007; Baranton et al., 2005; Zhao et al., 2005). Direct comparisons with this study are not possible as cathode catalysts in microbial fuel cell systems did not compare the catalytic activity using the Tafel slope, transfer coefficient α or the exchange current density i_0 which are commonly used in fuel cell studies to directly compare catalyst activity.

Also as most studies on alternative cathode catalysts used known substrates (such as acetate with PBS) as feed this suggests that not only platinum but also the non-precious metal catalysts are sensitive to deactivation or poisoning from substances in the wastewater. Therefore the most likely explanation for the low activity of platinum is the gradual inhibition and poisoning of the catalyst material by substances in the wastewater which pass through the microporous separator to the cathode. Sulphide is known to notably reduce the activity of platinum and FePc towards oxygen reduction due to sulphur formation on the electrode and precipitation of FeS on FePc cathodes (Harnisch et al., 2009b). Decomposition of organic matter produces sulphides (sulphur cycle) (Metcalf & Eddy. et al., 2003; Peavy et al., 1985). Wastewaters commonly contain sulphides. Though microbial fuel cells have been shown to remove sulphur pollutants (Zhang et al., 2010a; Zhao et al., 2009; Rabaey et al., 2006) even small amounts of sulphide diffusing through the membrane would noticeably reduce the cathode activity.

As a catalyst activated carbon is comparable to carbon black but with a greater specific surface area and more surface groups, both factors which should lead to higher activity. Following this conclusion (Duteanu N, 2010) reported good activity using nitric acid activated carbon cathodes in an air cathode system using acetate and PBS as substrate. Contrasting with these results the low activity observed in this study could be explained through deactivation of the material possibly by sulphide poisoning of the surface groups although this was not investigated further and was not observed for carbon black as cathode catalyst.

5.4.1.4 Polarisation studies
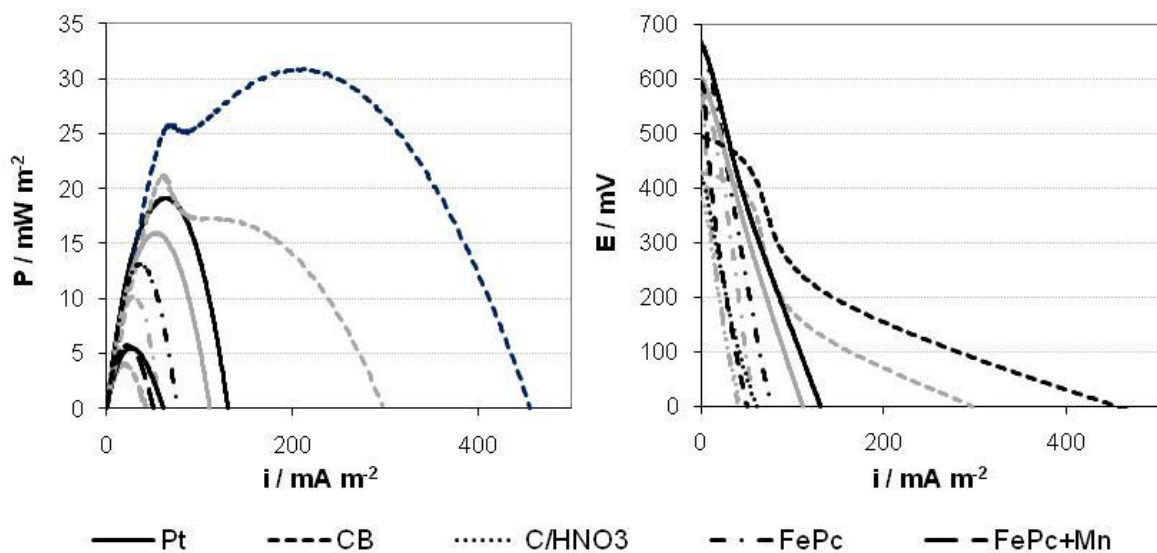
Figure 5.6: Linear sweep polarisation curves of cell potential and power density for the different cathodes using C/HNO$_3$ (grey) and FM30k (black) as anode material

Figure 5.6 shows the cell voltage and power density data achieved using activated carbon cloth (FM30k) as the anode for cells with all cathode materials. The most stable performance was observed in reactors using carbon black as cathode catalyst, which also achieved highest peak power densities of 21 mW m^{-2} at 60 mA m^{-2} and 355 mV with C/HNO$_3$ anodes and a third higher power densities of 31 mW m^{-2} at 201 mA m^{-2} and 154 mV using FM30k anodes. This was more than reactors using platinum catalysts achieved with 16 mW m^{-2} (at 51 mA m^{-2} and 311 mV) and 19 mW m^{-2} (at 61 mA m^{-2} and 312 mV) followed by FePc with 10 mW m^{-2} (at 27 mA m^{-2} and 369 mV) and 13 mW m^{-2} (at 34 mA m^{-2} and 377 mV) while FePc+Mn and C/HNO3 reached similarly

lowest power densities at 4 mW m^{-2} and 5.5 mW m^{-2} for C/HNO$_3$ and FM30k anodes respectively

5.4.2 Wastewater treatment efficiency

Figure 5.7 shows the change in pH and conductivity of the reactors using platinum, carbon black, FePc, FePC+Mn and activated carbon as cathode materials and the control reactor (feed under anaerobic conditions) using activated carbon powder (A;C) or activated carbon cloth (B;D) as anode material. The conductivity decreased for all MFC reactors over two days when activated carbon cloth was used as anode material. When C/HNO$_3$ was used as anode material, the conductivity in FePc and FePc+Mn reactor decreased only slowly after the first day. The conductivity in the control reactor remained, as expected, constant. Similarly to the conductivity, the pH showed a decrease over the first day, after which the pH stabilised when using C/HNO$_3$ anodes (Figure 5.7 C) and increased again when using activated carbon anodes (Figure 5.7 D).

The pH and conductivity decreased as any ions in the wastewater transfer from the anode chamber through the membrane to the cathode. Although protons are consumed at the cathode decrease in pH observed shows an accumulation of protons in the anode chamber. One possible explanation for this phenomenon is the preferential transfer of other cations through the membrane as their number is usually 1000 to 10 000 times higher than the amount of protons in the substrate (Rozendal et al., 2006). The conductivity as a measure of all ions in the solutions decreased. Therefore a more rapid decrease in conductivity over a batch should be an indicator of better performance of the reactor as more cations are used at the cathode whereas the decrease of the pH might also be dependent on the membrane used. In the control reactor (substrate under anaerobic conditions) the a less rapid decrease in pH was observed and the conductivity remained relatively constant since protons were not produced or cations consumed. Higher power production resulted in a more rapid decrease of the pH and conductivity thus showing that both can be used as an indicator for power performance in MFCs.
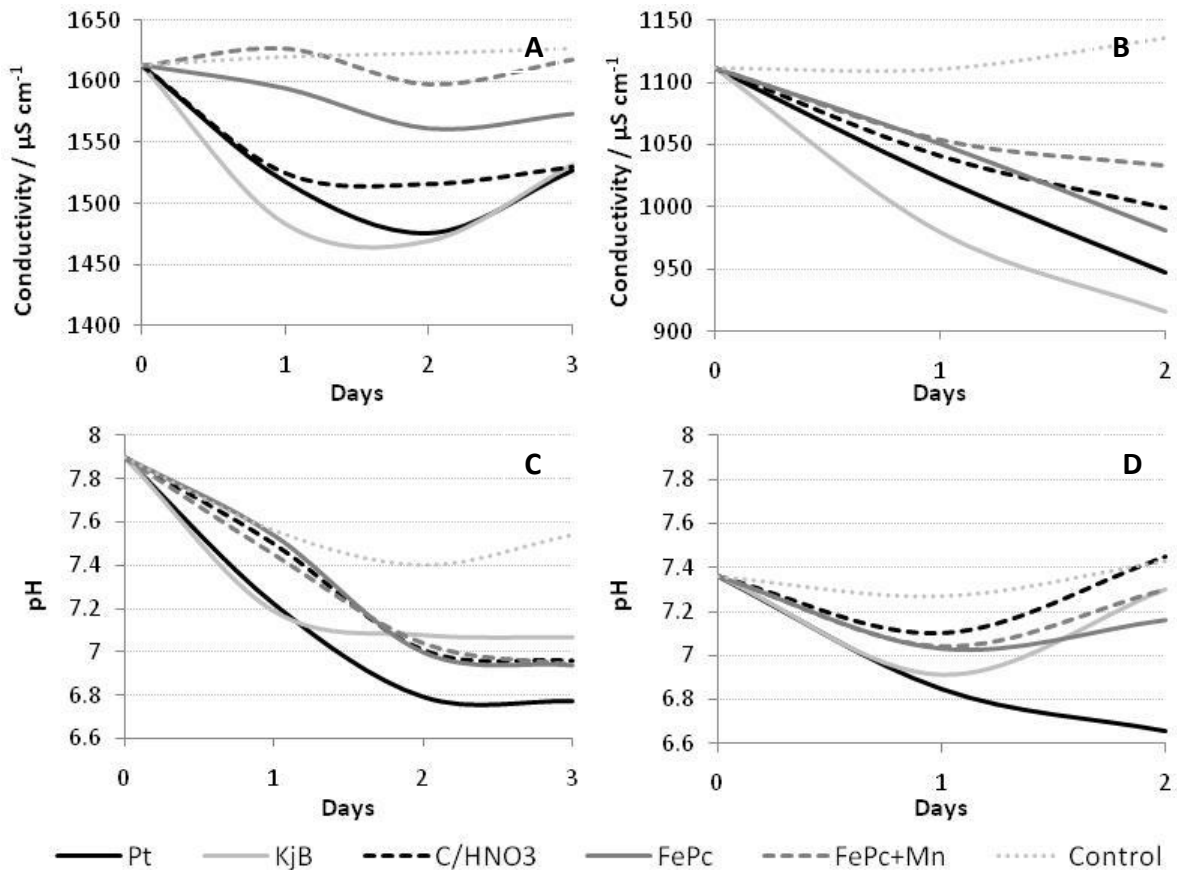
Figure 5.7: Conductivity (A;B) and pH (C;D) for the reactors, with different cathodes, using activated carbon powder (C/HNO$_3$) (A;C) and activated carbon cloth (B;D) as anode materials each over one batch.

The wastewater treatment efficiency (Figure 5.8) was on average 65%, 75% and 63% COD removal for batches starting on the 31st, 56th and 100th day whereas the control reactor (feed under anaerobic digestion) reached slightly lower COD removal of 50%, 61% and 56% for 31, 56 and 100 days respectively. The reactors with platinum, carbon black, C/HNO$_3$ and FePc reached higher COD removal with on average 70% than the reactors using FePc+Mn as cathode material. The MFC system achieved higher COD removal than the control reactor due to the current demand under 1000 Ω external load on the system.

The coulombic efficiencies achieved using C/HNO$_3$ anodes were high during the first sampling after 31 days. The highest CE was documented for platinum with 30% followed by FePC with 24%. Carbon black achieved 20% CE and activated carbon 17%. FePc+Mn reached the lowest CE with 10%. The decrease in power performance using C/HNO$_3$ anodes was reflected in the coulombic efficiencies which after 56 days were 11% for carbon black, followed by 7% for

101

platinum, 4% for FePc+Mn and 2% for C/HNO$_3$ and FePC both. The use of FM30k as anode material nearly doubled the coulombic efficiency for platinum and carbon black to 55% and 43% respectively. A less impressive increase was observed for FePc, C/HNO$_3$ and FePc+Mn with 27%, 19% and 17% respectively (Figure 5.8).
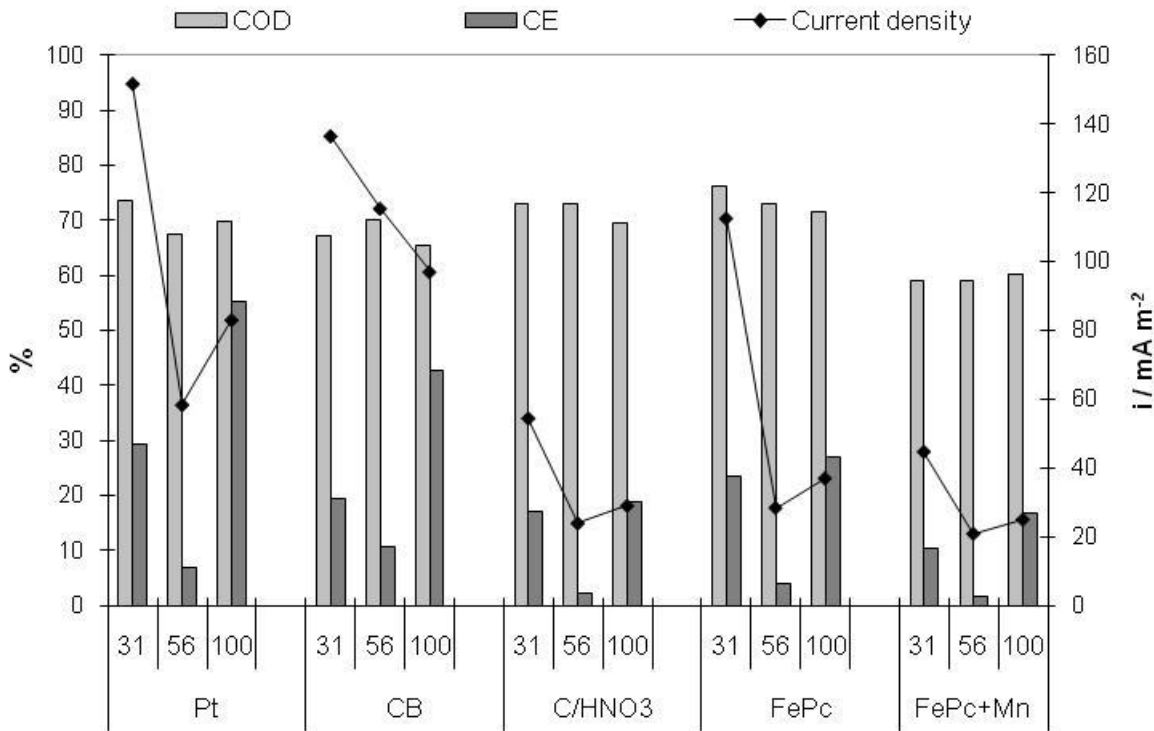
Figure 5.8: Percentage COD removal, coulombic efficiency and current produced over time using the different cathodes.

Reactors using activated carbon cloth achieved higher coulombic efficiencies even when lower power densities were reached than good performing reactors using activated carbon powder (C/HNO$_3$) as anode material. Higher coulombic efficiencies were achieved in better performing reactor which suggests that electricity production is one of the main processes happening in these reactors.

Typically coulombic efficiencies are low in wastewater fed microbial fuel cell due to the complexity of the substrate. Cheng *et al* (2006) reported a coulombic efficiency of 27% using wastewater as substrate whereas Li *et al.* (2010) reported coulombic efficiencies of up to 11.3% using wastewater supplemented with acetate as feed substrate. Consequently the high coulombic efficiencies achieved in this study highlight the attractiveness of activated carbon in cloth as anode material in microbial fuel cell reactors.

5.5   CONCLUSION

There was a loss in activity for all catalysts over time, as substances from the wastewater (putatively sulphides) are able to directly interact with the catalyst to inhibit, poison or deactivate it. The rapid decline over just 100 days in steady state power performance is a concerning trend for commercial use of microbial fuel cells using air diffusion cathodes in wastewater.

The carbon black cathode showed the best durability even though it was least active cathode material in half cell tests. In contrast platinum, FePc, FePc+Mn and activated carbon, all more active catalysts under ideal conditions, showed a rapid decline in power performance.

The better coulombic efficiencies using activated carbon cloth could be due to the higher specific surface area of the material, compared to the activated carbon powder, which is more suitable for microbial colonisation.

The rapid decline in power performance of the air cathodes suggest that catalyst materials have to be tested more rigorously under realistic conditions since crossover of inhibiting substances from wastewater is not completely preventable even when using a selective membrane, though this would probably cause a slower decline in power performance.

6 MEMBRANE STUDIES

ABSTRACT

In a microbial fuel cell the membrane separates the anode and cathode reactions. To achieve this, membranes need to be selective, durable, biocompatible, unsusceptible to fouling and clogging and be inexpensive.

A range of different membranes and separators were characterised for fouling, ion conductivity, and oxygen permeability. This lead to the investigation of the ion exchange membranes Nafion, two radiation grafted membranes bases on ethylene tetrafluoroethylene (ETFE) and polyvinylidene fluoride (PVDF), the microporous separators Rhinohide and carbon paper, as a membrane-less reactor with an internal cathode, in MFC reactor studies.

The membranes had a significant influence on the system which was illustrated by different profiles for the voltage evolution. The membrane-less reactors, using carbon paper with an internal cathode, showed the greatest potential during polarisation reaching a power density of 67 mW m^{-2}. Reactors using Nafion and ETFE ion exchange membranes achieved power densities of 61 mW m^{-2} and 59 mW m^{-2} respectively. Lower power densities were obtained with reactors using PVDF (26 mW m^{-2}) and Rhinohide (23 mW m^{-2}) during polarisation. Under a constant external resistance of 1000 Ω the reactors using Nafion and ETFE reached on average power densities of 29 mW m^{-2} and reactors using carbon paper achieved 24 mW m^{-2}. The worst performing reactors used Rhinohide (14 mW m^{-2}) and PVDF (11 mW m^{-2}).

The best performing reactors using the ion exchange membranes ETFE and Nafion showed a more pronounced decrease in pH over the first day of the batch and achieved high coulombic efficiencies with 92±6% and 71±12% respectively. Membranes-less reactors reached coulombic efficiencies of 68±11% followed by PVDF with 66±20% CE and 63±8% CE for Rhinohide.

6.1 INTRODUCTION

The function of a membrane in a fuel cell system is to separate the anode and cathode reaction and permit selective transport of protons from the anode to the cathode. In microbial fuel cells the membrane needs to be selective (proton conducting), durable, chemically stable, biocompatible, unsusceptible to fouling and clogging (especially when using fuels of unknown and changeable composition such as wastewater) and be inexpensive.

Challenges of using membranes and air cathode in a membrane-electrode-assembly (MEA) architecture are (Zhang et al., 2010b; Harnisch et al., 2009a; Chae et al., 2008; Harnisch et al., 2008; Rozendal et al., 2008; Kim et al., 2007)

- Oxygen transport through cathode and membrane into the anode chamber which reduces power densities and coulombic efficiencies due to oxygen scavenging of the microbial consortia;

- Substrate loss through the membrane;

- Cation, and other ion, transport through the membrane to the cathode where salts (i.e. carbonates) are formed, which might inhibit the activity of the cathode catalyst;

- Higher resistance to the proton transport through the membrane due to fouling and clogging over time, as microorganisms and complex substrates are used on the anode side;

- Cost- Nafion, the most commonly used proton exchange membrane (PEM) in microbial fuel cells, is too expensive for use in wastewater treatment.

Various strategies were investigated to provide a solution to these challenges. A range of cheaper cation, anion, monopolar and bipolar ion exchange membranes as well as ultrafiltration membranes have been tested in attempts to balance the pH difference between anode and cathode chamber due to ion transport through the membrane and also to reduce costs (Harnisch et al., 2009a; Pant, 2009; Sun et al., 2009; Harnisch et al., 2008; Kim et al., 2007; Rozendal et al., 2007; Grzebyk and Pozniak, 2005). Other studies used microporous battery separators, carbon paper, carbon cloth, glass beads, glass wool or glass fibre as low cost alternatives to membranes. In these studies the anode and cathode chamber are still separated

but not with a selective membrane. Consequently any substance in the substrate is able to transfer from the anode chamber to the cathode. Oxygen diffusion into the anode chamber depends on the porosity of the separator material and any additional layers (J-cloth) (Zhang et al., 2009b; Liu et al., 2008; Fan et al., 2007; Ghangrekar and Shinde, 2007; Scott et al., 2007; Jang et al., 2004; Liu and Logan, 2004). This architecture is in many studies called membrane-less, but this study identifies membrane-less microbial fuel cells as only those microbial fuel cells where the the anolyte solution (substrate and microorganisms) serves as a 'natural' boundary between anode and cathode chamber, as long as the electrode spacing is wide enough (Du et al., 2008).

All these studies have shown that understanding of the membrane/separator characteristics and their influence on microbial fuel cell performance is essential to attain high power densities and coulombic efficiencies. But few (Chae et al., 2008) have studied the membrane characteristics as well as reactors performance when used.

In this chapter a number of membranes and separators were characterised and the best performing separators and membranes were tested in microbial fuel cell reactors.

6.2   HYPOTHESIS

High power densities and coulombic efficiencies can be achieved using a cheap separator or the electrolyte itself as separator as well as with the use of an ion exchange membrane in wastewater fuelled microbial fuel cells.

6.3   MEMBRANE CHARACTERISTICS

6.3.1   Introduction

A membrane separator should be chosen depending on the characteristics weighted against the requirements of the system used. In microbial fuel cell system these requirements include (Arora and Zhang, 2004):

- Low oxygen diffusion coefficient;
- Minimal ionic resistance;
- Hydrophilic and readily wetted by the substrate;
- Proton or ion conducting depending on the cathode catalyst;
- Effective in preventing crossover/migration between the two electrodes;
- Resistant to fouling and degradation by the substrate and microorganisms and build-up of substances in the membrane pores;
- Sufficient chemical stability;
- Durable with sufficient physical strength to allow easy handling;
- Inexpensive.
- Biocompatible.

Depending on the application the importance of these requirements varies. Often a compromise must be reached i.e. when optimising performance and cost. For wastewater treatment low cost together with durability and resistance to fouling is the most important requirement for an economical viable system generation energy even though low oxygen diffusion, ionic resistance and crossover benefit power generation enormously.

6.3.2   Experimental

In this study a number of membranes and separators were characterised on fouling, oxygen diffusion and their ionic resistance. The membrane separators studied were either ion exchange membranes, or durable microporous or fibrous separators (Table 6.1). All membranes and separators studied were durable and inert and showed high chemical stability.

6.3.2.1 Materials

Table 6.1 lists the membranes and separators used:

- Rhinohide, an inexpensive microporous battery separator produced by Entek International, UK was used in previous experiments as membrane separator. It is a composite of ultra-high-molecular weight polyethylene and silica (UHMWPE/Si) and is characterised by its hydrophilicity, strength and porosity (55±5%).

- Five separator materials (Scimat), made out of polypropylene (PP) or composite polypropylene/polyethylene (PP/PE) fibres. The surface of the fibres has been grafted with polyacrylic acid to increase the hydrophilicity and provide an ion exchange function (around 0.8 meg g^{-1}, as characterised by Freudenberg, Germany). Scimat 700/30k and 700/40k have been neutralised and are in the potassium salt form, while the other materials are in the acid form. All Scimat materials were produced by Freudenberg.

- Tyvek (produced by DuPont, USA), a versatile separator made of spunbonded olefins (high density polytheylene fibres). It has outstanding chemical and rot and mildew resistance, high porosity and strength.

- Toray carbon paper (E-Tek, UK), which was studied in a membrane-less design as a conductive support for the cathode inside the anode chamber

- Nafion 117, a perfluorinated sulphonic acid (PFSA) membrane characterised through its mechanical strength, chemical stability, high electrical conductivity and permeable selectivity produced by DuPont, USA. It is most commonly used as a proton exchange membrane in fuel cell systems (Mauritz and Moore, 2004; Stenina et al., 2004; Lehmani et al., 1997; Unnikrishnan et al., 1997).

- Five radiation grafted membranes based on ETFE, PVDF and HDPE supplied by J.A. Horsfall, Cranfield University.

Table 6.1: Materials and use of the membranes tested.

Membrane	Use	Material
Nafion 117	Proton exchange membrane	PFSA/PTFE copolymer
Rhinohide	Microporous separator	UHMWPE/silica
Scimat 700/70	Nonwovens	PP fibres
Scimat 700/77	Nonwovens	PP fibres
Scimat 700/30k	Nonwovens	PP/PE fibres
Scimat 700/40k	Nonwovens	PP/PE fibres
Scimat 850/61	Nonwovens	PP fibres
Tyvek	Nonwovens	HDPE fibres
Carbon paper	Gas diffusion layer	Carbon paper
ETFE-g-PSSA D.O.G. 23%	Ion exchange membrane	ETFE/PSSA
ETFE-g-PSSA D.O.G. 35%	Ion exchange membrane	ETFE/PSSA
HDPE-g-PSSA D.O.G. 11%	Ion exchange membrane	HDPE/PSSA
CoPVDF-g-PSSA D.O.G. 10%	Ion exchange membrane	PVDF/PSSA
PVDF-g-PSSA D.O.G. 34%	Ion exchange membrane	PVDF/PSSA

Table 6.2 lists the radiation grafted membranes tested. For the radiation grafted membranes an inert polymer base was cross-linked through the use of γ radiation with a monomer forming a grafted copolymer. The radiation grafted membranes have a backbone based on ETFE, PVDF and HDPE which incorporates suphonic acid groups which provide ionic pathways for proton transport (Table 6.2) (Patel et al., 2009; Cheng et al., 2007; Gubler et al., 2005; Shen et al., 2005; Horsfall and Lovell, 2002; Scott et al., 2000; Lehtinen et al., 1998; Hietala et al., 1997; Gupta et al., 1996). The radiation grafting of polymer and monomer with different characteristics means the produced copolymer shows the desired hydrophilic properties without impairing the chemical resistance (Arora and Zhang, 2004). All ion exchange membranes were apparent smooth films.

Table 6.2: Radiation grafted ion exchange membranes with the characteristics supplied by J.A. Horsfall from Cranfield University.

Membrane	Base Film	Thickness (pre-grafting) / μm	Degree of Grafting / %	IEC / meq g^{-1}, Na^+ Form
3907P	**ETFE**	125	23	1.784
3911P	**PVDF Copolymer**	100	10	0.826
3986P	**PVDF**	30	34	2.268
3541P	**ETFE**	50	35	1.984
3546P	**HDPE**	40	11	0.568

6.3.2.2 Membranes fouling

The resistance of the membrane separators to fouling and degradation by the substrate and microorganisms in the wastewater was tested by immersion of the membranes in wastewater under anaerobic conditions. Over six month every two weeks the wastewater was pumped out of the batch reactors and refilled with new wastewater. The membranes were then dyed with DAPI and studied using a confocal microscope to visualise microorganisms on and especially inside the membrane separators.

6.3.2.3 Ion conductivity

The ion conductivity was measured in a steel electrochemical cell with a surface area of 3.2 cm^2 by measuring the resistance in the cell with a membrane in 1M phosphate buffer solution (PBS) using AC impedance. The background electrolyte resistance $R_{Electrolyte}$ was subtracted from the cell resistance R_{Cell} to obtain the membrane resistance R_{Mem}. As the electrolyte resistance accounted in most cases for 50% or more of the cell resistance this correction was essential.

$$R_{Mem} = R_{Cell} - R_{Electrolyte} \tag{6.1}$$

From the membrane resistance R_{Mem} the area resistance R_A, the resistivity ρ and the conductivity κ of the membranes can be calculated.

$$R_A = R_{Mem} \cdot A \tag{6.2}$$

$$\rho = \frac{R_A}{L_t} \tag{6.3}$$

$$\kappa = \frac{L_t}{R_A} \tag{6.4}$$

Where A is the membrane area and L_t the membrane thickness.

6.3.2.4 Oxygen mass transfer, diffusion coefficient and membrane permeability

The oxygen permeability of membranes and separators was determined for each membrane using a single chamber microbial fuel cell filled with nitrogen sparged water at 298 K. The anodic chamber was stirred continuously to ensure the same oxygen concentration throughout. A dissolved oxygen (DO) probe was placed in the anode chamber and the DO concentration in the chamber was recorded over time.

In a completely mixed two chamber system the mass balance of dissolved oxygen in the chamber is determined through (Chae et al., 2008; Kim et al., 2007; Logan, 1999):

$$V\frac{dc}{dt} = J_O A = \frac{D_O A}{L_t}(c_0 - c) \tag{6.5}$$

Where V is the chamber volume, J_O is the oxygen flux, A is the membrane area, L_t the membrane thickness, c_0 is the saturated oxygen concentration in the aerated chamber, c is the dissolved oxygen concentration at time t in the anode chamber.
The solution of which is

$$D_O = -\frac{VL_t}{At} \ln\left[\frac{c_0 - c}{c_0}\right] \tag{6.6}$$

Using equation 6.5 the diffusion coefficient D_O and the mass transfer coefficient k_O for a two chamber can be calculated as:

$$k_O = -\frac{V}{At} \ln\left[\frac{c_0 - c}{c_0}\right] \tag{6.7}$$

$$D_{O_2} = k_O L_t \tag{6.8}$$

In a single chamber microbial fuel cell system the aerated chamber is the air around itself. Thus the concentration of oxygen c_0 in the air chamber can be determined using Henrys law (Atkins and De Paula, 2009; Perry et al., 1984; R. Battino, 1966).

$$c_0 = \frac{k_H}{p_{g_{O_2}}}$$

(6.9)

Where k_H is Henry's coefficient for oxygen and p_{gO2} is the partial pressure of oxygen. The coefficient $k_H = 7.92 \cdot 10^4$ kPa kg mol^{-1} at 298 K was taken from Atkins (2009).

The membrane permeability P_M was calculated as (Ritchie et al., 1996)

$$P_M = \frac{k_{Transfer}}{A \cdot 1atm}$$

(6.10)

Where $k_{Transfer}$ is the transfer rate of oxygen into the anodic chamber.

6.3.3 Results and discussion

After the membrane separators were immersed in wastewater microorganisms were seen as a film which only partly covered the membranes. No visual evidence of the degradation of the ion exchange membranes through microorganisms was apparent. The radiation grafted membrane based on HDPE did not show a biofilm when studied under the confocal microscope. Like the ion exchange membranes Rhinohide showed a biofilm on the surface but no visual evidence for penetration of the microorganisms into the materials itself was observed. Scimat and Tyvek are obviously fibre grafted separators. Scimat 700/40k, 850/61 and Tyvek had the highest number of microorganisms accumulating between the fibres where the other separators showed little accumulation of microorganisms.

Conductivity measurements (Table 6.3) of the membrane separators showed that Tyvek and the radiation grafted membrane based on HDPE were as the most resistive materials with the lowest ion conductivity. Rhinohide and Scimat 700/30k achieved the highest ion conductivity followed by Scimat 700/70 and 700/77. An average conductivity between $8.5 \cdot 10^{-3}$ S cm^{-1} and $15.7 \cdot 10^{-3}$ S cm^{-1} was observed for both radiation grafted membranes based on ETFE and Scimat 700/40k followed by Nafion, Scimat 850/61 and for radiation grafted membranes based on PVDF.

Tyvek's high resistivity is probably attributed to its hydrophobic behaviour which makes wetting of the pores difficult and thus leads to low ion transfer through the pores.

Table 6.3: Conductivity measurements of the separators and membranes studied using AC impedance spectroscopy in 1M PBS.

Membrane Separator	Thickness / μm	Area resistance / Ω cm^2	Conductivity / S cm^{-1}	Resistivity / Ω cm
Nafion	183	1.93	$9.5 \cdot 10^{-3}$	105.65
Rhinohide	668	1.69	$39.4 \cdot 10^{-3}$	25.35
Scimat 700/70	127	0.49	$25.7 \cdot 10^{-3}$	38.85
Scimat 700/77	117	0.51	$23.0 \cdot 10^{-3}$	43.53
Scimat 700/30k	130	0.27	$48.3 \cdot 10^{-3}$	20.72
Scimat 700/40k	103	0.78	$13.2 \cdot 10^{-3}$	75.86
Scimat 850/61	91	1.07	$8.5 \cdot 10^{-3}$	117.51
Tyvek	146	31.09	$0.5 \cdot 10^{-3}$	2129.13
Carbon paper	300	n/a	n/a	n/a
ETFE-g-PSSA D.O.G. 23%	164	1.05	$15.7 \cdot 10^{-3}$	63.84
ETFE-g-PSSA D.O.G. 35%	66	0.48	$13.8 \cdot 10^{-3}$	72.32
HDPE-g-PSSA D.O.G. 11%	39	6.77	$0.6 \cdot 10^{-3}$	1734.70
CoPVDF-g-PSSA D.O.G. 10%	115	3.53	$3.3 \cdot 10^{-3}$	307.25
PVDF-g-PSSA D.O.G. 34%	45	0.49	$9.1 \cdot 10^{-3}$	109.63

There is little literature in microbial fuel cells on the ion conductivity of membranes. Only (Harnisch et al., 2008) studied the area resistance of Nafion with 9.2 Ω cm^2, and anion exchange membrane with 12.4 Ω cm^2 and a cation exchange membrane with 45.1 Ω cm^2 in 0.05 M PBS. This is much about 10 times higher than the area resistance observed in this study but this is presumably due to the 20 times lower phosphate buffer concentration used.

Studies of the oxygen diffusion behaviour of the membranes showed all Scimat separators to be very hydrophilic, so that water leaked through them even with a carbon black coating on the outside. This made the Scimat materials unsuitable as membranes in single chamber microbial fuel cell systems.

Table 6.4: Oxygen diffusion, mass transport coefficient and permeability of the membrane separators in water at 298 K.

Membrane separators	k_O / cm s^{-1}	D_O / cm^2 s^{-1}	P_M / mg l^{-1} s^{-1} cm^{-2} Pa
Nafion	$2.79 \cdot 10^{-3}$	$5.1 \cdot 10^{-5}$	$4.38 \cdot 10^{-6}$
Rhinohide	$2.44 \cdot 10^{-3}$	$16.3 \cdot 10^{-5}$	$4.52 \cdot 10^{-6}$
Tyvek	$2.62 \cdot 10^{-3}$	$3.82 \cdot 10^{-5}$	$4.61 \cdot 10^{-6}$
Carbon paper (wet proofed)	$3.73 \cdot 10^{-3}$	$11.2 \cdot 10^{-5}$	$8.62 \cdot 10^{-6}$
ETFE-g-PSSA D.O.G. 23%	$2.54 \cdot 10^{-3}$	$4.16 \cdot 10^{-5}$	$5.01 \cdot 10^{-6}$
ETFE-g-PSSA D.O.G. 35%	$2.17 \cdot 10^{-3}$	$1.43 \cdot 10^{-5}$	$8.2 \cdot 10^{-6}$
HDPE-g-PSSA D.O.G. 11%	$2.46 \cdot 10^{-3}$	$9.57 \cdot 10^{-6}$	$4.83 \cdot 10^{-6}$
PVDF Copolymer-g-PSSA D.O.G. 10%	$2.79 \cdot 10^{-3}$	$3.2 \cdot 10^{-5}$	$4.24 \cdot 10^{-6}$
PVDF-g-PSSA D.O.G. 34%	$2.74 \cdot 10^{-3}$	$1.23 \cdot 10^{-5}$	$4.25 \cdot 10^{-6}$

Table 6.4 shows the oxygen diffusion, mass transport coefficient and permeability of the membranes separators in water. Similar mass transfer coefficients (k_O) (around $2.6 \cdot 10^{-3}$ cm s^{-1}) were obtained for all membrane separators except for carbon carbon paper with a slightly higher mass transfer coefficient of $3.73 \ 10^{-3}$ cm s^{-1}. The oxygen diffusion coefficient (D_O) varied with membrane thickness. The lowest oxygen diffusion coefficient was observed for the HDPE radiation grafted membrane with $9.57 \cdot 10^{-6}$ cm^2 s^{-1}. The other membranes and separators showed similar values in the range of 10^{-5} cm^2 s^{-1} for k_0 which is 10 times higher than HDPE. Rhinohide showed the highest diffusion in this group with 16.3 cm^2 s^{-1}. The membrane permeability was similar for all materials with carbon paper and ETFE 35% grafted showing the highest oxygen permeability double the value of the other materials with $8.62 \cdot 10^{-6}$ mg l^{-1} s^{-1} cm^{-2} Pa and $8.2 \cdot 10^{-6}$ mg l^{-1} s^{-1} cm^{-2} Pa respectively.

The oxygen diffusion permeabilities observed in this study were similar to values reported in literature with $4.3 \ 10^{-6}$ cm^2 s^{-1}, $5.27 \ 10^{-6}$ cm^2 s^{-1}, and $2.4 \ 10^{-6}$ cm^2 s^{-1} although different electrolytes were used in the different studies (water instead of glucose or acetate with PBS) (Zhang et al., 2009b; Chae et al., 2008; Kim et al., 2007; Liu and Logan, 2004). This suggest that the influence of the electrolytes used in the different studies on oxygen permeabilities was negligible.

High resistivity with low conductivity were observed for Tyvek and HDPE as membrane separators making both materials unsuitable as efficient microbial fuel cell membranes. The Scimat materials are also unsuitable due to a mixture of high porosity and hydrophilic characteristics. Carbon paper is hydrophobic which presumably is the cause of the high ionic resistances. The highly grafted materials ETFE 35% and PVDF 34% showed themselves to be fragile during the experimental study which showed in warping and swelling of both materials due to their thickness and high percentage of grafting.

6.3.4 Conclusion

Based on durability, ion exchange capability and oxygen diffusion permeabilities Nafion, ETFE 23% grafted, PVDF 10% grafted and Rhinohide were chosen to be studied in MFC tests as three ion exchange membrane and one inexpensive separator. Additionally carbon paper was chosen to support a biocathode on the inside of the anode chamber opposite to the anode as gas diffusion cathode support.

6.4   REACTOR STUDIES

6.4.1   Introduction

Although characterising the membrane separator gives an idea of the possible capabilities of the materials in a reactor the actual performance of the membrane depends on the system conditions. Therefore realistic experiments are essential for biological systems such as wastewater treatment. The actual behaviour of the membrane will be affected by the complex composition of the substrate (wastewater) used.

The membranes used in reactors experiments were Nafion, Rhinohide, ETFE-g-PSSA D.O.G. 23% (ETFE), PVDF Copolymer-g-PSSA D.O.G. 10% (PVDF) and Carbon paper (CP) was used a gas diffusion support for a membrane-less reactor, where the cathode catalyst (carbon black) is placed inside the anodic chamber opposite the anode material with only the wastewater separating the electrodes. Carbon paper was chosen as gas diffusion support for the membrane less reactors due to its high oxygen diffusion coefficient and conductivity.

6.4.2   Experimental

In this study five different membrane materials were studied in a single chamber MFC using wastewater as feed substrate and activated carbon cloth (FM30k) as anode material. Carbon black as cathode catalyst was deposited directly onto the membrane material used with a load of 1 mg cm^{-2}. For reactors using Nafion, Rhinohide, ETFE and PVDF as a membrane the catalyst was applied on the outside of the membrane as an air cathode (Figure 6.1 A). Reactors using carbon paper, working as membrane-less reactors, had the catalyst applied on the inside of the chamber opposite to the anode (Figure 6.1 B).
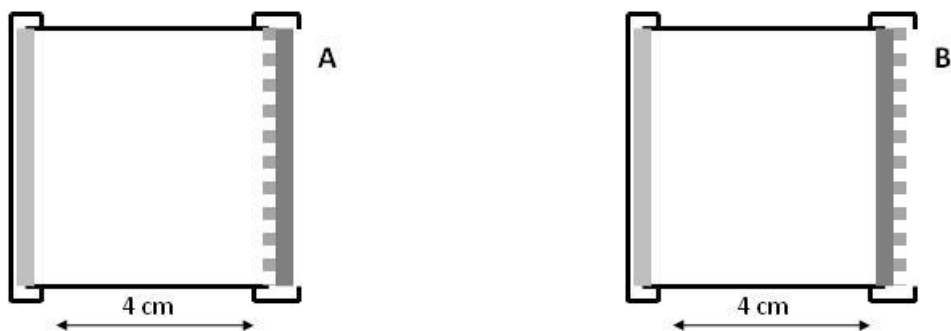
Figure 6.1: Reactor configurations used during the study with the cathode catalyst applied at the air-side of the membrane (A) or inside the anode chamber (B).

Domestic wastewater was used as both inoculums and feed substrate in the study. The detailed characteristics of the substrate before sampling are provided in Table 6.5.

Table 6.5: Physiochemical characteristics of the feed substrate (domestic wastewater) used in the present study.

Parameter	Wastewater
pH	7.36
COD /mg l^{-1}	256
SS / mg l^{-1}	202.2
VSS / %SS	11.0
Sulphate / ppm	93.58
Chloride /ppm	181.31
Phosphate /ppm	Not detected
Fluoride /ppm	Not detected
Conductivity / mS cm^{-1} at RT	1.493

Duplicate reactors were used in the experiment to ensure validity of the experimental observations. All results shown are the average of the two duplicate reactors.

6.4.3 Results and discussion

6.4.3.1 Power Performance

6.4.3.1.1 Variations in Voltage Evolution under 1kΩ

Figure 6.2 shows the voltage evolution of the different membranes under 1 kΩ and OCP over time. The activated carbon cloth anodes produced as expected little voltage over the first three batches for all reactors. After the third batch voltage production increased rapidly for reactors using PVDF and Nafion membranes with an apparent decrease in voltage generation after the 6th batch. The decrease continued till the end of the steady state investigation. Reactors using ETFE and carbon paper only started to produce voltage from the 5th batch onwards but from then on the voltage produced increased steadily. Reactors using Rhinohide as chamber separators took even longer to acclimatise and voltage production started increasing from the 7th batch (Figure 6.2).
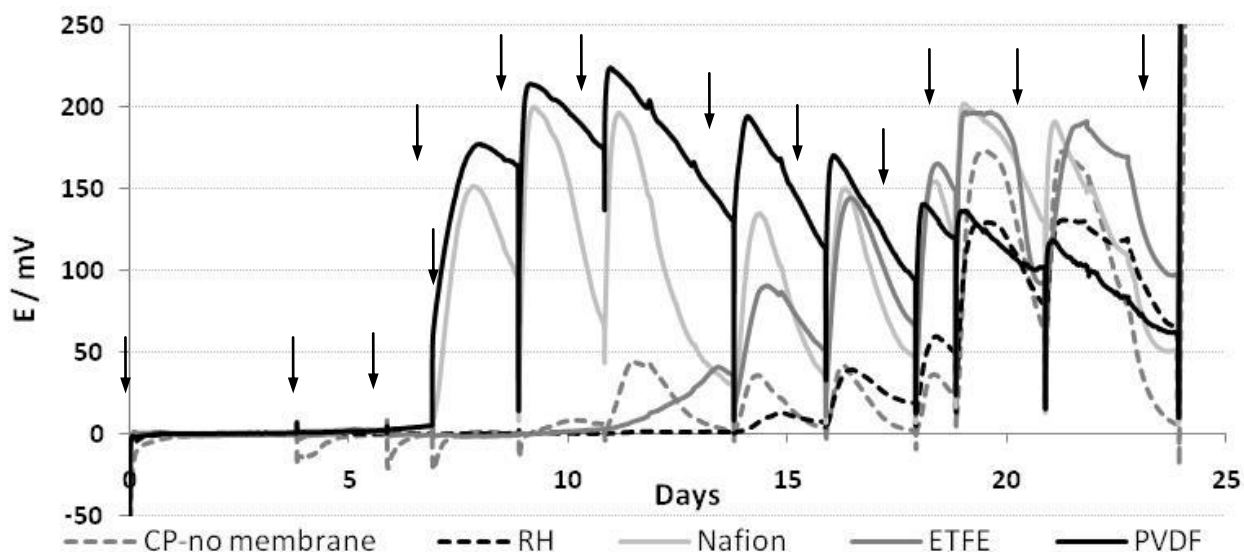
Figure 6.2: Voltage generation under 1 kΩ and OCP for the different membrane separators. Arrows indicate the start of the next batch as the reactors were refilled.

The differences in voltage generation and acclimatisation time show the significant influence of the membrane on the microbial fuel cell system. During the first three batches the anode materials is presumably colonised with a biofilm. This takes time as the activated carbon cloth (FM30k) used has antibacterial and strong adsorption properties. The rapid increase in voltage

evolution for PVDF and Nafion membranes is most likely due to high ion transfer capabilities from the anode to the cathode which decreases as substances either accumulate in the membranes or are transported to the cathode and inhibit the cathode activity. As the anodic chamber is 4 cm in length oxygen diffusion into the anodic chamber should not be responsible for the decrease in power performance. The slower acclimatisation for reactors using ETFE and Rhinohide membrane separators indicateed the oxygen transfer differences of the membranes and separators.

The formation of a biofilm at the anode as well as at the cathode could be a possible explanation for the slow acclimatisation for reactors using carbon paper support. Since the cathode catalyst is inside the anode chamber a cathodic biofilm has to be formed on the carbon black catalyst deposited on the carbon paper inside the anode chamber. This biofilm is sustained by oxygen diffusing through the carbon paper and using wastewater as feed substrate but oxygen as terminal electron acceptor.

Table 6.6 shows the average internal resistance for the reactors. The lowest internal resistance was observed for Nafion with 269±4 Ω, followed by ETFE with 269±4 Ω, carbon paper with 301±9 Ω and PVDF and Rhinohide with 316±2 Ω and 350±6 Ω internal resistance respectively. The reactors reaching higher voltage and therefore power under 1000 Ω showed lower internal resistance whereas higher internal resistances were observed in poorly performing reactors.

Table 6.6: Internal resistance of the reactors using different membranes.

	CP	RH	Nafion	ETFE	PVDF
Internal Resistance / Ω	301±9	350±6	269±4	294±5	316±2

The internal resistances measured agree with the conductivities measured previously where Rhinohide showed the highest conductivity which translated in the highest internal resistance. PVDF showed the lowest conductivity but this did not directly corresponded to the lowest internal resistance which is possibly due to accumulation of substances in the reactor as the internal resistance was measured at the end of the experiment.

6.4.3.1.2 Polarisation studies

Potential, current and power density achieved during polarisation are an indicator for the performance of a material. Figure 6.3 shows the cell potential and power curve of the reactors using different membranes. The highest peak power density was obtained for carbon paper; 67 mW m^{-2} at a current density of 203 mA m^{-2} and a potential of 330 mV. This was followed by reactors using Nafion membranes which reached 61 mW m^{-2} (at 238 mA m^{-2} and 251 mV) and reactors using ETFE membranes with 59 mW m^{-2} (at 244 mA m^{-2} and 243 mV). The lowest peak power densities were achieved using Rhinohide as membrane with 23 mW m^{-2} (at 167 mA m^{-2} and 140 mV) and PVDF membranes whit 26 mW m^{-2} (at 114 mA m^{-2} and 223 mV) (Figure 6.3). Reactors using carbon paper as diffusion support and Nafion and ETFE as membrane showed the highest potential for high power generation during polarisation.
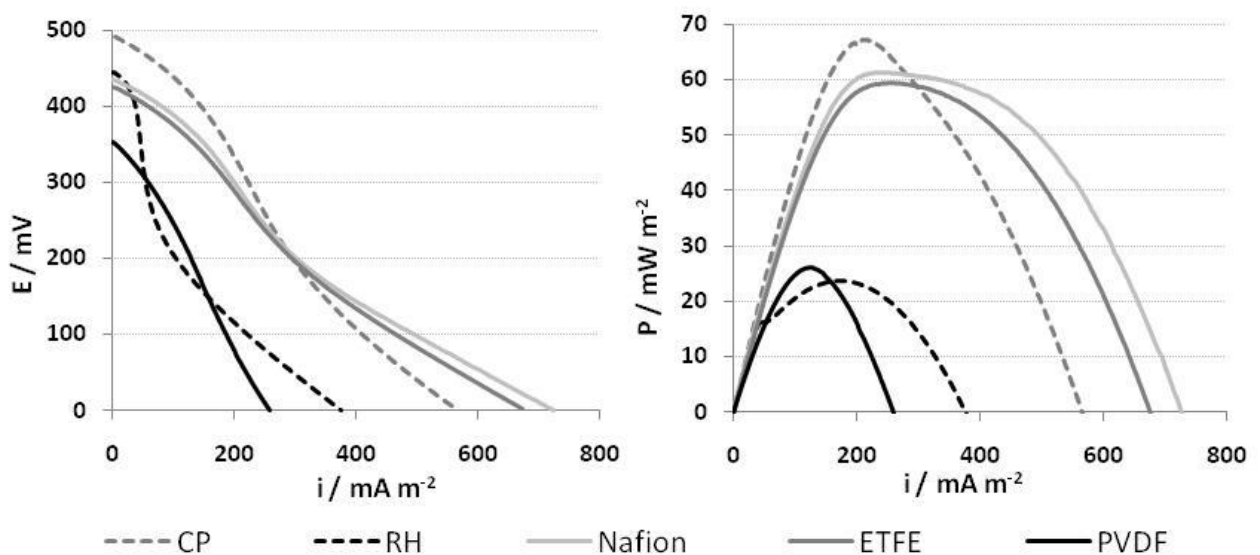
Figure 6.3: Linear sweep voltammogram showing the peak cell potential and power density for the reactors using different membranes during polarisation.

Average peak potential, current and power density during polarisation of the duplicate reactors showed little variability between the reactors using membranes or separators while the membrane-less reactors (CP) showed much higher variability presumably due to differences in the cathodic biofilm.

Table 6.7: Average potential, current and power density achieved during polarisation of the duplicate reactors using different membranes.

	E / mV	i / mA m^{-2}	P / mW m^{-2}
CP	252.5±77	224.5±21	55±12
Nafion	253.5±2.5	222±16	57±4
ETFE	227.5±15	254±10	57.5±1.5
PVDF	205.5±17	118.5±4.5	24.5±1.5
RH	139±1	162.5±4.5	22.5±0.5

6.4.3.1.3 Anode and cathode behaviour

Figure 6.4 shows the anode and cathode polarisation data of the reactor working at peak conditions using different membranes obtained at the end of the batch. The anode showed linear behaviour with an overpotential loss of 100 mV over 400 mA m^{-2} and only slight differences (about 20 mV) in onset potential for the different reactors.

The cathode behaviour varied widely with the different membrane materials. For reactors generating higher voltage using carbon paper, Nafion and ETFE high cathodic onset potentials with 270 mV, 206 mV and 190 mV respectively and also low overpotential losses at the cathode side with 120 mV, 60 mV and 50 mV respectively were observed. Cathodes in reactors using Rhinohide as separator showed a modest onset potential of 190 mV but high overpotential losses on the cathode side of 190 mV which lead to a poor power performance. The cathode in reactors using PVDF as membrane showed a low onset potential of 115 mV with similarly high overpotential losses of 180 mV. The best performing reactors (carbon paper, Nafion, ETFE) showed higher overpotential losses on the anode than the cathode over the whole current density reange which means the anode is more limiting, although carbon black was used as cathode catalyst. The poor performing reactors (PVDF and Rhinohide) showed higher overpotential losses on the cathode than the anode showing that the cathode was more limiting in those cases.

The carbon black cathodes showed their two wave profile, as discussed in Chapter 4, showing a change in oxygen reduction mechanisms over the profile. The reactors using better performing membrane separators, carbon paper, ETFE and Nafion showed a wide curved profile while Rhinohide showed a rapid decrease after the first wave before leading into the second wave. PVDF showed little curvature and only the first wave was clearly visible.
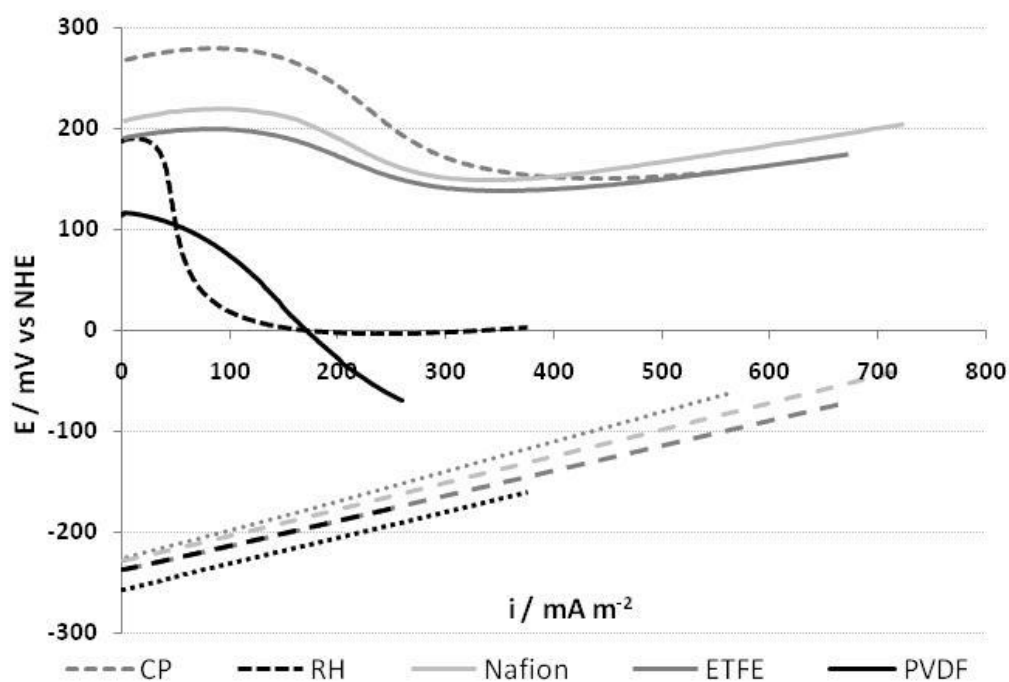
Figure 6.4: Linear sweep voltammetry of the iR corrected cathode (line for ion exchange membranes and dashed for separators) and anode (dotted for separators and long dashed for ion exchange membranes) behaviour of the reactors using different membrane separators. Reactors at peak performance are shown here.

Since the same materials were used as anode and cathode in this study differences in anode and cathode behaviour are presumably mainly due to the influence variations in the microbial consortia forming the biofilm on the anode, substances diffusing through the membrane and the proton exchange capacity of the membrane. The cathode is seemingly inhibited by lower proton transfer and diffusion of substances through the membranes which apparently inhibited the cathode potential as a much lower onset potential was observed for PVDF, followed by Rhinohide, ETFE and Nafion. As the cathode catalyst was inside the chamber for carbon paper anodes this could be an explanation for the high cathode onset potential observed as only oxygen has to diffuse through the carbon paper, which means the material will probably not congest as easily as the membranes and the separator used. The slight differences in the onset

potential of the anodes are probably a visible effect of differences in the microbial consortia forming the biofilm and as the variability was less than 8 % of the anode potentials measured the variation presumed to be not significant. The cathode potential and behaviour was the main influence on the system through the influence of the different membranes on the cathode performance.

6.4.3.1.4 Variations in Steady State

Figure 6.5 shows the average cell potential, current and power densities achieved for the different membrane materials. Reactors using ETFE and Nafion membranes achieved the highest steady state power densities with 29 ± 3.4 mW m^{-2} (at 152 ± 8.8 mA m^{-2} and 190 ± 11 mV) and 29 ± 2.6 mW m^{-2} (at 152 ± 6.7 mA m^{-2} and 190 ± 8 mV) respectively under 1kΩ. Closely following carbon paper achieved 24 ± 0.02 mW m^{-2} (at 138 ± 0.07 mA m^{-2} and 172 ± 0.09 mV) (Table 6.8). This was about half the instantaneous power achieved during polarisation with the same membranes. Reactors using Rhinohide separators reached power densities of 14 ± 2.2 mW m^{-2} (at 104 ± 8.2 mA m^{-2} and 130 ± 10.3 mV). The worst performing reactors used PVDF membranes and achieved power densities of 11 ± 0.5 mW m^{-2} (at 95 ± 2.1 mA m^{-2} and 118 ± 2.6 mV).
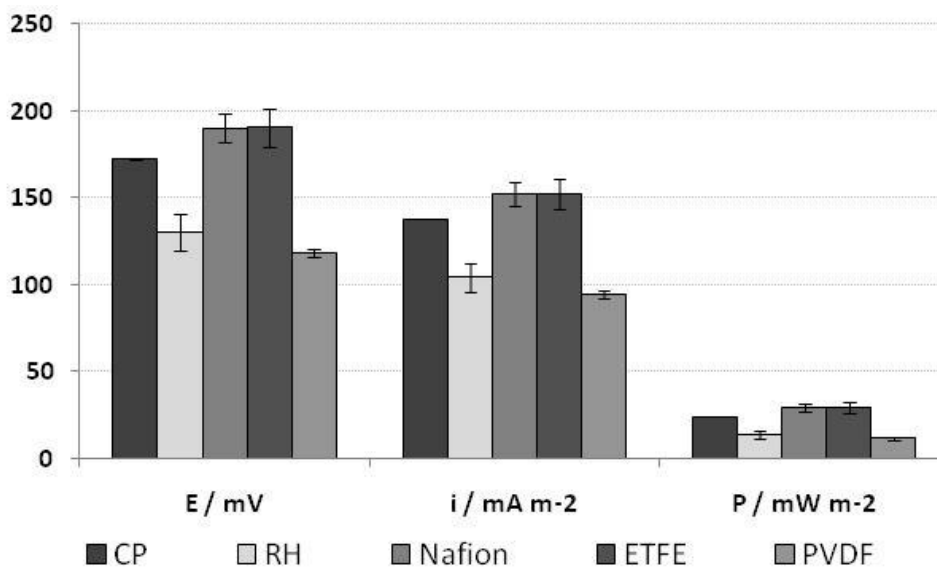
Figure 6.5: Average cell potential, power and current densities for the different materials under 1kΩ of the duplicate reactors over the batch.

Statistical analysis of the cell voltage, power density and current density showed the influence of the membrane materials to be statistical significant (with p=0.008 for cell voltage and current density and p=0.010 for power density) whereas the duplicates where statistically the same (p=0.565 for cell potential and current density and p=0.432 for power density).

Table 6.8: Average power and current densities and voltage under 1kΩ external load.

	E / mV	i / mAm^{-2}	P / mW m^{-2}
CP	172±0.09	138±0.07	24±0.02
RH	130±10.3	104±8.2	14±2.2
Nafion	190±8	152±6.7	29±2.6
ETFE	190±11	152±8.8	29±3.4
PVDF	118±2.6	95±2.1	11±0.5

Power performance in this study is difficult to directly compare with the literature due to the different reactors designs and substrates used. Thus although higher power densities were achieved in a number of studies, using acetate as substrate, lower power results in this study are significant, as power is generated from actual wastewater. Agreeing with this study trends visible in literature show membrane-less reactors and reactors using anion exchange membranes to achieve higher power densities compared to reactors using cation exchange membranes (e.g. Nafion) (Zhang et al., 2009b; Du et al., 2008; Logan, 2008; Kim et al., 2007; Liu and Logan, 2004).

6.4.3.2 Wastewater treatment efficiency

Substrate conductivity and pH were measured to observe the ion flux over the batch. Figure 6.6 shows the pH and conductivity of the different membranes over one batch. The pH and conductivity decreased, stabilised and then fell again over the batch with smaller changes in pH in the control reactor. The pH and conductivity decreased faster in reactors using ion exchange membranes (Nafion, ETFE and PVDF) than in reactors using separators which showed faster decrease than the control reactor. The power performance of the reactors with the best performing membranes coincided with a higher decrease in pH and conductivity for all reactors except those using carbon paper as cathode support.
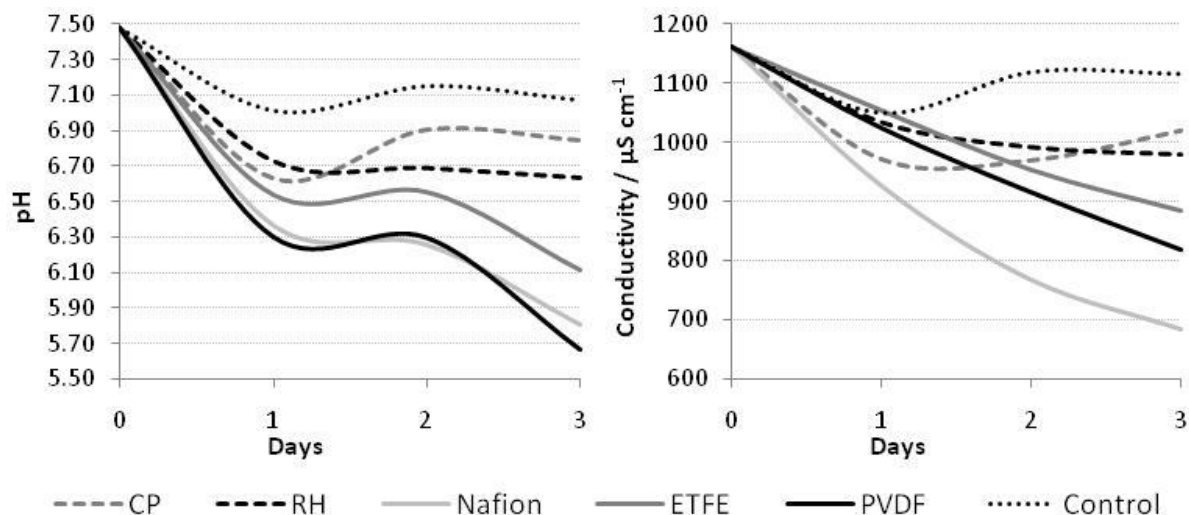
Figure 6.6: Variations in pH and conductivity for the different membranes over a batch.

Interestingly the ion exchange membranes showed a more rapid decrease in conductivity as well as a more rapid decrease in the pH. The decrease in conductivity can be explained through ions, other than protons being used at the cathode thus fewer ions were in the wastewater over time and the production of weak electrolytes through other degradation processes occurring in the anode chamber. In contrast to the results shown protons should be preferentially used (especially when using cation exchange membranes) in the cathode reaction, but the decreasing pH shows an accumulation of protons in the anode chamber. An explanation for decreasing conductivity together with increasing proton concentrations in the anode chamber, could be the preferential transfer and use of other ions through the membrane to the cathode, difficulties to transfer protons to the cathode through the 4 cm reactor length, as only diffusion processes were used or that more protons were produced at the anode than used at the cathode. Since wastewater does not have much buffering capacity, the continuing decrease in pH and conductivity might lead to acidic pH and very low conductivity. These changes could results in a gradual decrease in the power performance of the systems.

Reactors using carbon paper as cathode support and Rhinohide as separator showed less decrease in pH and conductivity. The lower decrease in pH for Rhinohide and carbon paper reactors could be due to a greater number of protons being able to easily diffuse to the cathode and react there. As the protons only have to travel through the electrolyte for carbon

paper and although ions are used by the cathodic biofilm, the cathodic biofilm, depending on the reduction processes used, presumably also produces ions and therefore act as a buffer in the solution (He and Angenent, 2006; Bergel et al., 2005; Rhoads et al., 2005). Similarly could the hydrophilic and microporous structure of Rhinohide be easily accessible for proton transfer which the ion exchange membranes were not.

The rapid pH change in the anode chamber can decrease the power performance at pH values lower than pH 6. Although at the same time higher power densities were observed at lower pH, less efficient COD removal was also observed at lower pH by Raghavulu *et al.* (2009). Accordingly a further drop in pH over a long batch would supposedly result in lower wastewater treatment and power performances since the microbial community would be stressed or die at acidic conditions. But a pH change between pH 8 and 6 did not visibly influence power and wastewater treatment performance in this study contrasting with findings presented by Harnisch *et al.* (2008) and Rozendal *et al.* (2008).

Figure 6.7 shows the dissolved oxygen measured in the anodic chamber of the MFC and the control reactor (substrate under anaerobic conditions). Dissolved oxygen measurements showed a comparable decrease in oxygen concentrations in all reactors over the batch with ETFE showing the highest reduction. Only the control reactors showed nearly complete anaerobic conditions as very low dissolved oxygen concentrations were observed (Figure 6.7).
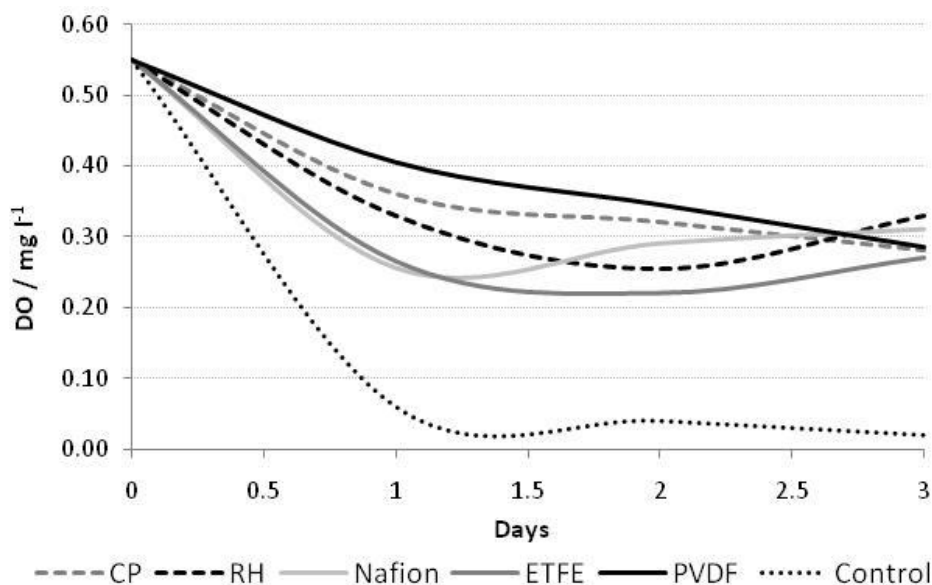
Figure 6.7: Dissolved oxygen measured in the anodic chamber for all reactors.

Oxygen diffusion into the anode chamber is an often reported problem in microbial fuel cells leading to reduced coulombic efficiencies as substrate is degraded aerobically (Zhang et al., 2009b; Cheng et al., 2006a; Liu and Logan, 2004; Min and Logan, 2004). The extent of the problems though seems to be mainly dependent on the size of the anodic chamber and only in reactors using small anode spacing oxygen flux into the chamber significanctly reduces the anode potential.

Figure 6.8 shows the COD removal, coulombic efficiency and current density of MFCs with the different membranes under 1 kΩ load. COD removal efficiencies between 65% and 80% were achieved by the MFC reactors with the control reactor reaching 64% COD removal. Rhinohide achieved the highest COD removal with 79±5% followed by Nafion, ETFE, PVDF, CP with 77±3%, 74%, 67±18 and 65% COD removal respectively. The control reactor reached slightly lower COD removal with 64%.
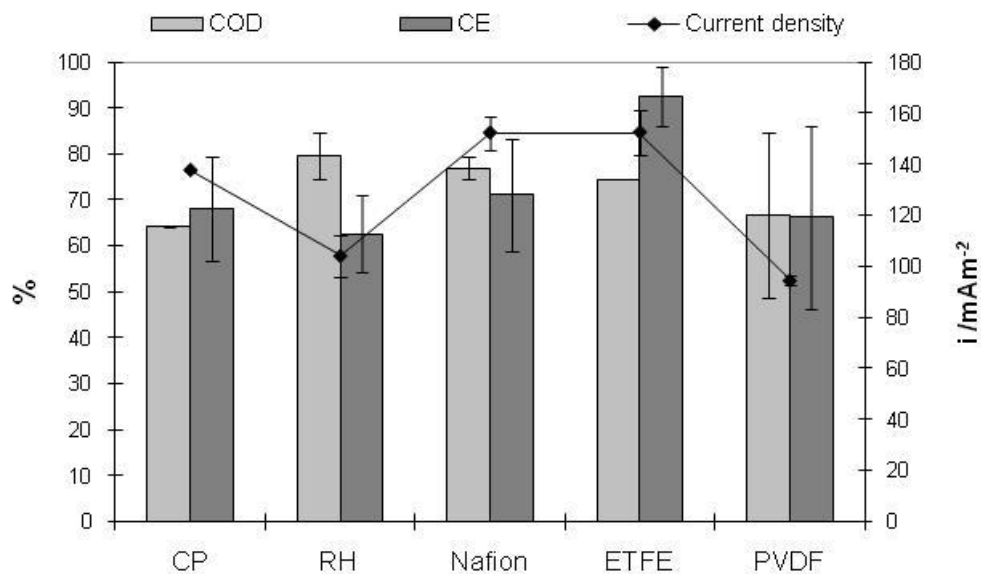
Figure 6.8: COD, CE and current density produced by the reactors using different membranes under 1kΩ external load measured at the end of the batch.

Surprisingly high coulombic efficiencies for wastewater as substrate were observed in this study (Figure 6.8). Reactors using ETFE membranes achieved the highest coulombic efficiencies; on average 92±6%, which is approximately 15% higher than average results observed for the other reactors with 71±12% CE for Nafion, 68±11% CE for carbon paper, 66±20% CE for PVDF and

63±8% CE for Rhinohide. The average COD removal and coulombic efficiencies for all reactors was 72% each, which is good for COD removal but higher than previously reported for coulombic efficiencies achieved using wastewater as substrate.

The membrane-less reactor using carbon paper as support reached high coulombic efficiencies. Since substrate is consumed by the aerobic cathodic biofilm inside the anode chamber, lower coulombic efficiencies were expected. Accordingly 68% CE is a notable result for microbial fuel cell with an inner biocathode.

Interestingly Rhinohide achieved the highest COD removal as well as the lowest coulombic efficiencies while low current was produced. Apparently competing degradation processes to electricity generation are more active in the reactors using Rhinohide separators than in the reactors using other membrane separators. A higher variability in CE between duplicate reactors was observed in reactors working less efficiently.

Statistical analysis of the COD removal and coulombic efficiencies showed neither the influence of the membranes nor the duplicates to be statistically significant. This is probably due to the high variability, especially in coulombic efficiencies between duplicate reactors.

Results in this study concur with a number of studies in literature which showed that either a better membrane (Nafion to salt-bridge) (Min et al., 2005) a separator (Kim et al., 2007) or no-membrane (the electrolyte as separator) is able to improve the proton/ion transport due to transport limitations in ion exchange membranes at low salt concentrations, which particularly is the case in microbial fuel cell systems using wastewater as substrate. Dlugolecki *et al.* (2010) showed exactly this when investigating the electrical resistance of ion exchange membranes at different solution concentrations.

ETFE radiation grafted cation exchange membranes showed impressive results, after a slow start-up, with comparatively high power densities and remarkable coulombic efficiencies of on average 92%. Nafion produced as high power densities with on average 72% CE. Membrane-less reactors using carbon paper supports reached high power densities and coulombic efficiencies of 68%.

Comparing these results with the previous studies variations between duplicate reactors in the power performance were more apparent in reactors achieving low coloumbic efficiencies which presumably coincides with lower similarities in the microbial community. If this can be confirmed in further studies is would suggest higher reproducibility in duplicate reactors, possibly due to very similar microbial communities, when high colombic efficiencies are reached. Thus when energy generation is the main or one of the main processes in the reactors higher reproducibility can be achieved between duplicate reactors.

6.4.3.3 Cost/performance ratio

The cost of the membranes was approximated using producer pricing for carbon paper, Rhinohide and Nafion. For the radiation grafted membranes ETFE and PVDF the cost of the base film was multiplied by 10 to estimate the cost of the final membrane.

Table 6.9 shows the cost in correlation to average power densities and percentage coulombic efficiency. The lowest cost (£) per power (mW) were observed for ETFE followed by PVDF and Rhinohide with 0.10 £ mW^{-1}, 0.18 £ mW^{-1} and 0.11 £ mW^{-1} respectively. Very high cost per power was observed for carbon paper with 16.5 £ mW^{-1} and Nafion with 51 £ mW^{-1}. Similarly reached Nafion the highest cost per percentage coulombic efficiency with 20.8 £ m^{-2} %$^{-1}$ followed by carbon paper with 5.7 £ m^{-2} %$^{-1}$. Rhinohide and PVDF reached 0.24 £ m^{-2} %$^{-1}$ and 0.15 £ m^{-2} %$^{-1}$ respectively and ETFE showed the lowest cost per %CE with 0.01 £ m^{-2} %$^{-1}$.

Table 6.9: Cost-performance ratio for the different membrane materials. Cost was linked to power density and coulombic efficiency.

	Cost / £ m^{-2}	P / mW m^{-2}	Cost/P £ mW^{-1}	CE / %	Cost/%CE / £ m^{-2} %$^{-1}$	Lifetime of 10 years / kWh m^{-2}	Total cost over 10 years / £
CP	390	24±0.02	16.5	68±11	5.7	2.1	0.17
RH	1.5	14±2.2	0.11	63±8	0.02	1.2	0.10
Nafion	1478	29±2.6	51	71±12	20.8	2.5	0.20
ETFE	3	29±3.4	0.10	92±6	0.03	2.5	0.20
PVDF	2	11±0.5	0.18	66±20	0.03	1	0.08

Assuming a 10 year lifetime of MFC technology in wastewater treatment and a price of 8 p kWh^{-1} the importance of inexpensive separator materials becomes clear when looking at the cost per watt (Table 6.9). Over the assumed lifetime of 10 years the reactor using the comparatively best performing membrane ETFE would produce 2.5 kWh m^{-2} of membrane material. This would not even cover the capital cost of the membrane although it does only costs as £3 m^{-2}. None of the membrane and separators tested would produce enough power to cover their costs. The only difference would be that the use of higher priced materials Nafion and carbon paper would lead to 1000 and 100 times more expensive power respectively than if a good performing low cost membranes such as ETFE were used.

The high cost per watt and cost per coulombic efficiency of Nafion and carbon paper is due to the high material costs making both materials uneconomical in MFCs. ETFE, as a cheap membrane, showed that using a membrane in MFCs can be more economical than using a membrane-less design (carbon paper). Long-term investigation and research for inexpensive current collectors for membrane-less reactors would further elucidate the issue of material costs in MFCs and could help decide if a membrane of no-membrane would be more cost-efficient.

6.4.4 Conclusion

Microbial fuel cell reactors were operated using an ion exchange membrane (Nafion, ETFE and PVDF), a separator (Rhinohide) or membrane-less using carbon paper as cathode support with the cathode catalyst inside the anode chamber opposite to the anode.

Appropriate characterisation of a membrane for bioelectrochemical system made the choice of membrane for reactor tests easier and lead to higher reactor performance. Only long-term experiment will show the actual power and wastewater treatment performance of a membrane in a system, as the undefined composition of the wastewater might affect the membrane in a manner which only becomes apparent after a long period of operation.

The considerable influence of the membrane on the microbial fuel cell system was apparent in different acclimatisation profiles and generated voltage. Every voltage/time plot showed a

markedly different profile for the various membranes used. Reactors using PVDF and Nafion membranes reached high power rapidly after three batches, but the performance decreased gradually over the subsequent batches for PVDF, whereas Nafion decreased and then recovered again after a number of batches. The pH change in a batch system became more pronounced the better the reactor performed.

Oxygen diffusion into the anode chamber is a major barrier to high power performance. As small concentration of oxygen will diffuse through even the most selective ion exchange membranes it is perhaps better to use the oxygen in the chamber through a biocathode in the anodic chamber. This approach would also simplify the system architecture (as both electrodes are inside one chamber). An advantage of using biocathodes would be lower costs, assuming the microbial consortia are able to consistently produce high power without inhibition, deactivation of poisoning by the wastewater used as substrate.

ETFE radiation grafted ion exchange membranes showed impressive results, after a slow start-up, with high power densities and average coulombic efficiencies of 92%. Nafion produced comparable power densities with, on average, 72% CE. The membrane-less reactors reached high power densities and surprisingly high coulombic efficiencies of, on average, 68% CE. Since the substrate is consumed by the aerobic cathodic biofilm inside the anode chamber, lower coulombic efficiencies were expected.

The high power densities and coulombic efficiencies achieved using cation exchange membranes ETFE and Nafion showed the importance of good proton conduction through the membrane. A membrane has to be chosen carefully with the application it will be used for already in mind. PVDF is an example for a poorly chosen membrane which worked very well for a small number of batches, but the performance declined rapidly possibly due to clogging of the ion conduction mechanisms. It would be interesting to see how ETFE and Nafion perform over a longer period of operation. This could influence the choice of an ion exchange membrane or a membrane-less design with a biological cathode in the anode chamber for bioelectrochemical wastewater treatment systems. The advantage of no-membrane would obviously be lower costs as long as an inexpensive cathode support is used.

7 REACTOR STUDIES

ABSTRACT

The performance of a flat plate reactor with 0.5 cm electrode spacing (electrode area 100 cm^2) and three reactors, set up as an factorial design with electrode spacings of 1 cm, 2 cm and 4 cm (electrode area 12.5 cm^2), were studied under 50 Ω, 500 Ω and 1000 Ω external resistance under continuous flow using domestic wastewater as substrate. All four reactors were operated at a flow rate of flow rate of 0.75±0.07 ml min^{-1}.

The flat plate reactor showed low power performance reaching the highest power density with 10.5 mW m^{-2} under 1000 Ω and coulombic efficiencies up to 6.4±0.2% under 50 Ω.

The reactors operated with different electrode spacing reached very low coulombic efficiencies and power densities. Thus although the statistical analysis showed external resistance and electrode distance to be statistically significant, depending on responses analysed, concluding on the importance of either effect and their interactions is difficult, as only 0.2% to 2% of the organic substrate was degraded for power generation.

The low coulombic efficiencies achieved in all four continuous flow reactors showed energy production to be a minor process in the reactors. The low power performance could be due to the flowrate used, which lead to different HRTs in the reactors and influenced the biofilm, and also be due to high biological activity in the influent wastewater which lead to rapid degradation of the substrates using competitive processes instead of electrogenesis.

7.1 INTRODUCTION

Reactor architecture of a microbial fuel cell consists of the reactor dimensions including the size of the electrodes, volume of the anodic chamber and the electrode spacing. The reactor architecture of a microbial fuel cell significantly influences its power performance (Logan, 2008; Rozendal et al., 2008; Du et al., 2007; Logan et al., 2006; Angenent et al., 2004). For that the reactor architecture has to enable thermodynamic laws to work hand in hand with the biological aspects, the biocatalyst, to produce viable and sustainable amounts of energy.

Electrochemically only the surface area of the materials used facing membrane and cathode is able to effortlessly transfer the produced protons through the membrane to the cathode where the second half reaction occurs. Thus only microorganisms on the anode side facing the membrane, and therefore cathode, are able to easily transfer electrons to the anode and protons to the cathode and play a significant part in energy generation.

In wastewater fed MFC reactors the low conductivity and therefore high internal resistance means that the electrode distance is a main influence on the system. But oxygen diffusing into the anode chamber decreases the anode potential as more oxygen reaches the anode decreasing the power performance. Consequently a balance has to be found between electrode spacing and decrease in the anode potential.

The external resistance has been shown to seemingly attune the anodic community to current generation and lower external resistance is often linked to higher power densities (Aelterman et al., 2008; Logan and Regan, 2006). The maximum sustainable power density is the amount of power the system can continuously generate under a known external resistance. It varies depending on system design and microbial community (Menicucci et al., 2006). The external resistance is therefore influenced by the reactor design and application and interacts with it which is visible in the power generated.

To investigate the influence of electrode spacing and external resistance in a continuous flow system, four continuous flow reactors were studied under different external resistances at a flowrate of 0.75 ± 0.07 ml min^{-1}.

- A flat plate reactor (FP) was run for three month with 100 cm^2 electrodes using FePc (loading 1 mg cm^{-2}), deposited on the microporous membrane separator Rhinohide (produced by Entek International, UK) as cathode materials and a graphite sheet as anode material with 0.5 cm distance between the electrodes, thus having an anodic chamber of 50 ml.

- Three reactors were run for eight weeks at two levels, high (high), low (low) and a midpoint (mid), were used to study the influence and interactions of external load and volume, electrode distance in a factorial design (Table 7.1). Anode and cathode materials used were activated carbon cloth FM30k as anode material and carbon black (load 1 mg cm^{-2}) deposited on Rhinohide as membrane separator.

The factorial design used enabled the statistical analysis of the influence and interaction of external load and electrode spacing on MFC performance which to our knowledge has not been used when studying microbial fuel cell performance till now.

Table 7.1: Factorial design used to study the influence and interactions of volume, electrode distance and external resistance.

Levels	high	mid	low
Electrode distance / cm	4	2	1
External resistance / Ω	1000	500	50
Volume / ml	50	25	12.5

7.1.1 Design of Experiments – Factorial Experimental Design

Traditionally during an experiment, one factor is varied while all other conditions/factors are held at a set level. But this method can be time consuming, require large amounts of resources and interactions between factors studied might be missed. An alternative method is to investigate factors using a statistically designed experiment.

In a factorial design factors are varied simultaneously testing the effect of all factors on the response. Because of this the least number of experiments is used to gain the most information from the experiments as the effects of each factor and interactions between factors can be studied at the same time (Berthouex and Brown, 2002; Sokal and Rohlf, 1994). In a two-level design the response is assumed to be approximately linear over the range the levels were chosen. In a three level design curvature can be modelled A third level for a continuous factor enables the investigation of a quadratic relationship (curves/non-linear) between the response and each factor.

In a microbial fuel cell the electrode distance and external resistance shows a non-linear influence on the performance, as both factors are assumed to show an optimum performance under a certain external resistance and electrode distance. Thus a 3^2 factorial design matrix was used as basis of the experimental design to investigate into the main effects and interactions of the external resistance and electrode spacing on microbial fuel cell performance (Table 7.2).

Table 7.2: 3^2 factorial design studying the influence of electrode distance and external resistance on microbial fuel cell performance.

		External Resistance / Ω		
		50 (0)	*500 (1)*	*1000 (2)*
Electrode	*1 (0)*	00	01	02
Distance / cm	*2 (1)*	10	11	12
	4 (2)	20	21	22

Cell voltage, current density, power density, COD removal and coulombic efficiency were analysed statistically as response measurements and the significance of main effects and interactions was assessed. Responses were visualised in interaction plots where the orientation of the lines indicates the existence of main effects and interaction.

7.2   HYPOTHESIS

External resistance and electrode distance determine the power performance in a continuous flow MFC using domestic wastewater as substrate.

7.3 EXPERIMENTAL

One flat plate reactor (FP) and three cube reactors were set up as continuous flow reactors to study the influence of the external resistance and the electrode distance in a flow through system using domestic wastewater as substrate. For this the reactors were acclimatised at 50 Ω external load and once voltage stabilised the load was varied and samples taken.
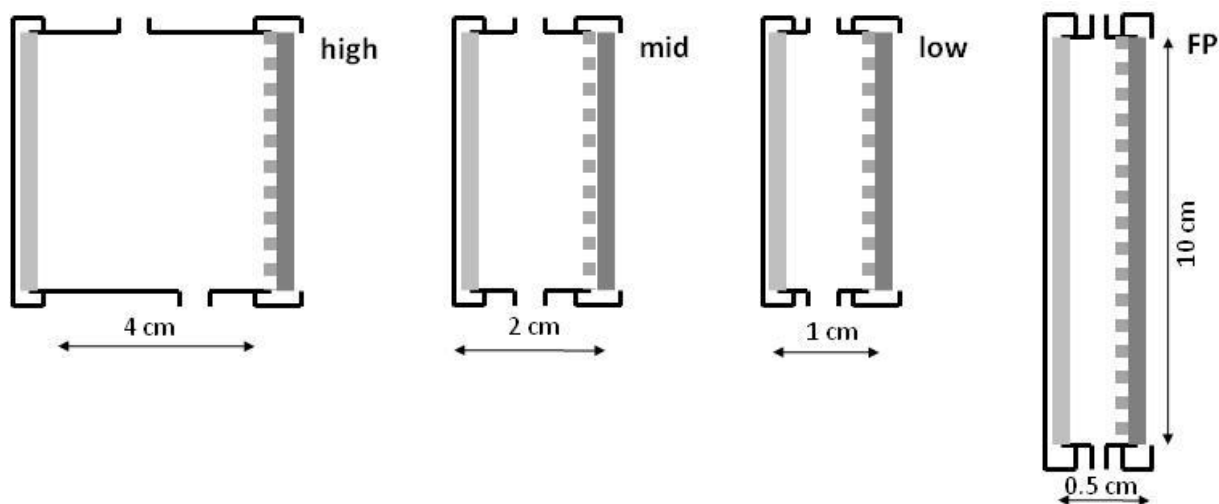
Figure 7.1: Single chamber microbial fuel cell reactors with the anode (light grey line), membrane (grey dotted line) and the cathode (dark grey). Reactor. Reactor configurations high, mid and low were used in a factorial designed experiment to study the electrode spacing in a flow through system and configuration FP was designed as a flat plate reactor with an internal spacing of 0.5 cm and a working volume of 50 ml.

Figure 7.1 shows the single chamber designs used for the flat plate reactor and the reactors used in the factorial design experiment. The flat plate reactors used a graphite plate as anode and FePc as cathode catalyst directly deposited onto the separator (Rhinohide) used as membrane material in a 50 ml chamber with 0.5 cm electrode spacing.

For the factorial design the reactors used activated carbon cloth as anode material, carbon black directly deposited onto the separator. Rhinohide was used as membrane separator.

Influent COD for all four continuous flow reactors was 288 mg l^{-1} under 50 Ω, 224 mg l^{-1} under 500 Ω and 560 mg l^{-1} under 1000 Ω. The physiochemical parameter for the wastewater used can be found in Table 5.1.

Table 7.3: Physiochemical characteristics of the feed substrate (domestic wastewater) used in the present study.

Parameter	Wastewater
SS / mg l^{-1}	995.6
VSS / %SS	24.7
Sulphate / ppm	101.32
Chloride /ppm	66.42
Phosphate /ppm	19.88
Fluoride /ppm	5.39
Conductivity / mS cm^{-1} at RT	1.213

Following research into literature the continuous reactors were run at a flowrate of 0.75±0.07 ml min^{-1}.

7.4   RESULTS AND DISCUSSION

7.4.1   *Flat plate reactor*

7.4.1.1 Power performance

7.4.1.1.1 Voltage Evolution under differing external load

The flat plate reactor was operated at a hydraulic retention time (HRT) of 1 hour (flow rate 0.75±0.07 ml min^{-1}) over three months with a 50 Ω resistor. The voltage generated under continuous flow in the system did not stabilise until the influent temperature was stabilised at 25±2 °C in a waterbath. Figure 7.2 shows the voltage produced after acclimatisation by the flat plate reactor under 50 Ω, 500 Ω and 1000 Ω.
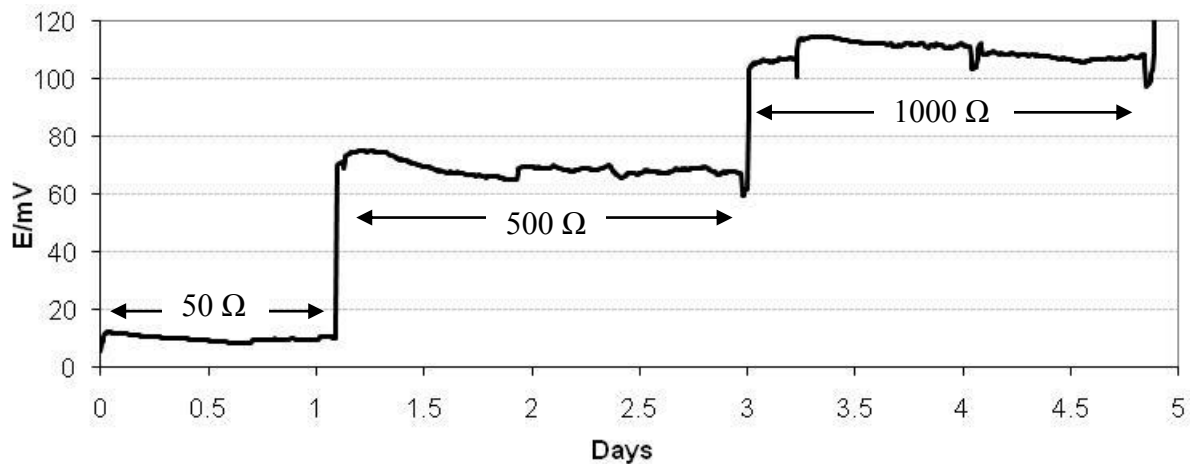
Figure 7.2: Voltage evolution of the flat plate reactor under 50 Ω, 500 Ω and 1000 Ω after the voltage stabilised.

Figure 7.3 shows the average voltage, current and power density the flat plate reached under the different loads. Under 50 Ω the flat plate reactors achieved an average power density of 0.2 mW m^{-2} at a current density of 19.6 mA m^{-2} and a voltage of 9.8 mV. Average power densities increased under higher load with the flat plat reactor reaching 8.9 mW m^{-2} (at 119.4 mA m^{-2} and 74.6 mV) and 10.5 mW m^{-2} (at 91.6 mA m^{-2} and 114.5 mV) for 500 Ω and 1000 Ω respectively. The internal resistance measured after polarising was 140 Ω.
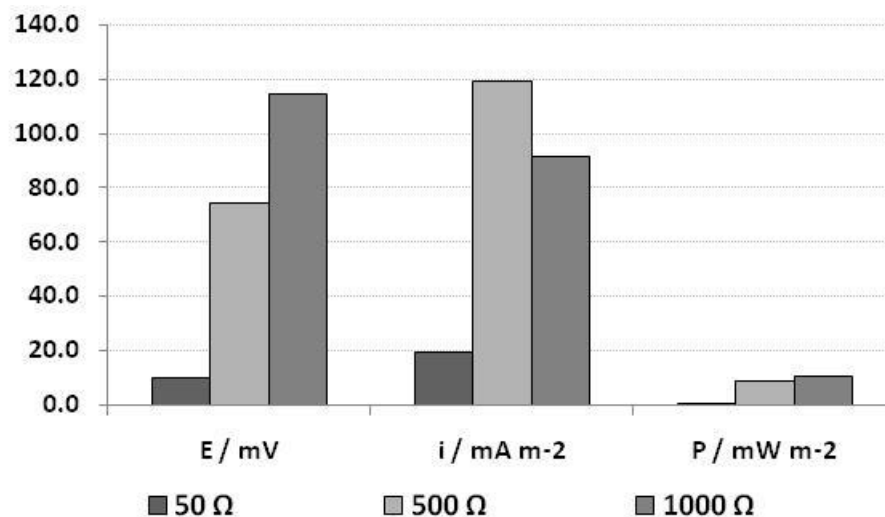
Figure 7.3: Average voltage, current and power density of the flat plate reactor under different external load.

As the internal resistance with 140 Ω is higher than the lowest external resistance with 50 Ω this might have affected the current production and therefore a much lower power performance was observed.

Higher power densities were observed under higher external resistance which agree with results obtained in the previous study on anode materials (Chapter 4) where power densities increased for all anode materials with increasing external resistance. In contrast Aelterman *et al.* (2008) reported higher power densities under lower load when changing the external resistance from 50 Ω to 10.5 Ω (85±5 mW m^{-2} TAC to 104±8 mW m^{-2} TAC) using 1 g l^{-1} acetate as substrate. But this was only visible at high substrate loading rate (3.3 g COD l^{-1} TAC day $^{-1}$) which was achieved through a flowrate of 26.6 ml h^{-1}. At a lower flowrate of 13.3 ml h^{-1} the power density decreased slightly when changing the external resistance from 40±19 mW m^{-2} TAC under 10.5 Ω to 43±7 mW m^{-2} TAC under 50 Ω. As the influent COD in this study is around ¼ of the influent COD Alterman *et al.* (2008) used the lower flowrate and decrease in power density observed agrees with tentatively with results observed in this study.

The power densities of 10.5 mW m^{-2} reached under 1000 Ω were a third lower than those reached in the previous study on cathode materials (Chapter 5) using FePc on the cathode side and carbon black on the anode side. Compared with literature power densities reached in the flat plate reactor were low. Min and Logan (2004) obtained an average power density of 72 mW m^{-2} using domestic wastewater as substrate at a similar HRT of 1.1 h.

7.4.1.1.2 Polarisation studies

Figure 7.4 shows the cell potential and power density as well as anode and cathode behaviour during polarisation. Cathode and cell potential were iR corrected. The cathode declined smoothly showing an overpotential loss of 530 mV over 38 mA m^{-2}. The anode increased nearly linear with a smaller overpotential loss of 100 mV. Therefore the cathode is more limiting in the system.

The flat plate reactor gave very low power reaching 3.1 mW m^{-2} at 14.7 mA m^{-2} and 77 mV during polarisation. The power curve was iR corrected to show capabilities of the flat plate

reactor without internal resistance. iR corrected power densities showed a slight increase to 3.5 mW m^{-2}, showing very little improvement in the power performance of the reactor.
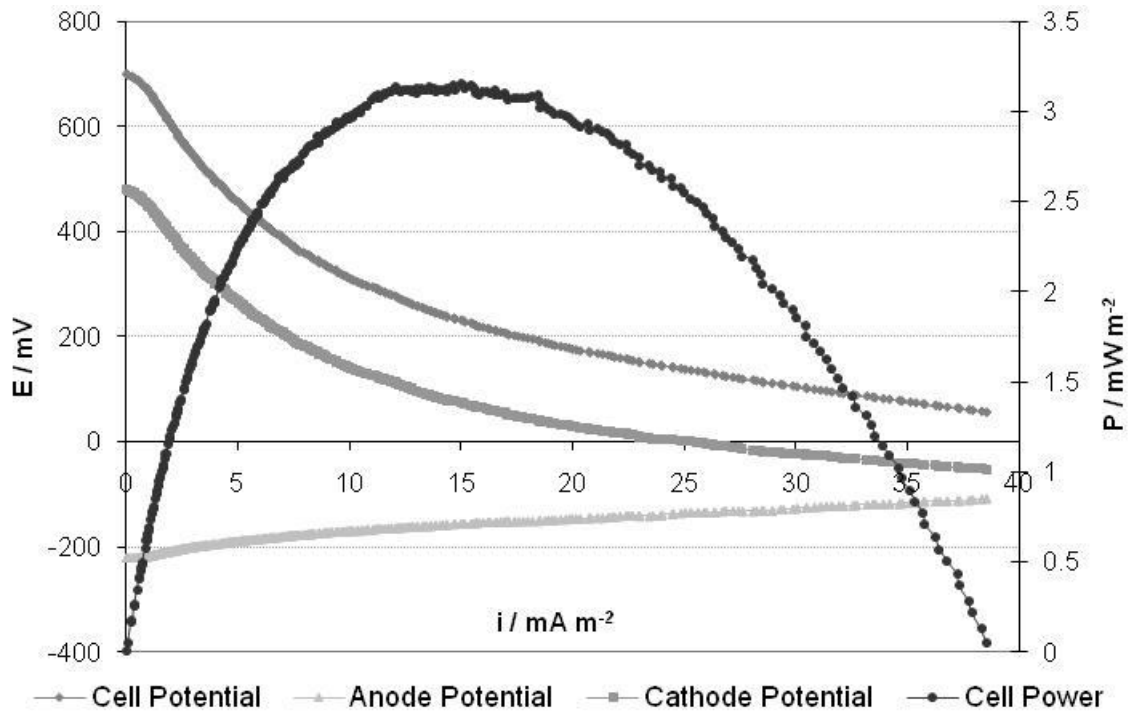
Figure 7.4: Linear sweep voltammogram of the flat plate reactor during polarisation showing, anode vs NHE, iR corrected cathode vs NHE, iR corrected cell potential and power density at a scan rate of 1 mV s^{-1}.

Curiously the polarisation results showed lower possible power densities than achieved under constant external load. The under 50 Ω acclimatised biofilm could presumably have been put under stress as the current demand on the system increased steeply during the polarisation and therefore performed better under a constant external resistance of 500 Ω and 1000 Ω. This could possibly also explain the very low power densities reached under 50 Ω.

7.4.1.2 Wastewater treatment efficiency

Figure 7.5 shows the percentage COD removal, percentage coulombic efficiency and current density the flat plate reactor achieved under different external loads. The flat plate reactor achieved moderate COD removal with 48±2% under 50 Ω, 45±2% under 500 Ω and 45±1% COD removed under 1000 Ω. The coulombic efficiency decreased with increasing load from

6.4±0.2%, 5.3±0.4% and 3.1±0.6% under 50 Ω, 500 Ω and 1000 Ω respectively. The current density showed a maximum under 500 Ω with 119 mA m^{-2}, followed by 92 mA m^{-2} under 1000 Ω and the lowest current density was observed under 50 Ω with 20 mA m^{-2}.
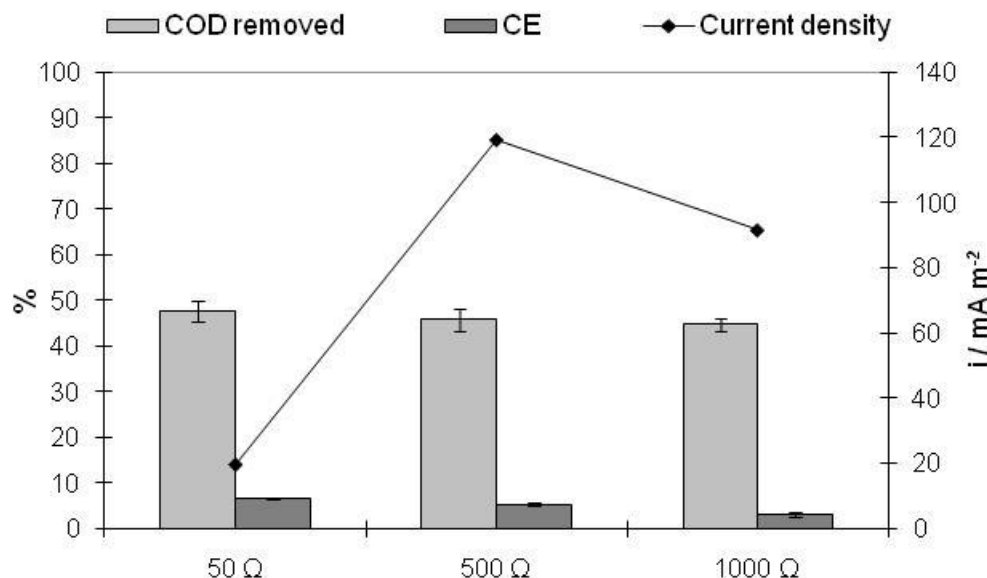
Figure 7.5: Average COD, CE and current density of the flat plate reactor under 50 Ω, 500 Ω and 1000 Ω.

Moderate COD removal efficiency is possibly due to the HRT of 1 h. As expected the coulombic efficiency decreased with increasing external resistance. This trend agreed with observations apparent in earlier studies on anode materials (Chapter 4) where also very low coulombic efficiencies were observed. Under lower external resistances a higher current demand is on the electroactiv biofilm which results in higher coulombic efficiencies. The low coulombic efficiencies of 6.5% and under show that power generation was not the main process degrading the substrate. An explanation for this inefficiency could be the HRT of 1 h. But as the HRT was not changed this could not be proven.

COD removal in literature showed comparable (40-50% COD removal) and higher results (80-90%) using domestic wastewater was substrate in continuous flow reactors than observed in this study (Di Lorenzo et al., 2009a; Cheng et al., 2006a; Chang et al., 2004). This shows a broad variability in COD removal efficiencies which is probably due to the different wastewater compositions, the hydraulic retention time used and variations in the microbial consortia, but could also be a feature of the reactor architecture used. Di Lorenzo *et al.* (2009b) reported

higher COD removal and power densities using higher influent COD loading. As the HRT determines the COD loading rate of a reactors this could have been a problem in the reactors used. But the low coulombic efficiencies in contrast to literature studies show that the reactors were very inefficient as MFCs as most substrate was degraded using other processes and not for energy generation.

7.4.2 Factorial design

7.4.2.1 Power performance

7.4.2.1.1 Variations in voltage evolution, current and power density under different external load

The reactors were acclimatised under 50 Ω external load for 6 weeks, before the external load was varied. Samples were taken under each different external load. Voltage evolution was very erratic in the reactor with 1 cm electrode spacing which stabilised when the influent for all three reactors was kept at constant 25±2 °C. The three continuous flow reactors were operated at a flow rate of 0.75±0.07 ml min^{-1} and a hydraulic retention time of 1 h, 30 min and 15 min for the reactors with 4 cm, 2 cm and 1 cm electrode spacing respectively. Figure 7.6 shows the voltage evolution of the three continuous flow reactor operated with different electrode spacing (low: 1 cm, mid: 2 cm and high: 4 cm) under three different external loads (50 Ω, 500 Ω and 1000 Ω). While the reactors using 2 cm and 4 cm electrode spacing showed relative constant voltage production the reactor using 1 cm electrode spacing high variability even under these conditions under all three external loads.
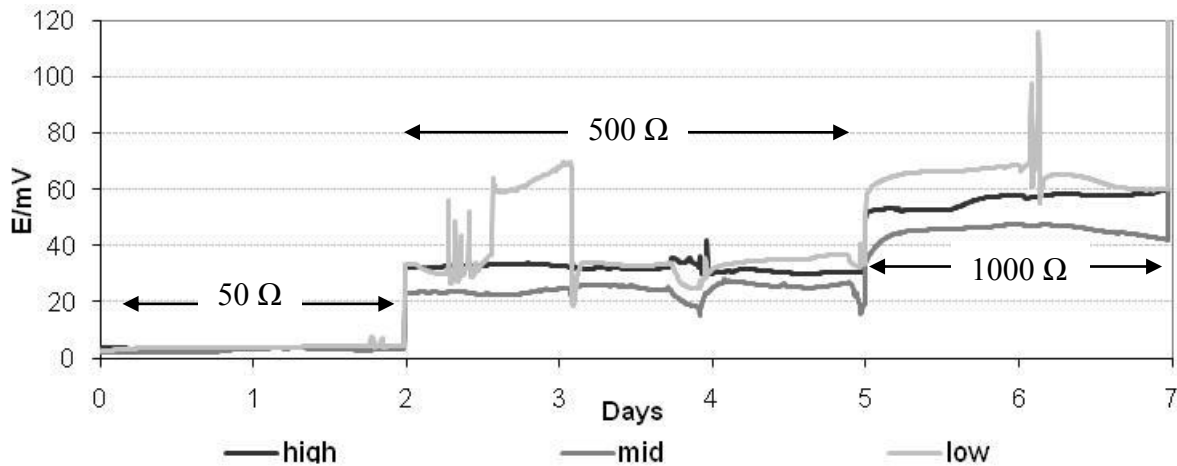
Figure 7.6: Voltage evolution of the three continuous flow reactors operated as a factorial design.

Figure 7.7 shows the average cell voltage, current and power density over time for the three reactors under different external loads. All reactors reached very low power densities. The reactor with 2 cm electrode spacing reached the lowest power densities with 0.1 mW m^{-2} at 41 mA m^{-2} and 2.6 mV under 50 Ω increasing slightly to 1.1 mW m^{-2} (at 42 mA m^{-2} and 26 mV) under 500 Ω and to 1.8 mW m^{-2} at 38 mA m^{-2} and 48 mV under 1000 Ω. The reactor using 4 cm electrode spacing reached slightly higher power densities with 0.26 mW m^{-2} (at 66 mA m^{-2} and 4.1 mV), 1.9 mW m^{-2} (at 55 mA m^{-2} and 34 mV) and 2.9 mW m^{-2} (at 47 mA m^{-2} and 60 mV) under 50 Ω, 500 Ω and 1000 Ω respectively. The highest power densities under any external load were reached by the reactor using 1 cm electrode spacing with 0.3 mW m^{-2} (at 68 mA m^{-2} and 4.3 mV) under 50 Ω , 2.2 mW m^{-2} (at 58 mA m^{-2} and 34 mV) under 500 Ω and to 3.8 mW m^{-2} at 55 mA m^{-2} and 69 mV under 1000 Ω.
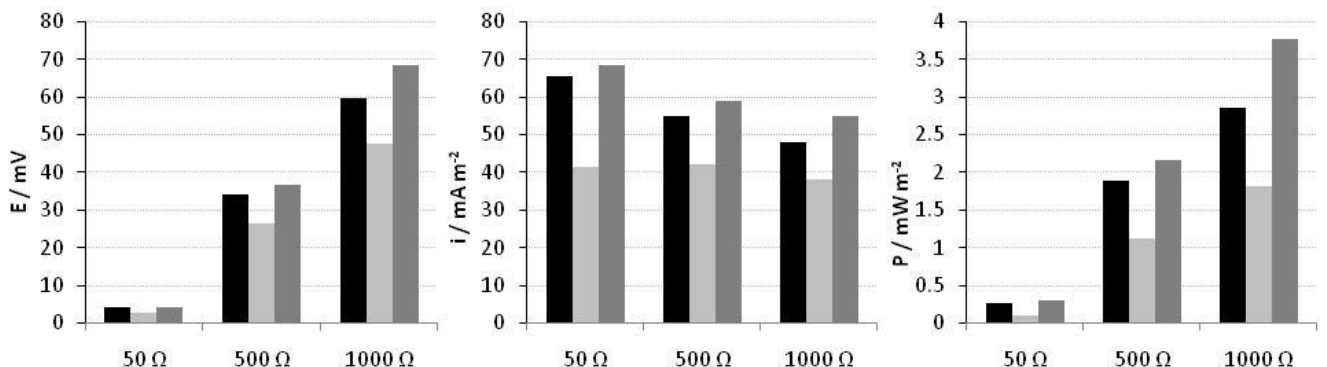
Figure 7.7: Average cell voltage, current density and power density for high (black), mid (light grey) and low (grey) at 50 Ω, 500 Ω, and 1000 Ω external load.

The internal resistance measured using impedance spectroscopy for the different reactors was very high with 79675 Ω for reactors with 4 cm electrode spacing, 76267 Ω for reactors with 2 cm electrode spacing and 33140 Ω for reactors with 1 cm electrode spacing. As these results were unrealistic the internal resistance was also estimated using the power density peak method (Logan, 2008). The power density peak method gives an estimate of the internal resistance based on the maximum power transfer theorem. This theorem states that maximum power is transferred in a circuit when the resistance of load and source are equal. As the theorem is derived on the basis of a battery or fixed power supply, it can only be applied when the source resistance is fixed. This is not the case in fuel cells where the internal resistance will change potential and current because of resistances due to kinetic and mass transfer losses and membrane resistance. In a battery only the membrane resistance is significant as the other two are negligible. Thus to use the power density peak method in microbial fuel cells kinetic and mass transfer resistances have to assumed to be negligible.

The resulting internal resistance estimates were 25 Ω for reactors with 4 cm electrode spacing, 204 Ω for reactors using 2 cm electrode distance and 25 Ω for reactors using 1 cm electrode spacing. The high internal resistance estimated for 2 cm electrode spacing explains the low power voltage, current and power densities observed under 50 Ω, 500 Ω and 1000 Ω.

In contrast to expectation the highest power densities were observed for the reactor with 1 cm electrode spacing which can be explained through the lower internal resistance, the reactor with 2 cm electrode spacing performed surprisingly poor whereas the best performance was expected from this reactors since Liu *et al.* (2005) achieved a 40 % increase in power densities when reducing the electrode spacing from 4 cm to 2 cm in batch-fed reactors. Furthermore reported Cheng *et al.* (2006a) a nearly 50 % decrease in power density when decreasing the electrode spacing from 2 cm to 1 cm in continuous flow reactors. Part of these contrasting results might be explained by the poor performance of all three reactors through the high influence of the internal resistance and possibly the different HRT of the reactors.

7.4.2.1.2 Polarisation Studies and Anode and Cathode Behaviour

Figure 7.8 shows the power density and cell voltage of the reactors during polarisation. All reactors reached low power densities. The highest power density was reached using reactors with 1 cm electrode spacing with 5.5 mW m^{-2} at 52 mA m^{-2} and 105 mV followed by the reactor using 4 cm electrode spacing with 4.7 mW m^{-2} (at 37 mA m^{-2} and 136 mV). The reactor using 2 cm electrode spacing showed the worst performance with 3.4 mW m^{-2} (at 8.6 mA m^{-2} and 311 mV).
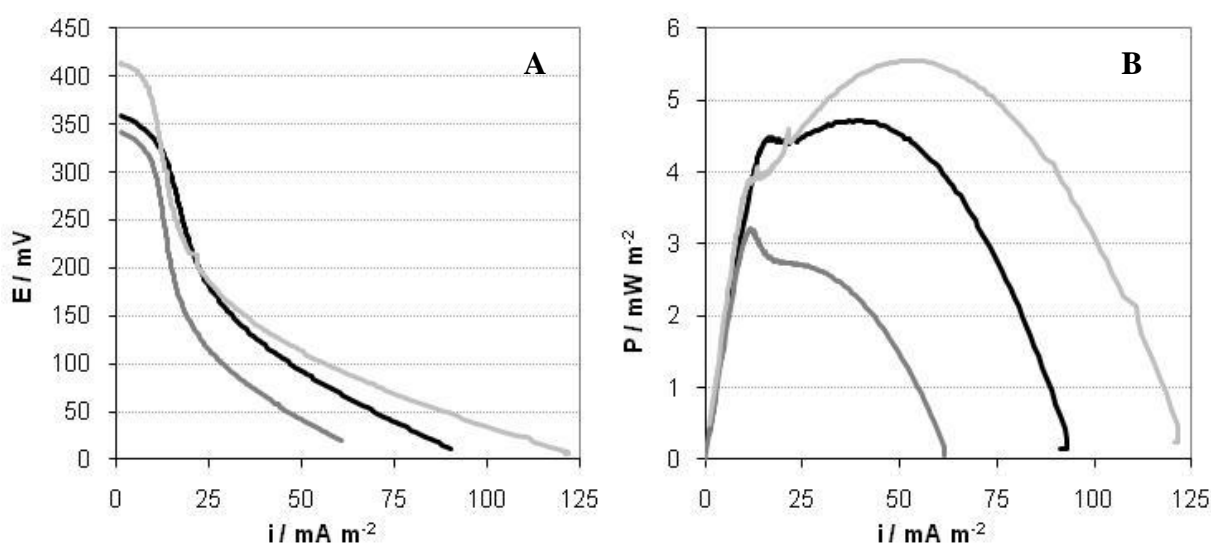
Figure 7.8: Linear sweep voltammograms showing the power density (B) and cell voltage (A) of the reactors set up as a factorial design with high (black), mid (grey), low (light grey).

Cathode, cell and power density were internal resistance corrected using the estimated result from the power density peak method. The two wave form of the cell potential, which is discussed below, indicated that the cathode potential influenced the cell potential and therefore power performance of the reactors.

Figure 7.9 shows the anode and iR corrected cathode behaviour of the three continuous flow reactors as measured during the polarisation. The reactor using 4 cm electrode spacing showed an overpotential loss of 60 mV at the anode and 300 mV at the cathode over a current density of 90 mA m^{-2}. The reactor using 2 cm electrode spacing showed a slightly lower overpotential loss of 44 mV at the anode and 294 mV at the cathode over a current density of 60 mA m^{-2}.

Interestingly the reactor with 1 cm electrode spacing showed a high overpotential loss of 335 mV at the anode and low overpotential loss of 80 mV at the cathode over a current density of 120 mA m^{-2}.
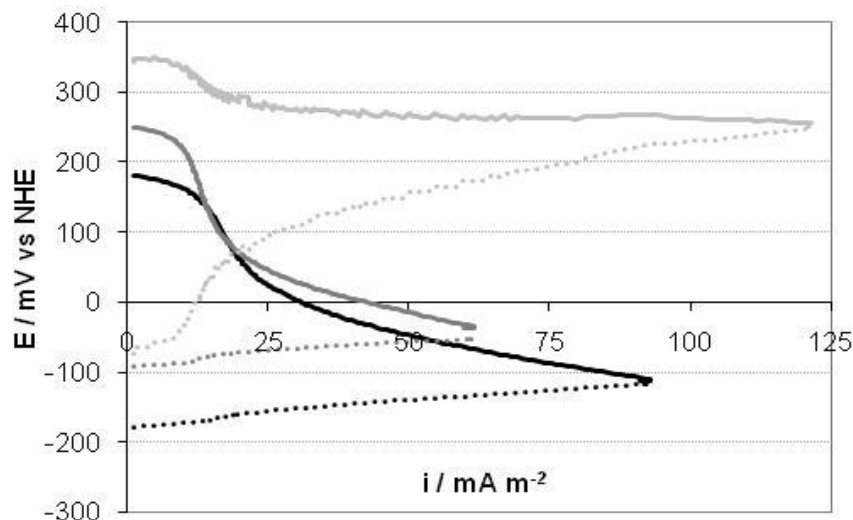
Figure 7.9: Linear sweep voltammograms of the anode (dotted) and cathode (line) behaviour during polarisation of the three reactors using different electrode spacing with high (black), mid (grey), low (light grey).

Similarly to observation under fed batch mode (Chapter 4) smaller electrode distance led to a shift in the anode potential with an onset potential of -178 mV at 4 cm, -92 mV at 2 cm and 72 mV when using 1 cm electrode spacing.

The difference in behaviour may be partly affected by the oxygen transfer into the reactor. Oxygen reaches the anodic biofilm more readily using a smaller electrode spacing, thus leading to a higher decrease in anode potential which is readily visible when looking at the anode behaviour of the reactor using 1 cm electrode spacing. The continuous flow system, in this study, did not reduce the shift in anode potential when decreasing the electrode distance.

Concurring with observations made in Chapter 4 to 6 the cathode potential showed two waves during the polarisation both possibly corresponding two different reaction mechanisms for oxygen reduction to peroxide due to the high accessibility of the carbon black surfaces at different sites on the carbon surface (Vielstich et al., 2003; Pirjamali and Kiros, 2002; Appleby and Marie, 1979).

7.4.2.2 Wastewater treatment efficiency

Samples to measure the COD were taken once the voltage stabilised under the different external loads. Figure 7.10 shows the average COD removal, coulombic efficiency and current density of the three reactors under different external load. The highest COD removal was observed for reactors using 4 cm electrode spacing and a HRT of 1 h with 90±6% under 1000 Ω, 80±8% under 500 Ω and 78±3% under 50 Ω. The reactor using 2 cm electrode spacing with a HRT of 30 min achieved slightly less COD removal with 83±5% under 1000 Ω, 60±1.4% under 500 Ω and 74±4% under 50 Ω. The reactors using 1 cm electrode spacing and a HRT of 15 min showed the worst COD removal with 56±12% under 1000 Ω, 47±9% under 500 Ω and 32±6% under 50 Ω. As expected higher COD removal was observed for greater electrode spacing as the substrates stayed longest in the anode chamber due to the long HRT (1 h) as well as higher external resistance.
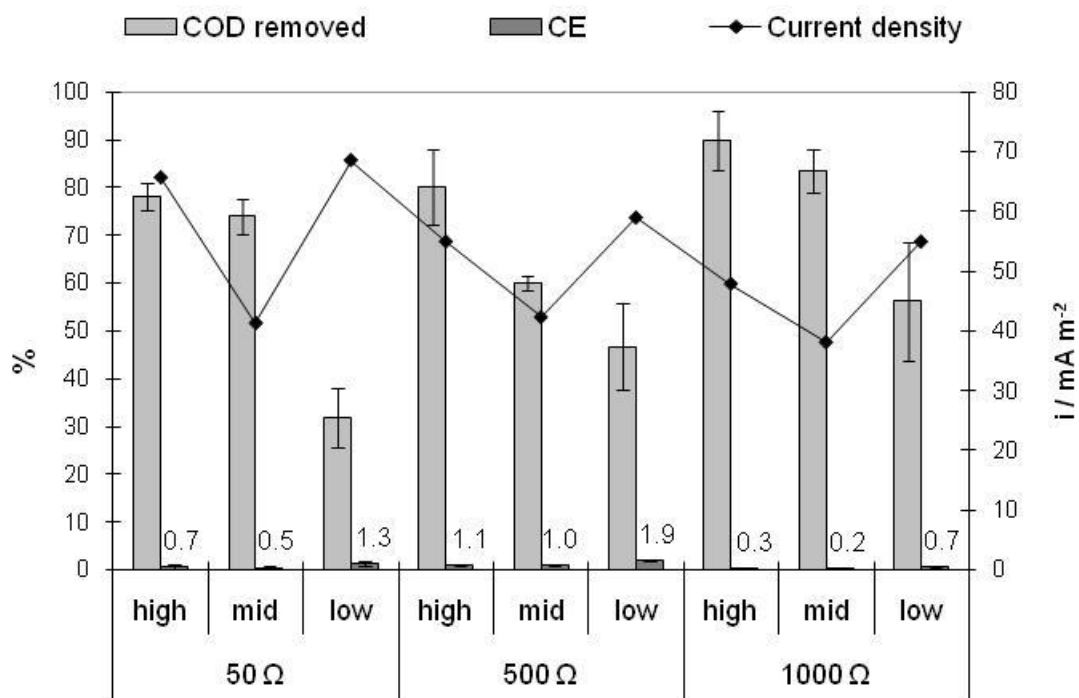
Figure 7.10: Average COD removal, CE and current density of the reactors used in the factorial design experiment under 50 Ω, 500 Ω and 1000 Ω.

Coulombic efficiencies for all reactors were very low ranging from 0.2% to 1.9%. The lowest CE was observed for reactors using 2 cm electrode spacing under any external resistance and under 500 Ω all reactors reached, in comparison, the highest C with 1.9% CE, 1.1% CE and 1.0%

CE for the reactor with 1 cm electrode spacing, 4 cm electrode spacing and 2 cm electrode spacing respectively.

COD removal improved for all three reactors with increasing external resistance. The reactor with 1 cm electrode spacing showed the lowest COD removal due to an HRT of 15 min, this was followed by the reactor with 2 cm electrode spacing and an HRT of 30 min while the reactor with 4 cm electrode spacing and an HRT of 1 h achieved the best COD removal. The very low coulombic efficiencies show the poor power performance of the reactors. The low coulombic efficiencies also showed power generation to be a minor process in the continuous flow system.

7.4.2.3 Statistical analysis of the factorial design

Figure 7.11 shows the interaction plots of the factors 'external resistance' and 'electrode distance' for the different results/responses (cell potential (A), current density (B), power density (C), COD removed (D) and CE (E)). These plots are a visualisation of main effects and interactions of the two factors at three levels.

Both voltage and power density (Figure 7.11 A and C) increased with increasing external resistance and decreasing distance, with the highest voltage reached at 1 cm electrode distance under 1000 Ω external resistance. Statistical analysis of responses showed that the effect of the external resistance is statistically significant (p=0.00 for voltage, p=0.005 for power density) whereas the electrode distance is not significant (p=0.112 for voltage, p=0.099 for power density).

The current density (Figure 7.11 B) decreased with increasing external resistance inversely to both voltage and power density. Reactors with 1 and 4 cm electrode distance showed a more pronounced decrease in current density from 50 Ω to 1000 Ω than the reactor with 2 cm electrode spacing which reached current densities in the same range at all three external resistances. Using the current density as response the electrode distance had a significant

effect (p=0.008) while the external resistance did not show a statistical significant effect (p=0.063).
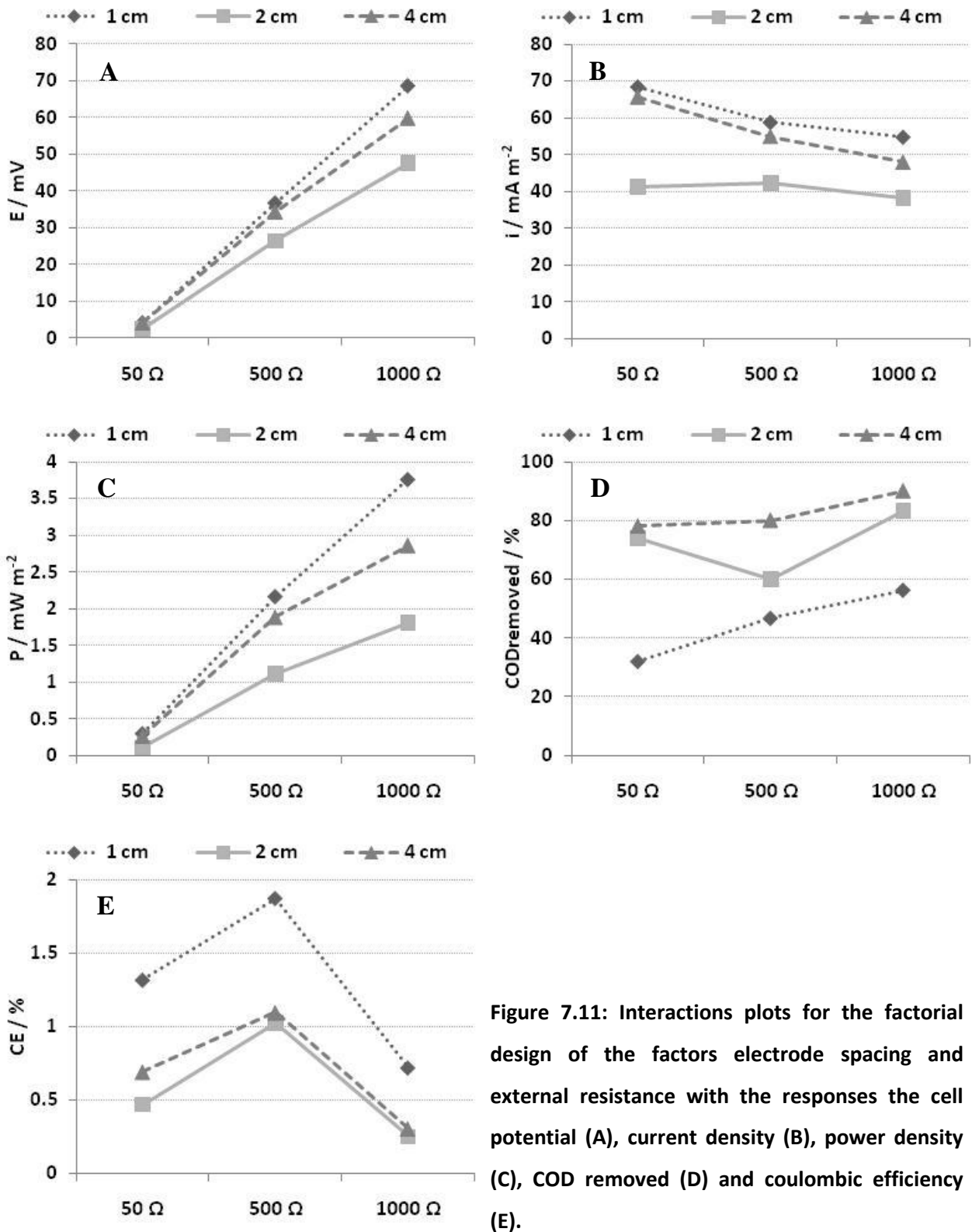
Figure 7.11: Interactions plots for the factorial design of the factors electrode spacing and external resistance with the responses the cell potential (A), current density (B), power density (C), COD removed (D) and coulombic efficiency (E).

The COD removal (Figure 7.11 D) increased slightly with increasing external resistance and as expected also with increasing electrode spacing. Statistically only the effect of the electrode distance was significant (p=0.008 for electrode spacing, p=0.113 for the external resistance). Coulombic efficiencies (Figure 7.11 E) reached the highest percentage under 500 Ω, followed by 50 Ω and the lowest coulombic efficiencies under 1000 Ω while at the same time reaching the highest coulombic efficiencies with 1 cm electrode distance, followed by 4 cm and 2 cm. Both effects were statistically significant (with p=0.002 for the external resistance and p=0.004 for the electrode distance).

An unexpected result was that reactors using 4 cm electrode distance reached higher voltage, current and power density and correlating coulombic efficiencies under all three external resistances than reactors with 2 cm electrode distance.

7.5   CONCLUSION

All four continuous flow reactors showed low power performance, moderate to good COD removal efficiencies and very low coulombic efficiencies. Thus electricity generation was a minor process in all of them which makes reaching conclusion on the MFC system difficult. Interestingly the flat plate reactors reached higher power densities under 500 Ω and 1000 Ω than while polarising the cell.

Low coulombic efficiencies achieved by all three reactors showed that energy generation was a minor process degrading the organic substrates in the wastewater. Thus although the statistical analysis showed external resistance and electrode distance to be statistically significant, depending on responses analysed, concluding on the importance of either effect and their interactions is difficult as only 0.2-2% of the organic substrate was degraded for power generation.

Partly the inefficient power performance could be due to the flow rate used, which lead to different HRTs in the reactors and influenced the microbial biofilm. Or it could be explained by

the high activity in the influent wastewater which lead to fast degradation of substrates using other processes than electrogenesis.

8 OVERALL CONCLUSIONS & FUTURE WORK

8.1 OVERALL CONCLUSION

Microbial fuel cells have been operated in fed batch and continuous mode using different anode, cathode and membrane materials and changing the reactor architecture while using wastewater as substrate.

The anode materials tested (carbon cloth, carbon black, C/HNO$_3$, C/PANI and three different activated carbon cloths), with the exception of carbon cloth, showed surprisingly consistent anode behaviour with low charge transfer resistivites. The most active and stable materials were a range of activated carbon cloth and activated carbon black (powdered carbon black activated with nitric acid) supported on carbon cloth. The high surface area, conductivity, porosity, and adsorption capabilities of the activated materials presumably gave the microorganisms a large surface to adhere to and facilitated extensive contact between microorganisms (biocatalyst), substrate and current collector. The low anode charge transfer resistivity achieved with these materials reflected the relatively high activity of the biocatalyst.

Activated carbon as anode material achieved comparatively high coulombic efficiencies and good power and wastewater treatment efficiencies. Activated carbon cloth showed great potential as anode material during polarisation, but a decline in power performance under constant external load was observed over time. In contrast coulombic efficiencies increased considerably from 23% CE to 42% CE over time while COD removal remained constant.

The community analysis of activated and modified anode materials revealed the significant influence of the external load on the anodic biofilm. The surface chemistry of the anode may have affected the selection of the microbial consortia when domestic wastewater was used as substrate. These results supported the hypothesis that the microbial community could be selected based on external load and surface chemistry of the anode material if power generation is the most important process in the system.

Brewery wastewater as part of the substrate (0.5%) seemingly inhibited power generation and masked the influence of the anode materials on the reactor performance. It was associated with very low coulombic efficiencies presumably due to preferential degradation of the high carbohydrate content by fermentation.

Power densities produced were limited largely by high ohmic losses (internal resistance) which were mainly due to the low conductivity of the substrate (wastewater). Reducing the electrode spacing to 2 mm decreased the internal resistance to 12 Ω (for low distance activated carbon cloth) or lower (1-7 Ω for the mesh anodes). An expected increase in power performance was offset by oxygen diffusion into the anode chamber which decreased the anode potential by 100 mV.

The batch reactors studied showed higher overpotential losses at the cathode than the anode. This strengthened the observation that the cathode activity was more limiting than the anode even taking into account the slow reaction kinetics of the biocatalyst (microorganisms). Investigation of the durability of different cathode catalysts with an inexpensive separator and wastewater as substrate (platinum, carbon black, C/HNO$_3$, FePc, FePc+Mn) showed a rapid decline in power performance over the relatively short period of 100 days. Carbon black showed the greatest durability with less decrease in activity over the 100 period.

Variation of the membrane or separator in the reactor showed a significant influence on the power performance through different profiles for voltage evolution. The highest power densities were reached with reactors using the ion exchange membranes ETFE and Nafion followed closely by the membrane-less reactor. These reactors also reached very high coulombic efficiencies with 92±6%, 71±12%, 68±11%, 66±20% and 63±8% for EFTE, Nafion, the membrane-less reactor, PVDF and Rhinohide respectively. The high power densities and coulombic efficiencies obtained using ion exchange membranes ETFE and Nafion showed the importance of good proton conduction through the membrane. Only long-term experiments will show the actual power and wastewater treatment performance of a membrane in a system, as the undefined composition of the wastewater might affect the membrane in a manner which only becomes apparent after a long period of operation. The good power

performance and high coulombic efficiency achieved using membrane-less reactors might be advantaged through lower costs and long-term durability when an inexpensive cathode support is used.

Oxygen diffusion into the anode chamber is a major barrier to overcome for high power performance. As slight amounts of oxygen will diffuse through even the most selective ion exchange membranes it is perhaps better to reduce the oxygen in the chamber through a biocathode on the membrane opposite to the anode inside the anodic chamber. This approach would also mean simpler system architecture as both electrodes are inside one chamber. An advantage of biocathodes would be lower costs, assuming the microbial consortia are able to consistently produce high power without inhibition, deactivation or poisoning by the wastewater.

The pH change in the batch system became more pronounced the better the reactor performed, but supposedly only leads to a reduction in power generation when the pH falls below 6. Reductions in the pH are presumably less important in continuous flow systems, as the flow through the system will replenish ions and therefore keep pH fluctuations to a minimum.

The continuous flow reactors studied showed low power performance, modest to good COD removal and very low coulombic efficiencies. This was presumably mainly due to the chosen flow rate and high biological activity in the wastewater.

The findings of the present research suggest that a lowered ohmic resistance through reduced electrode spacing, the use of a cost-effective and selective membrane which limits oxygen diffusion into the anode chamber, and more active cathode catalysts should considerably increase the power production. High coulombic efficiencies achieved in this research using cost-effective materials suggest that there is potential for the use of microbial fuel cell systems for economical energy generation from wastewater.

To ensure long-term viability anodes, air cathodes and membranes have to be tested more rigorously under realistic conditions since crossover of inhibiting substances from wastewater is not completely preventable even when using a selective membrane. It is crucial to spend more

time studying and understanding long-term durability and performance of the materials used and the influence of the system architecture especially on power performance in fed-batch and continuous flow wastewater-fed systems.

8.2 FUTURE WORK

Major limitations of the system architecture on microbial fuel cell performance are oxygen diffusion into the anode chamber and the high internal resistance due to the substrate (wastewater) used. The influence of oxygen diffusion on the microbial biofilm becomes more pronounced at lower electrode spacing which leads to reduced power performance. However when the electrode distance is increased the resulting high internal resistance also decreases the power output.

Limited durability and a loss in power performance was observed over time for the activated carbon cloth tested as anode material and the cathode catalysts investigated. The membrane materials studied performed comparatively well over the time they were studied under fed-batch operation. Since wastewaters are complex substrates it is important to study membranes used in MFC systems over longer periods (month to years) to gain knowledge of their long-term feasibility in wastewater treatment.

Investigation of the influence of external load and electrode distance in reactors operating under continuous flow resulted in very low power performances and coulombic efficiencies. To address the low performance further studies investigating the influence of the materials, MFC architecture and operational parameters are necessary.

Future research on materials and design with the aim to an operating pilot scale MFC using wastewater as substrate should focus on

- Reducing the internal resistance in the system while at the same time reducing oxygen diffusion into the anode chamber;
- Long-term investigation of the anode, cathode and membrane materials used to understand their performance over their lifetime;

- Implementation of materials and researched system architecture in continuous flow systems;
- Pilot/large scale experiments using wastewater fed MFCs.

Furthermore more efficient optimisation of MFC technology will be possible when the underlying processes are understood in detail. To understand underlying processes, research should further focus on electron transfer mechanisms, syntrophic behaviour and the interaction inside the microbial consortia and interaction with the anode and cathode support in mixed community biofilms.

9 REFERENCES

Aelterman, P., Versichele, M., Marzorati, M., Boon, N. and Verstraete, W. (2008) 'Loading rate and external resistance control the electricity generation of microbial fuel cells with different three-dimensional anodes', *Bioresource Technology,* 99, (18), pp. 8895-8902.

Angenent, L. T., Karim, K., Al-Dahhan, M. H. and Domiguez-Espinosa, R. (2004) 'Production of bioenergy and biochemicals from industrial and agricultural wastewater', *Trends in Biotechnology,* 22, (9), pp. 477-485.

Appleby, A. J. and Marie, J. (1979) 'Kinetics of Oxygen Reduction on Carbon Materials in Alkaline-Solution', *Electrochimica Acta,* 24, (2), pp. 195-202.

Arora, P. and Zhang, Z. M. (2004) 'Battery separators', *Chemical Reviews,* 104, (10), pp. 4419-4462.

Atkins, P. W. and De Paula, J. (2009) *Atkins' Physical chemistry.* Oxford: Oxford University Press.

Balkema A. J., P. H. A., Otterpohl R., Lambert F.J.D. (2002) 'Indicators for the sustainability assessment of wastewater treatment systems', *Urban Water*, (4), pp. 153-161.

Baranton, S., Coutanceau, C., Leger, J. M., Roux, C. and Capron, P. (2005) 'Alternative cathodes based on iron phthalocyanine catalysts for mini- or micro-DMFC working at room temperature', *Electrochimica Acta,* 51, (3), pp. 517-525.

Bard, A. J. and Faulkner, L. R. (2001) *Electrochemical methods : fundamentals and applications.* New York: Wiley.

Barton, S. C. (2005) 'Oxygen transport in composite mediated biocathodes', *Electrochimica Acta,* 50, (10), pp. 2145-2153.

Behera, M. and Ghangrekar, M. M. (2009) 'Performance of microbial fuel cell in response to change in sludge loading rate at different anodic feed pH', *Bioresource Technology,* 100, (21), pp. 5114-5121.

Bennetto, H. P., Stirling, J. L., Tanaka, K. and Vega, C. A. (1983) 'Anodic Reactions in Microbial Fuel-Cells', *Biotechnology and Bioengineering,* 25, (2), pp. 559-568.

Bergel, A., Feron, D. and Mollica, A. (2005) 'Catalysis of oxygen reduction in PEM fuel cell by seawater biofilm', *Electrochemistry Communications,* 7, (9), pp. 900-904.

Berthouex, P. M. and Brown, L. C. (2002) *Statistics for environmental engineers.* London.: Lewis Publishers.

Bitton, G. and Ebooks Corporation. (2005) *Wastewater Microbiology.* Hoboken: John Wiley & Sons Inc.

Bleda-Martinez, M. J., Lozano-Castello, D., Morallon, E., Cazorla-Amoros, D. and Linares-Solano, A. (2006) 'Chemical and electrochemical characterization of porous carbon materials', *Carbon,* 44, (13), pp. 2642-2651.

Bleda-Martinez, M. J., Macia-Agullo, J. A., Lozano-Castello, D., Morallon, E., Cazorla-Amoros, D. and Linares-Solano, A. (2005) 'Role of surface chemistry on electric double layer capacitance of carbon materials', *Carbon,* 43, (13), pp. 2677-2684.

Boehm, H. P. (1994) 'Some Aspects of the Surface-Chemistry of Carbon-Blacks and Other Carbons', *Carbon,* 32, (5), pp. 759-769.

Bond, D. R. and Lovley, D. R. (2003) 'Electricity production by Geobacter sulfurreducens attached to electrodes', *Applied and Environmental Microbiology,* 69, (3), pp. 1548-1555.

Boudou, J. P. (2003) 'Surface chemistry of a viscose-based activated carbon cloth modified by treatment with ammonia and steam', *Carbon,* 41, (10), pp. 1955-1963.

Bramucci, M., Kane, H., Chen, M. and Nagarajan, V. (2003) 'Bacterial diversity in an industrial wastewater bioreactor', *Applied Microbiology and Biotechnology,* 62, (5-6), pp. 594-600.

Chae, K. J., Choi, M., Ajayi, F. F., Park, W., Chang, I. S. and Kim, I. S. (2008) 'Mass transport through a proton exchange membrane (Nafion) in microbial fuel cells', *Energy & Fuels,* 22, (1), pp. 169-176.

Chang, I. S., Jang, J. K., Gil, G. C., Kim, M., Kim, H. J., Cho, B. W. and Kim, B. H. (2004) 'Continuous determination of biochemical oxygen demand using microbial fuel cell type biosensor', *Biosensors & Bioelectronics,* 19, (6), pp. 607-613.

Cheng, H., Scott, K., Lovell, K., Horsfall, J. A. and Waring, S. C. (2007) 'Evaluation of new ion exchange membranes for direct borohydride fuel cells', *Journal of Membrane Science,* 288, (1-2), pp. 168-174.

Cheng, S., Liu, H. and Logan, B. E. (2006a) 'Increased power generation in a continuous flow MFC with advective flow through the porous anode and reduced electrode spacing', *Environmental Science & Technology,* 40, (7), pp. 2426-2432.

Cheng, S., Liu, H. and Logan, B. E. (2006b) 'Power densities using different cathode catalysts (Pt and CoTMPP) and polymer binders (Nafion and PTFE) in single chamber microbial fuel cells', *Environmental Science & Technology,* 40, (1), pp. 364-369.

Cheng, S. A. and Logan, B. E. (2007) 'Ammonia treatment of carbon cloth anodes to enhance power generation of microbial fuel cells', *Electrochemistry Communications,* 9, (3), pp. 492-496.

Chu, Y. Q., Ma, C. A., Zhao, F. M. and Huang, H. (2004) 'Electrochemical reduction of oxygen on multi-walled carbon nanotubes electrode in alkaline solution', *Chinese Chemical Letters,* 15, (7), pp. 805-807.

Clauwaert, P., Van der Ha, D., Boon, N., Verbeken, K., Verhaege, M., Rabaey, K. and Verstraete, W. (2007) 'Open air biocathode enables effective electricity generation with microbial fuel cells', *Environmental Science & Technology,* 41, (21), pp. 7564-7569.

Deng, Q., Li, X. Y., Zuo, J. E., Ling, A. and Logan, B. E. (2010) 'Power generation using an activated carbon fiber felt cathode in an upflow microbial fuel cell', *Journal of Power Sources,* 195, (4), pp. 1130-1135.

Di Lorenzo, M., Curtis, T. P., Head, I. M. and Scott, K. (2009a) 'A single-chamber microbial fuel cell as a biosensor for wastewaters', *Water Research,* 43, (13), pp. 3145-3154.

Di Lorenzo, M., Scott, K., Curtis, T. P. and Head, I. M. (2010) 'Effect of increasing anode surface area on the performance of a single chamber microbial fuel cell', *Chemical Engineering Journal,* 156, (1), pp. 40-48.

Di Lorenzo, M., Scott, K., Curtis, T. P., Katuri, K. P. and Head, I. M. (2009b) 'Continuous Feed Microbial Fuel Cell Using An Air Cathode and A Disc Anode Stack for Wastewater Treatment', *Energy & Fuels,* 23, pp. 5707-5716.

Dlugolecki, P., Anet, B., Metz, S. J., Nijmeijer, K. and Wessling, M. (2010) 'Transport limitations in ion exchange membranes at low salt concentrations', *Journal of Membrane Science,* 346, (1), pp. 163-171.

Donnet, J.-B., Bansal, R. C. and Wang, M.-J. (1993) *Carbon black : science and technology.* New York: Dekker.

Du, Z. W., Li, H. R. and Gu, T. Y. (2007) 'A state of the art review on microbial fuel cells: A promising technology for wastewater treatment and bioenergy', *Biotechnology Advances,* 25, (5), pp. 464-482.

Du, Z. W., Li, Q. H., Tong, M., Li, S. H. and Li, H. R. (2008) 'Electricity Generation Using Membrane-less Microbial Fuel Cell during Wastewater Treatment', *Chinese Journal of Chemical Engineering,* 16, (5), pp. 772-777.

Duteanu N, E. B., Senthil Kumar SM, Ghangrekar MM, Scott K. (2010) 'Effect of chemically modified Vulcan XC-72R on the performance of air-breathing cathode in a single-chamber microbial fuel cell.', *Bioresource Technology,* 101, (14), pp. 5250–5255.

Eaton, A. D., Clesceri, L. S., Greenberg, A. E., Franson, M. A. H., American Public Health Association., American Water Works Association. and Water Environment Federation. (1998) *Standard methods for the examination of water and wastewater.* Washington, DC: American Public Health Association.

El-Naas, M. H., Al-Zuhair, S. and Abu Alhaija, M. (2010) 'Reduction of COD in refinery wastewater through adsorption on date-pit activated carbon', *Journal of Hazardous Materials,* 173, (1-3), pp. 750-757.

Fan, Y. Z., Hu, H. Q. and Liu, H. (2007) 'Enhanced Coulombic efficiency and power density of air-cathode microbial fuel cells with an improved cell configuration', *Journal of Power Sources,* 171, (2), pp. 348-354.

Feng, C. H., Ma, L., Li, F. B., Mai, H. J., Lang, X. M. and Fan, S. S. (2010a) 'A polypyrrole/anthraquinone-2,6-disulphonic disodium salt (PPy/AQDS)-modified anode to improve performance of microbial fuel cells', *Biosensors & Bioelectronics,* 25, (6), pp. 1516-1520.

Feng, Y., Wang, X., Logan, B. E. and Lee, H. (2008) 'Brewery wastewater treatment using air-cathode microbial fuel cells', *Applied Microbiology and Biotechnology,* 78, (5), pp. 873-880.

Feng, Y. J., Yang, Q., Wang, X. and Logan, B. E. (2010b) 'Treatment of carbon fiber brush anodes for improving power generation in air-cathode microbial fuel cells', *Journal of Power Sources,* 195, (7), pp. 1841-1844.

Franz, J. A., Williams, R. J., Flora, J. R., Meadows, M. E. and Irwin, W. G. (2002) 'Electrolytic oxygen generation for subsurface delivery: effects of precipitation at the cathode and an assessment of side reactions', *Water Research,* 36, (9), pp. 2243-2254.

Freguia, S., Masuda, M., Tsujimura, S. and Kano, K. (2009) 'Lactococcus lactis catalyses electricity generation at microbial fuel cell anodes via excretion of a soluble quinone', *Bioelectrochemistry,* 76, (1-2), pp. 14-18.

Freguia, S., Rabaey, K., Yuan, Z. and Keller, J. (2007) 'Non-catalyzed cathodic oxygen reduction at graphite granules in microbial fuel cells', *Electrochimica Acta,* 53, (2), pp. 598-603.

Freguia, S., Rabaey, K., Yuan, Z. G. and Keller, J. (2008) 'Sequential anode-cathode configuration improves cathodic oxygen reduction and effluent quality of microbial fuel cells', *Water Research,* 42, (6-7), pp. 1387-1396.

Freguia, S., Tsujimura, S. and Kano, K. (2010) 'Electron transfer pathways in microbial oxygen biocathodes', *Electrochimica Acta,* 55, (3), pp. 813-818.

Funt, B. L. and P. M. Hoang (1983). 'Electrochemical Characteristics of Electrodes Coated with Films of Poly(Vinyl-Para-Benzoquinone) and Its Co-Polymer with Styrene.' *Journal of Electroanalytical Chemistry* 154(1-2): 229-238.

Ghangrekar, M. M. and Shinde, V. B. (2007) 'Performance of membrane-less microbial fuel cell treating wastewater and effect of electrode distance and area on electricity production', *Bioresource Technology,* 98, (15), pp. 2879-2885.

Gil, G. C., Chang, I. S., Kim, B. H., Kim, M., Jang, J. K., Park, H. S. and Kim, H. J. (2003) 'Operational parameters affecting the performance of a mediator-less microbial fuel cell', *Biosensors & Bioelectronics,* 18, (4), pp. 327-334.

Gorby, Y. A., Yanina, S., McLean, J. S., Rosso, K. M., Moyles, D., Dohnalkova, A., Beveridge, T. J., Chang, I. S., Kim, B. H., Kim, K. S., Culley, D. E., Reed, S. B., Romine, M. F., Saffarini, D. A., Hill, E. A., Shi, L., Elias, D. A., Kennedy, D. W., Pinchuk, G., Watanabe, K., Ishii, S., Logan, B., Nealson, K. H. and Fredrickson, J. K. (2006) 'Electrically conductive bacterial nanowires produced by Shewanella oneidensis strain MR-1 and other microorganisms', *Proceedings of the National Academy of Sciences of the United States of America,* 103, (30), pp. 11358-11363.

Grzebyk, M. and Pozniak, G. (2005) 'Microbial fuel cells (MFCs) with interpolymer cation exchange membranes', *Separation and Purification Technology,* 41, (3), pp. 321-328.

Gubler, L., Gursel, S. A. and Scherer, G. G. (2005) 'Radiation grafted membranes for polymer electrolyte fuel cells', *Fuel Cells,* 5, (3), pp. 317-335.

Gupta, B., Buchi, F. N., Scherer, G. G. and Chapiro, A. (1996) 'Crosslinked ion exchange membranes by radiation grafting of styrene/divinylbenzene into FEP films', *Journal of Membrane Science,* 118, (2), pp. 231-238.

Ha, P. T., Moon, H., Kim, B. H., Ng, H. Y. and Chang, I. S. (2010) 'Determination of charge transfer resistance and capacitance of microbial fuel cell through a transient response analysis of cell voltage', *Biosensors & Bioelectronics,* 25, (7), pp. 1629-1634.

Hami, M. L., Al-Hashimi, M. A. and Al-Doori, M. M. (2007) 'Effect of activated carbon on BOD and COD removal in a dissolved air flotation unit treating refinery wastewater', *Desalination,* 216, (1-3), pp. 116-122.

HaoYu, E., Cheng, S., Scott, K. and Logan, B. (2007) 'Microbial fuel cell performance with non-Pt cathode catalysts', *Journal of Power Sources,* 171, (2), pp. 275-281.

Harnisch, F., Schroder, U. and Scholz, F. (2008) 'The suitability of monopolar and bipolar ion exchange membranes as separators for biological fuel cells', *Environmental Science & Technology,* 42, (5), pp. 1740-1746.

Harnisch, F., Warmbier, R., Schneider, R. and Schroder, U. (2009a) 'Modeling the ion transfer and polarization of ion exchange membranes in bioelectrochemical systems', *Bioelectrochemistry,* 75, (2), pp. 136-141.

Harnisch, F., Wirth, S. and Schroder, U. (2009b) 'Effects of substrate and metabolite crossover on the cathodic oxygen reduction reaction in microbial fuel cells: Platinum vs. iron(II) phthalocyanine based electrodes', *Electrochemistry Communications,* 11, (11), pp. 2253-2256.

He, Z. and Angenent, L. T. (2006) 'Application of bacterial biocathodes in microbial fuel cells', *Electroanalysis,* 18, (19-20), pp. 2009-2015.

He, Z., Huang, Y. L., Manohar, A. K. and Mansfeld, F. (2008) 'Effect of electrolyte pH on the rate of the anodic and cathodic reactions in an air-cathode microbial fuel cell', *Bioelectrochemistry,* 74, (1), pp. 78-82.

He, Z., Minteer, S. D. and Angenent, L. T. (2005) 'Electricity generation from artificial wastewater using an upflow microbial fuel cell', *Environmental Science & Technology,* 39, (14), pp. 5262-5267.

He, Z., Wagner, N., Minteer, S. D. and Angenent, L. T. (2006) 'An upflow microbial fuel cell with an interior cathode: Assessment of the internal resistance by impedance Spectroscopy', *Environmental Science & Technology,* 40, (17), pp. 5212-5217.

Hernandez, M. E., Kappler, A. and Newman, D. K. (2004) 'Phenazines and other redox-active antibiotics promote microbial mineral reduction', *Applied and Environmental Microbiology,* 70, (2), pp. 921-928.

Hietala, S., Holmberg, S., Karjalainen, M., Nasman, J., Paronen, M., Serimaa, R., Sundholm, F. and Vahvaselka, S. (1997) 'Structural investigation of radiation grafted and sulfonated poly(vinylidene fluoride), PVDF, membranes', *Journal of Materials Chemistry,* 7, (5), pp. 721-726.

Ho, J. C. K. and Piron, D. L. (1995) 'Real Active Surface-Area Determination by Adsorption/Desorption of Overpotential Deposited Hydrogen', *Journal of the Electrochemical Society,* 142, (4), pp. 1144-1149.

Horsfall, J. A. and Lovell, K. V. (2002) 'Synthesis and characterisation of sulfonic acid-containing ion exchange membranes based on hydrocarbon and fluorocarbon polymers', *European Polymer Journal,* 38, (8), pp. 1671-1682.

Ibrahim, M. and Koglin, E. (2005) 'Spectroscopic study of polyaniline emeraldine base: Modelling approach', *Acta Chimica Slovenica,* 52, (2), pp. 159-163.

Isaac, P. C. G. (1978) 'Environmental protection: new aims and real costs', *Chemistry and Industry*, pp. 497-503.

Jang, J. K., Pham, T. H., Chang, I. S., Kang, K. H., Moon, H., Cho, K. S. and Kim, B. H. (2004) 'Construction and operation of a novel mediator- and membrane-less microbial fuel cell', *Process Biochemistry,* 39, (8), pp. 1007-1012.

Jankowska, H., Neffe, S. and Swiatkowski, A. (1981) 'Investigations of the Electrochemical Properties of Activated Carbon and Carbon-Black', *Electrochimica Acta,* 26, (12), pp. 1861-1866.

Jasinski, R. (1964) 'A New Fuel Cell Cathode Catalyst', *Nature,* 201, pp. 1212 - 1213

Jiang, D. Q. and Li, B. K. (2009) 'Granular activated carbon single-chamber microbial fuel cells (GAC-SCMFCs): A design suitable for large-scale wastewater treatment processes', *Biochemical Engineering Journal,* 47, (1-3), pp. 31-37.

Johnson, W. P. and Logan, B. E. (1996) 'Enhanced transport of bacteria in porous media by sediment-phase and aqueous-phase natural organic matter', *Water Research,* 30, (4), pp. 923-931.

Karube, I., Matsunaga, T., Tsuru, S. and Suzuki, S. (1977) 'Biochemical Fuel-Cell Utilizing Immobilized Cells of Clostridium-Butyricum', *Biotechnology and Bioengineering,* 19, (11), pp. 1727-1733.

Kiely, G. (1997) *Environmental engineering.* New York: McGraw-Hill Book Co.

Kim, J. R., Cheng, S., Oh, S. E. and Logan, B. E. (2007) 'Power generation using different cation, anion, and ultrafiltration membranes in microbial fuel cells', *Environmental Science & Technology,* 41, (3), pp. 1004-1009.

Kinoshita, K. (1992) *Electrochemical oxygen technology.* New York: Wiley.

Kruusenberg, I., Alexeyeva, N. and Tammeveski, K. (2009) 'The pH-dependence of oxygen reduction on multi-walled carbon nanotube modified glassy carbon electrodes', *Carbon,* 47, (3), pp. 651-658.

Lahaye, J. and Ehrburgerdolle, F. (1994) 'Mechanisms of Carbon-Black Formation - Correlation with the Morphology of Aggregates', *Carbon,* 32, (7), pp. 1319-1324.

Larrosa, A., Lozano, L. J., Katuri, K. P., Head, I., Scott, K. and Godinez, C. (2009) 'On the repeatability and reproducibility of experimental two-chambered microbial fuel cells', *Fuel,* 88, (10), pp. 1852-1857.

Laspidou, C. S., Rittmann B.E. (2005) 'Modeling biofilm complexity by including active and inert biomass and extracellular polymeric substances', *Cambridge University Press*, (1), pp. 285–291.

Lehmani, A., Turq, P., Perie, M., Perie, J. and Simonin, J. P. (1997) 'Ion transport in Nafion(R) 117 membrane', *Journal of Electroanalytical Chemistry,* 428, (1-2), pp. 81-89.

Lehtinen, T., Sundholm, G., Holmberg, S., Sundholm, F., Bjornbom, P. and Bursell, M. (1998) 'Electrochemical characterization of PVDF-based proton conducting membranes for fuel cells', *Electrochimica Acta,* 43, (12-13), pp. 1881-1890.

Levett, P. N. (1990) *Anaerobic bacteria : a functional biology.* Milton Keynes ; Philadelphia: Open University Press.

Li, B. K. and Logan, B. E. (2004) 'Bacterial adhesion to glass and metal-oxide surfaces', *Colloids and Surfaces B-Biointerfaces,* 36, (2), pp. 81-90.

Li, F. X., Sharma, Y., Lei, Y., Li, B. K. and Zhou, Q. X. (2010a) 'Microbial Fuel Cells: The Effects of Configurations, Electrolyte Solutions, and Electrode Materials on Power Generation', *Applied Biochemistry and Biotechnology,* 160, (1), pp. 168-181.

Li, W.-W. L., Guo-Ping Sheng, Xian-Wei Liua and Han-Qing Yua. (2010) 'Recent advances in the separators for microbial fuel cells ', *Bioresource Technology*.

Li, X., Hu, B. X., Suib, S., Lei, Y. and Li, B. K. (2010b) 'Manganese dioxide as a new cathode catalyst in microbial fuel cells', *Journal of Power Sources,* 195, (9), pp. 2586-2591.

Liu, H., Cheng, S., Huang, L. P. and Logan, B. E. (2008) 'Scale-Lip of membrane-free single-chamber microbial fuel cells', *Journal of Power Sources,* 179, (1), pp. 274-279.

Liu, H., Cheng, S. A. and Logan, B. E. (2005) 'Power generation in fed-batch microbial fuel cells as a function of ionic strength, temperature, and reactor configuration', *Environmental Science & Technology,* 39, (14), pp. 5488-5493.

Liu, H. and Logan, B. E. (2004) 'Electricity generation using an air-cathode single chamber microbial fuel cell in the presence and absence of a proton exchange membrane', *Environmental Science & Technology,* 38, (14), pp. 4040-4046.

Liu, H. S., Song, C. J., Zhang, L., Zhang, J. J., Wang, H. J. and Wilkinson, D. P. (2006) 'A review of anode catalysis in the direct methanol fuel cell', *Journal of Power Sources,* 155, (2), pp. 95-110.

Logan, B., Cheng, S., Watson, V. and Estadt, G. (2007) 'Graphite fiber brush anodes for increased power production in air-cathode microbial fuel cells', *Environmental Science & Technology,* 41, (9), pp. 3341-3346.

Logan, B. E. (1999) *Environmental transport processes.* New York: J. Wiley.

Logan, B. E. (2009) 'Exoelectrogenic bacteria that power microbial fuel cells', *Nature Reviews Microbiology,* 7, (5), pp. 375-381.

Logan, B. E. and Ebooks Corporation. (2008) *Microbial Fuel Cells.* Hoboken: John Wiley & Sons Inc.

Logan, B. E., Hamelers, B., Rozendal, R. A., Schrorder, U., Keller, J., Freguia, S., Aelterman, P., Verstraete, W. and Rabaey, K. (2006) 'Microbial fuel cells: Methodology and technology', *Environmental Science & Technology,* 40, (17), pp. 5181-5192.

Logan, B. E. and Regan, J. M. (2006) 'Electricity-producing bacterial communities in microbial fuel cells', *Trends in Microbiology,* 14, (12), pp. 512-518.

Loutfy, R. O. (1986) 'Electrochemical Characterization of Carbon-Black', *Carbon,* 24, (2), pp. 127-130.

Lovley, D. R. (2006) 'Bug juice: harvesting electricity with microorganisms', *Nature Reviews Microbiology,* 4, (7), pp. 497-508.

Lowy, D. A., Tender, L. M., Zeikus, J. G., Park, D. H. and Lovley, D. R. (2006) 'Harvesting energy from the marine sediment-water interface II - Kinetic activity of anode materials', *Biosensors & Bioelectronics,* 21, (11), pp. 2058-2063.

Lyon, D. Y., Buret, F., Vogel, T. M. and Monier, J. M. (2010) 'Is resistance futile? Changing external resistance does not improve microbial fuel cell performance', *Bioelectrochemistry,* 78, (1), pp. 2-7.

Madigan, M. T. and T. D. Brock (2009). *Brock biology of microorganisms*. San Francisco, CA, Pearson/Benjamin Cummings.

Magrez, A., Kasas, S., Salicio, V., Pasquier, N., Seo, J. W., Celio, M., Catsicas, S., Schwaller, B. and Forro, L. (2006) 'Cellular toxicity of carbon-based nanomaterials', *Nano Letters,* 6, (6), pp. 1121-1125.

Marcus, A. K., Torres, C. I. and Rittmann, B. E. (2007) 'Conduction-based modeling of the biofilm anode of a microbial fuel cell', *Biotechnology and Bioengineering,* 98, (6), pp. 1171-1182.

Mauritz, K. A. and Moore, R. B. (2004) 'State of understanding of Nafion', *Chemical Reviews,* 104, (10), pp. 4535-4585.

Menicucci, J., Beyenal, H., Marsili, E., Veluchamy, R. A., Demir, G. and Lewandowski, Z. (2006) 'Procedure for determining maximum sustainable power generated by microbial fuel cells', *Environmental Science & Technology,* 40, (3), pp. 1062-1068.

Metcalf & Eddy., Tchobanoglous, G., Burton, F. L. and Stensel, H. D. (2003) *Wastewater engineering : treatment and reuse.* Boston: McGraw-Hill.

Min, B. and Logan, B. E. (2004) 'Continuous electricity generation from domestic wastewater and organic substrates in a flat plate microbial fuel cell', *Environmental Science & Technology,* 38, (21), pp. 5809-5814.

Min, B. K., Cheng, S. A. and Logan, B. E. (2005) 'Electricity generation using membrane and salt bridge microbial fuel cells', *Water Research,* 39, (9), pp. 1675-1686.

Misra, S. C. K. and Angelucci, R. (2001) 'Polyaniline thin film-porous silicon sensors for detection of microorganisms', *Indian Journal of Pure & Applied Physics,* 39, (11), pp. 726-730.

Mohan, D., Singh, K. R. and Singh, V. K. (2008) 'Wastewater treatment using low cost activated carbons derived from agricultural byproducts - A case study', *Journal of Hazardous Materials,* 152, (3), pp. 1045-1053.

Muhammad-Tahir, Z. and Alocilja, E. C. (2003) 'Fabrication of a disposable biosensor for Escherichia coli O157 : H7 detection', *Ieee Sensors Journal,* 3, (4), pp. 345-351.

Murguia, M. and Villasenor, J. L. (2003) 'Estimating the effect of the similarity coefficient and the cluster algorithm on biogeographic classifications', *Annales Botanici Fennici,* 40, (6), pp. 415-421.

Myers, C. R. and Myers, J. M. (1992) 'Localization of Cytochromes to the Outer-Membrane of Anaerobically Grown Shewanella-Putrefaciens Mr-1', *Journal of Bacteriology,* 174, (11), pp. 3429-3438.

Newman, D. K. and Kolter, R. (2000) 'A role for excreted quinones in extracellular electron transfer', *Nature,* 405, (6782), pp. 94-97.

Niessen, J., Schroder, U., Rosenbaum, M. and Scholz, F. (2004) 'Fluorinated polyanilines as superior materials for electrocatalytic anodes in bacterial fuel cells', *Electrochemistry Communications,* 6, (6), pp. 571-575.

Nohl, H., Jordan, W. and Youngman, R. J. (1986) 'Quinones in Biology - Functions in Electron-Transfer and Oxygen Activation', *Advances in Free Radical Biology and Medicine,* 2, (1), pp. 211-279.

O'Toole, G., Kaplan, H. B. and Kolter, R. (2000) 'Biofilm formation as microbial development', *Annual Review of Microbiology,* 54, pp. 49-79.

Okada, T., Moller-Holst, S., Gorseth, O. and Kjelstrup, S. (1998) 'Transport and equilibrium properties of Nafion (R) membranes with H+ and Na+ ions', *Journal of Electroanalytical Chemistry,* 442, (1-2), pp. 137-145.

Oniciu, L. (1976) *Fuel cells.* Tunbridge Wells: Abacus Press.

Pant, D., G. Van Bogaerta, M. De Smeta, L. Dielsa and K. Vanbroekhoven. (2009) 'Use of novel permeable membrane and air cathodes in acetate microbial fuel cells ', *Electrochimica Acta,* xxx, (xxx), pp. xxx.

Pant, D., Van Bogaert, G., Diels, L. and Vanbroekhoven, K. (2010) 'A review of the substrates used in microbial fuel cells (MFCs) for sustainable energy production', *Bioresource Technology,* 101, (6), pp. 1533-1543.

Park, D. H., Kim, S. K., Shin, I. H. and Jeong, Y. J. (2000) 'Electricity production in biofuel cell using modified graphite electrode with Neutral Red', *Biotechnology Letters,* 22, (16), pp. 1301-1304.

Park, D. H. and Zeikus, J. G. (2002) 'Impact of electrode composition on electricity generation in a single-compartment fuel cell using Shewanella putrefaciens', *Applied Microbiology and Biotechnology,* 59, (1), pp. 58-61.

Patel, R., Park, J. T., Lee, W. S., Kim, J. H. and Min, B. R. (2009) 'Composite polymer electrolyte membranes comprising P(VDF-co-CTFE)-g-PSSA graft copolymer and zeolite for fuel cell applications', *Polymers for Advanced Technologies,* 20, (12), pp. 1146-1151.

Peavy, H. S., Rowe, D. R. and Tchobanoglous, G. (1985) *Environmental engineering.* New York: McGraw-Hill.

Perry, R. H., Green, D. W. and Maloney, J. O. (1984) *Perry's Chemical engineers' handbook.* New York: McGraw-Hill.

Pham, T. H., Aelterman, P. and Verstraete, W. (2009) 'Bioanode performance in bioelectrochemical systems: recent improvements and prospects', *Trends in Biotechnology,* 27, (3), pp. 168-178.

Pirjamali, M. and Kiros, Y. (2002) 'Effects of carbon pretreatment for oxygen reduction in alkaline electrolyte', *Journal of Power Sources,* 109, (2), pp. 446-451.

Pozio, A., De Francesco, M., Cemmi, A., Cardellini, F. and Giorgi, L. (2002) 'Comparison of high surface Pt/C catalysts by cyclic voltammetry', *Journal of Power Sources,* 105, (1), pp. 13-19.

Prasad, D., Arun, S., Murugesan, A., Padmanaban, S., Satyanarayanan, R. S., Berchmans, S. and Yegnaraman, V. (2007) 'Direct electron transfer with yeast cells and construction of a mediatorless microbial fuel cell', *Biosensors & Bioelectronics,* 22, (11), pp. 2604-2610.

Prescott, L. M., J. P. Harley, et al. (2005). *Microbiology*. Dubuque, IA, McGraw-Hill.

Qiao, Y., Bao, S. J., Li, C. M., Cui, X. Q., Lu, Z. S. and Guo, J. (2008) 'Nanostructured polyanifine/titanium dioxide composite anode for microbial fuel cells', *Acs Nano,* 2, (1), pp. 113-119.

Qiao, Y., Li, C. M., Bao, S. J. and Bao, Q. L. (2007) 'Carbon nanotube/polyaniline composite as anode material for microbial fuel cells', *Journal of Power Sources,* 170, (1), pp. 79-84.

R. Battino, H. L. C. (1966) 'The Solubility of Gases in Liquids', *Chemical Reviews,* 66, (4), pp. 395–463.

Rabaey, K., Boon, N., Hofte, M. and Verstraete, W. (2005a) 'Microbial phenazine production enhances electron transfer in biofuel cells', *Environmental Science & Technology,* 39, (9), pp. 3401-3408.

Rabaey, K., Boon, N., Siciliano, S. D., Verhaege, M. and Verstraete, W. (2004) 'Biofuel cells select for microbial consortia that self-mediate electron transfer', *Applied and Environmental Microbiology,* 70, (9), pp. 5373-5382.

Rabaey, K., Clauwaert, P., Aelterman, P. and Verstraete, W. (2005b) 'Tubular microbial fuel cells for efficient electricity generation', *Environmental Science & Technology,* 39, (20), pp. 8077-8082.

Rabaey, K. and Keller, J. (2008) 'Microbial fuel cell cathodes: from bottleneck to prime opportunity?', *Water Science and Technology,* 57, (5), pp. 655-659.

Rabaey, K., Ossieur, W., Verhaege, M. and Verstraete, W. (2005c) 'Continuous microbial fuel cells convert carbohydrates to electricity', *Water Science and Technology,* 52, (1-2), pp. 515-523.

Rabaey, K., Van de Sompel, K., Maignien, L., Boon, N., Aelterman, P., Clauwaert, P., De Schamphelaire, L., Pham, H. T., Vermeulen, J., Verhaege, M., Lens, P. and Verstraete, W. (2006) 'Microbial fuel cells for sulfide removal', *Environmental Science & Technology,* 40, (17), pp. 5218-5224.

Rabaey, K. and Verstraete, W. (2005) 'Microbial fuel cells: novel biotechnology for energy generation', *Trends in Biotechnology,* 23, (6), pp. 291-298.

Raghavulu, S. V., Mohan, S. V., Goud, R. K. and Sarma, P. N. (2009) 'Effect of anodic pH microenvironment on microbial fuel cell (MFC) performance in concurrence with aerated and ferricyanide catholytes', *Electrochemistry Communications,* 11, (2), pp. 371-375.

Ralph, T. R., Hards, G. A., Keating, J. E., Campbell, S. A., Wilkinson, D. P., Davis, M., StPierre, J. and Johnson, M. C. (1997) 'Low cost electrodes for proton exchange membrane fuel cells - Performance in single cells and Ballard stacks', *Journal of the Electrochemical Society,* 144, (11), pp. 3845-3857.

Reguera, G., McCarthy, K. D., Mehta, T., Nicoll, J. S., Tuominen, M. T. and Lovley, D. R. (2005) 'Extracellular electron transfer via microbial nanowires', *Nature,* 435, (7045), pp. 1098-1101.

Rhoads, A., Beyenal, H. and Lewandowski, Z. (2005) 'Microbial fuel cell using anaerobic respiration as an anodic reaction and biomineralized manganese as a cathodic reactant', *Environmental Science & Technology,* 39, (12), pp. 4666-4671.

Ritchie, A. C., Bowry, K., Fisher, A. C. and Gaylor, J. D. S. (1996) 'A novel automated method for the determination of membrane permeability in gas-liquid transfer applications', *Journal of Membrane Science,* 121, (2), pp. 169-174.

Rittmann, B. E. and McCarty, P. L. (2001) *Environmental biotechnology : principles and applications.* Boston, MA ; London: McGraw-Hill.

Roche, I. and Scott, K. (2009) 'Carbon-supported manganese oxide nanoparticles as electrocatalysts for oxygen reduction reaction (orr) in neutral solution', *Journal of Applied Electrochemistry,* 39, (2), pp. 197-204.

Rodriguez, J. M. D., Melian, J. A. H. and Pena, J. P. (2000) 'Determination of the real surface area of Pt electrodes by hydrogen adsorption using cyclic voltammetry', *Journal of Chemical Education,* 77, (9), pp. 1195-1197.

Roller, S. D., H. P. Bennetto, et al. (1984). 'Electron-Transfer Coupling in Microbial Fuel-Cells .1. Comparison of Redox-Mediator Reduction Rates and Respiratory Rates of Bacteria.' *Journal of Chemical Technology and Biotechnology B-Biotechnology* **34**(1): 3-12.

Rouquerol, F. o., Rouquerol, J. and Sing, K. S. W. (1999) *Adsorption by powders and porous solids : principles, methodology and applications.* San Diego, Calif.: Academic Press.

Rozendal, R. A., Hamelers, H. V. M. and Buisman, C. J. N. (2006) 'Effects of membrane cation transport on pH and microbial fuel cell performance', *Environmental Science & Technology,* 40, (17), pp. 5206-5211.

Rozendal, R. A., Hamelers, H. V. M., Molenkmp, R. J. and Buisman, J. N. (2007) 'Performance of single chamber biocatalyzed electrolysis with different types of ion exchange membranes', *Water Research,* 41, (9), pp. 1984-1994.

Rozendal, R. A., Hamelers, H. V. M., Rabaey, K., Keller, J. and Buisman, C. J. N. (2008) 'Towards practical implementation of bioelectrochemical wastewater treatment', *Trends in Biotechnology,* 26, (8), pp. 450-459.

Salitra, G., Soffer, A., Eliad, L., Cohen, Y. and Aurbach, D. (2000) 'Carbon electrodes for double-layer capacitors - I. Relations between ion and pore dimensions', *Journal of the Electrochemical Society,* 147, (7), pp. 2486-2493.

Schroder, U., Niessen, J. and Scholz, F. (2003) 'A generation of microbial fuel cells with current outputs boosted by more than one order of magnitude', *Angewandte Chemie-International Edition,* 42, (25), pp. 2880-2883.

Scott, K., Cotlarciuc, I., Hall, D., Lakeman, J. B. and Browning, D. (2008) 'Power from marine sediment fuel cells: the influence of anode material', *Journal of Applied Electrochemistry,* 38, (9), pp. 1313-1319.

Scott, K. and Murano, C. (2007) 'A study of a microbial fuel cell battery using manure sludge waste', *Journal of Chemical Technology and Biotechnology,* 82, (9), pp. 809-817.

Scott, K., Rimbu, G. A., Katuri, K. P., Prasad, K. K. and Head, I. M. (2007) 'Application of modified carbon anodes in microbial fuel cells', *Process Safety and Environmental Protection,* 85, (B5), pp. 481-488.

Scott, K., Taama, W. M. and Argyropoulos, P. (2000) 'Performance of the direct methanol fuel cell with radiation-grafted polymer membranes', *Journal of Membrane Science,* 171, (1), pp. 119-130.

Seredych, M., Hulicova-Jurcakova, D., Lu, G. Q. and Bandosz, T. J. (2008) 'Surface functional groups of carbons and the effects of their chemical character, density and accessibility to ions on electrochemical performance', *Carbon,* 46, (11), pp. 1475-1488.

Setton, R., Bernier, P. and Lefrant, S. (2002) *Carbon molecules and materials.* London: Taylor & Francis.

Shen, M., Roy, S., Kuhlmann, J. W., Scott, K., Lovell, K. and Horsfall, J. A. (2005) 'Grafted polymer electrolyte membrane for direct methanol fuel cells', *Journal of Membrane Science,* 251, (1-2), pp. 121-130.

Shi, H. (1996) 'Activated carbons and double layer capacitance', *Electrochimica Acta,* 41, (10), pp. 1633-1639.

Shukla, A. K., Suresh, P., Berchmans, S. and Rajendran, A. (2004) 'Biological fuel cells and their applications', *Current Science,* 87, (4), pp. 455-468.

Silva, S. A. M., Perez, J., Torresi, R. M., Luengo, C. A. and Ticianelli, E. A. (1999) 'Surface and electrochemical investigations of a fullerene soot', *Electrochimica Acta,* 44, (20), pp. 3565-3574.

Simon, E., Halliwell, C. M., Toh, C. S., Cass, A. E. G. and Bartlett, P. N. (2002) 'Immobilisation of enzymes on poly(aniline)-poly(anion) composite films. Preparation of bioanodes for biofuel cell applications', *Bioelectrochemistry,* 55, (1-2), pp. 13-15.

Sing, K. S. W. (1994) 'Physisorption of Gases by Carbon-Blacks', *Carbon,* 32, (7), pp. 1311-1317.

Sleutels, T. H. J. A., Lodder, R., Hamelers, H. V. M. and Buisman, C. J. N. (2009) 'Improved performance of porous bio-anodes in microbial electrolysis cells by enhancing mass and charge transport', *International Journal of Hydrogen Energy,* 34, (24), pp. 9655-9661.

Sokal, R. R. and Rohlf, F. J. (1994) *Biometry : the principles and practice of statistics in biological research.* New York: Freeman.

Stafford, D. A., Wheatley, B. I. and Hughes, D. E. (1980) *Anaerobic digestion : proceedings of the first International Symposium on Anaerobic Digestion, held at University College, Cardiff, Wales, September 1979.* London: Applied Science Publishers.

Stams, A. J. M., de Bok, F. A. M., Plugge, C. M., van Eekert, M. H. A., Dolfing, J. and Schraa, G. (2006) 'Exocellular electron transfer in anaerobic microbial communities', *Environmental Microbiology,* 8, (3), pp. 371-382.

Stams, A. J. M. and Plugge, C. M. (2009) 'Electron transfer in syntrophic communities of anaerobic bacteria and archaea', *Nature Reviews Microbiology,* 7, (8), pp. 568-577.

Stenina, I. A., Sistat, P., Rebrov, A. I., Pourcelly, G. and Yaroslavtsev, A. B. (2004) 'Ion mobility in Nafion-117 membranes', *Desalination,* 170, (1), pp. 49-57.

Stenstrom, M. K. and Rosso, D. (2007) 'Energy conservation and recovery: Two requirements for sustainable wastewater treatment', *Water Environment Research,* 79, (8), pp. 819-820.

Stoeckli, F. and Centeno, T. A. (2005) 'On the determination of surface areas in activated carbons', *Carbon,* 43, (6), pp. 1184-1190.

Stoodley, P., Sauer, K., Davies, D. G. and Costerton, J. W. (2002) 'Biofilms as complex differentiated communities', *Annual Review of Microbiology,* 56, pp. 187-209.

Sun, J., Hu, Y. Y., Bi, Z. and Cao, Y. Q. (2009) 'Improved performance of air-cathode single-chamber microbial fuel cell for wastewater treatment using microfiltration membranes and multiple sludge inoculation', *Journal of Power Sources,* 187, (2), pp. 471-479.

Tarasevich, M. R., Bogdanovskaya, V. A. and Zagudaeva, N. M. (1987) 'Redox Reactions of Quinones on Carbon Materials', *Journal of Electroanalytical Chemistry,* 223, (1-2), pp. 161-169.

Torres, C. I., Marcus, A. K., Lee, H. S., Parameswaran, P., Krajmalnik-Brown, R. and Rittmann, B. E. (2010) 'A kinetic perspective on extracellular electron transfer by anode-respiring bacteria', *Fems Microbiology Reviews,* 34, (1), pp. 3-17.

Uchimiya, M. and Stone, A. T. (2009) 'Reversible redox chemistry of quinones: Impact on biogeochemical cycles', *Chemosphere,* 77, (4), pp. 451-458.

Unden, G. (1998) 'Transcriptional regulation and energetics of alternative respiratory pathways in facultatively anaerobic bacteria', *Biochimica Et Biophysica Acta-Bioenergetics,* 1365, (1-2), pp. 220-224.

Unnikrishnan, E. K., Kumar, S. D. and Maiti, B. (1997) 'Permeation of inorganic anions through Nafion ionomer membrane', *Journal of Membrane Science,* 137, (1-2), pp. 133-137.

Vielstich, W., Gasteiger, H. A. and Lamm, A. (2003) *Handbook of fuel cells : fundamentals, technology and applications.* Chichester: Wiley.

von Canstein, H., Ogawa, J., Shimizu, S. and Lloyd, J. R. (2008) 'Secretion of flavins by Shewanella species and their role in extracellular electron transfer', *Applied and Environmental Microbiology,* 74, (3), pp. 615-623.

Wang, L. H., Toyoda, M. and Inagaki, M. (2008a) 'Dependence of electric double layer capacitance of activated carbons on the types of pores and their surface areas', *New Carbon Materials,* 23, (2), pp. 111-115.

Wang, X., Cheng, S. A., Feng, Y. J., Merrill, M. D., Saito, T. and Logan, B. E. (2009) 'Use of Carbon Mesh Anodes and the Effect of Different Pretreatment Methods on Power Production in Microbial Fuel Cells', *Environmental Science & Technology,* 43, (17), pp. 6870-6874.

Wang, X., Feng, Y. J. and Lee, H. (2008b) 'Electricity production from beer brewery wastewater using single chamber microbial fuel cell', *Water Science and Technology,* 57, (7), pp. 1117-1121.

Watt-Smith, M. J., Friedrich, J. M., Rigby, S. P., Ralph, T. R. and Walsh, F. C. (2008) 'Determination of the electrochemically active surface area of Pt/C PEM fuel cell electrodes using different adsorbates', *Journal of Physics D-Applied Physics,* 41, (17), pp. -.

Wen, Q., Wu, Y., Cao, D. X., Zhao, L. X. and Sun, Q. (2009) 'Electricity generation and modeling of microbial fuel cell from continuous beer brewery wastewater', *Bioresource Technology,* 100, (18), pp. 4171-4175.

Wen, Q., Wu, Y., Zhao, L. X. and Sun, Q. (2010) 'Production of electricity from the treatment of continuous brewery wastewater using a microbial fuel cell', *Fuel,* 89, (7), pp. 1381-1385.

Williams, M. C. (2004) *Fuel Cell Handbook.* EG&G Technical Services, Inc., U.S. Department of Energy, Office of Fossil Energy.

You, S. J., Zhao, Q. L., Zhang, J., Liu, H., Jiang, J. Q. and Zhao, S. Q. (2008) 'Increased sustainable electricity generation in up-flow air-cathode microbial fuel cells', *Biosensors & Bioelectronics,* 23, (7), pp. 1157-1160.

You, S. J., Zhao, Q. L., Zhang, J. N., Jiang, J. Q., Wan, C. L., Du, M. A. and Zhao, S. Q. (2007) 'A graphite-granule membrane-less tubular air-cathode microbial fuel cell for power generation under continuously operational conditions', *Journal of Power Sources,* 173, (1), pp. 172-177.

Zengin, H., Zhou, W. S., Jin, J. Y., Czerw, R., Smith, D. W., Echegoyen, L., Carroll, D. L., Foulger, S. H. and Ballato, J. (2002) 'Carbon nanotube doped polyaniline', *Advanced Materials,* 14, (20), pp. 1480-+.

Zhang, B. G., Zhou, S. G., Zhao, H. Z., Shi, C. H., Kong, L. C., Sun, J. J., Yang, Y. and Ni, J. R. (2010a) 'Factors affecting the performance of microbial fuel cells for sulfide and vanadium (V) treatment', *Bioprocess and Biosystems Engineering,* 33, (2), pp. 187-194.

Zhang, F., Cheng, S. A., Pant, D., Van Bogaert, G. and Logan, B. E. (2009a) 'Power generation using an activated carbon and metal mesh cathode in a microbial fuel cell', *Electrochemistry Communications,* 11, (11), pp. 2177-2179.

Zhang, J. N., Zhao, Q. L., Aelterman, P., You, S. J. and Jiang, J. Q. (2008) 'Electricity generation in a microbial fuel cell with a microbially catalyzed cathode', *Biotechnology Letters,* 30, (10), pp. 1771-1776.

Zhang, L. J. and Wan, M. X. (2002) 'Synthesis and characterization of self-assembled polyaniline nanotubes doped with D-10-camphorsulfonic acid', *Nanotechnology,* 13, (6), pp. 750-755.

Zhang, X. Y., Cheng, S. A., Huang, X. and Logan, B. E. (2010b) 'Improved performance of single-chamber microbial fuel cells through control of membrane deformation', *Biosensors & Bioelectronics,* 25, (7), pp. 1825-1828.

Zhang, X. Y., Cheng, S. A., Wang, X., Huang, X. and Logan, B. E. (2009b) 'Separator Characteristics for Increasing Performance of Microbial Fuel Cells', *Environmental Science & Technology,* 43, (21), pp. 8456-8461.

Zhao, F., Harnisch, F., Schroder, U., Scholz, F., Bogdanoff, P. and Herrmann, I. (2005) 'Application of pyrolysed iron(II) phthalocyanine and CoTMPP based oxygen reduction catalysts as cathode materials in microbial fuel cells', *Electrochemistry Communications,* 7, (12), pp. 1405-1410.

Zhao, F., Harnisch, F., Schrorder, U., Scholz, F., Bogdanoff, P. and Herrmann, I. (2006) 'Challenges and constraints of using oxygen cathodes in microbial fuel cells', *Environmental Science & Technology,* 40, (17), pp. 5193-5199.

Zhao, F., Rahunen, N., Varcoe, J. R., Chandra, A., Avignone-Rossa, C., Thumser, A. E. and Slade, R. C. T. (2008) 'Activated carbon cloth as anode for sulfate removal in a microbial fuel cell', *Environmental Science & Technology,* 42, (13), pp. 4971-4976.

Zhao, F., Rahunen, N., Varcoe, J. R., Roberts, A. J., Avignone-Rossa, C., Thumser, A. E. and Slade, R. C. T. (2009) 'Factors affecting the performance of microbial fuel cells for sulfur pollutants removal', *Biosensors & Bioelectronics,* 24, (7), pp. 1931-1936.

Zehnder, A. J. B. (1988). Biology of anaerobic microorganisms. New York, Wiley.

Zou, Y. J., Xiang, C. L., Yang, L. N., Sun, L. X., Xu, F. and Cao, Z. (2008) 'A mediatorless microbial fuel cell using polypyrrole coated carbon nanotubes composite as anode material', *International Journal of Hydrogen Energy,* 33, (18), pp. 4856-4862.

Zuo, Y., Cheng, S., Call, D. and Logan, B. E. (2007) 'Tubular membrane cathodes for scalable power generation in microbial fuel cells', *Environmental Science & Technology,* 41, (9), pp. 3347-3353.
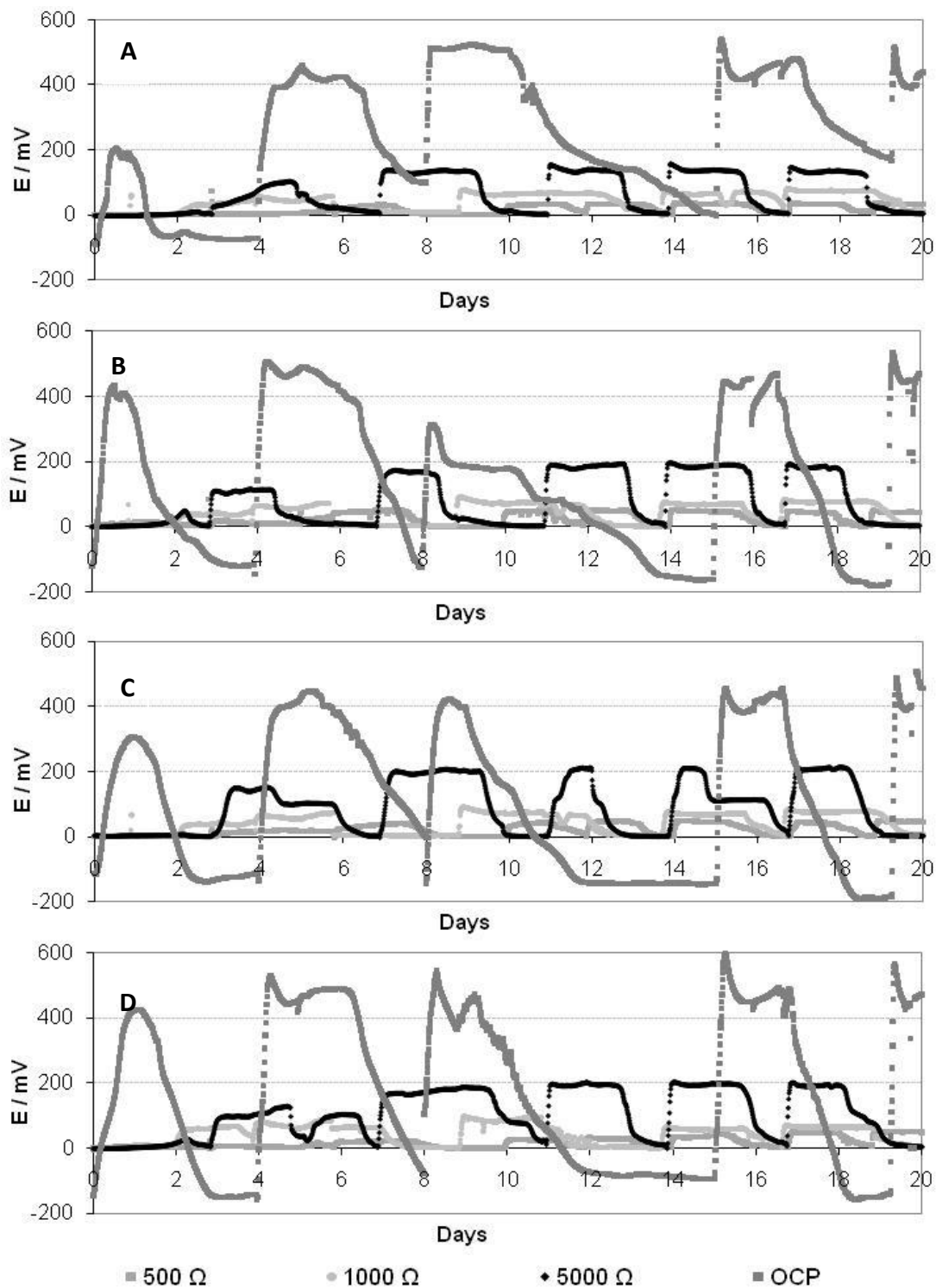
10 APPENDICES

10.1 ANODE MATERIALS

Figure 10.1 Voltage evolution for the different anode materials, CC (A), CB (B), C/HNO$_3$ (C), C/PANI (D) under different external loads.
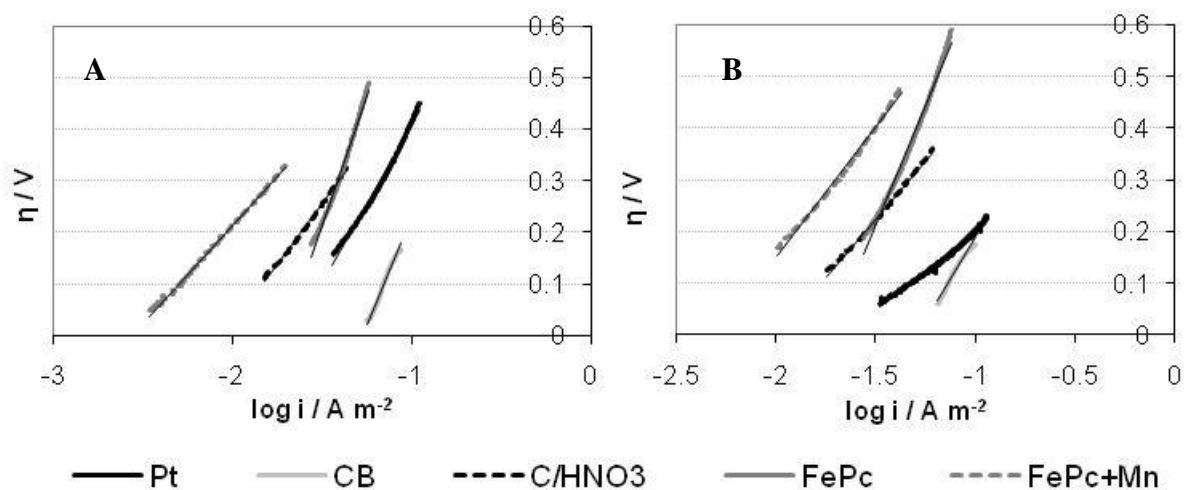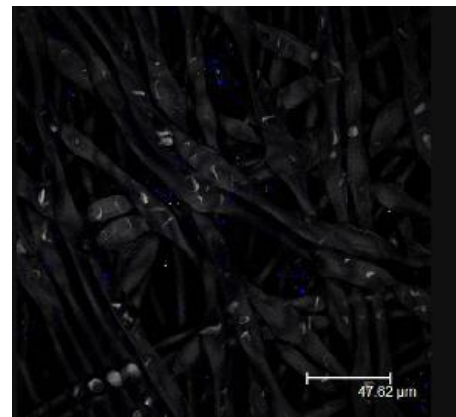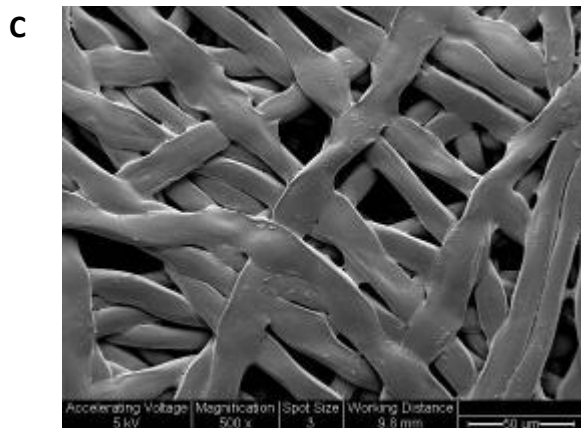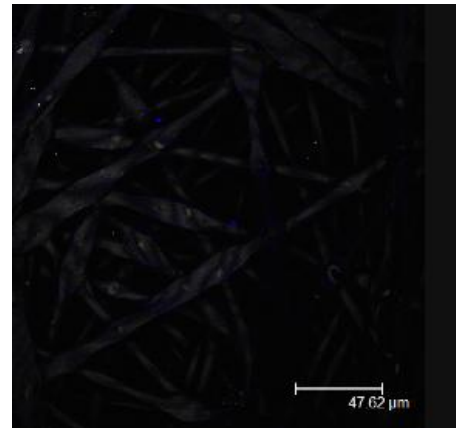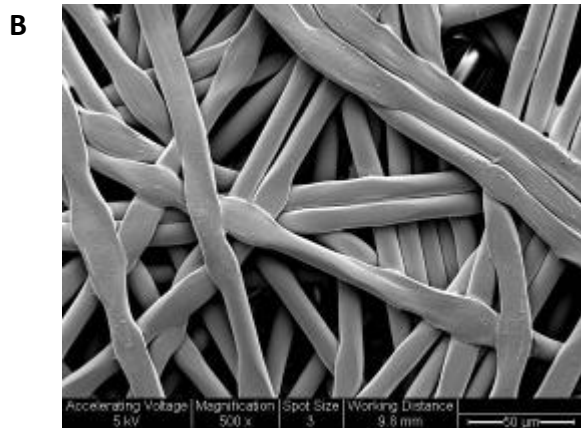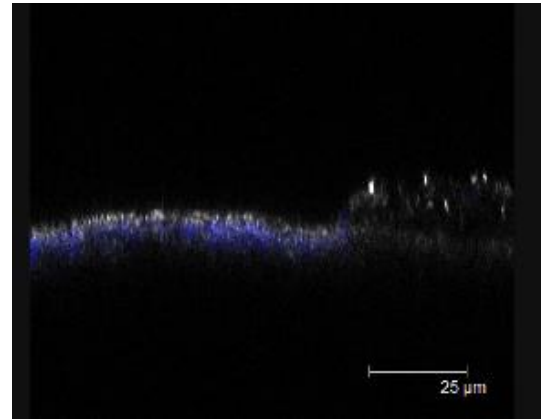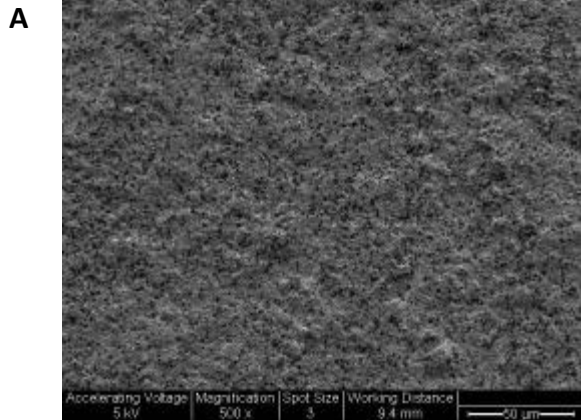
10.2 CATHODE MATERIALS

Figure 10.2: IR corrected Tafel plots calculated using the geometric cathode area for the different cathodes in a reactor using C/HNO₃ anodes (A) and activated carbon cloth anodes (B) (E vs NHE).

10.3 MEMBRANE MATERIALS

SEM pictures with a magnification of 500x.   **Confocal imaging pictures of the materials using DAPI to dye the microorganisms.**
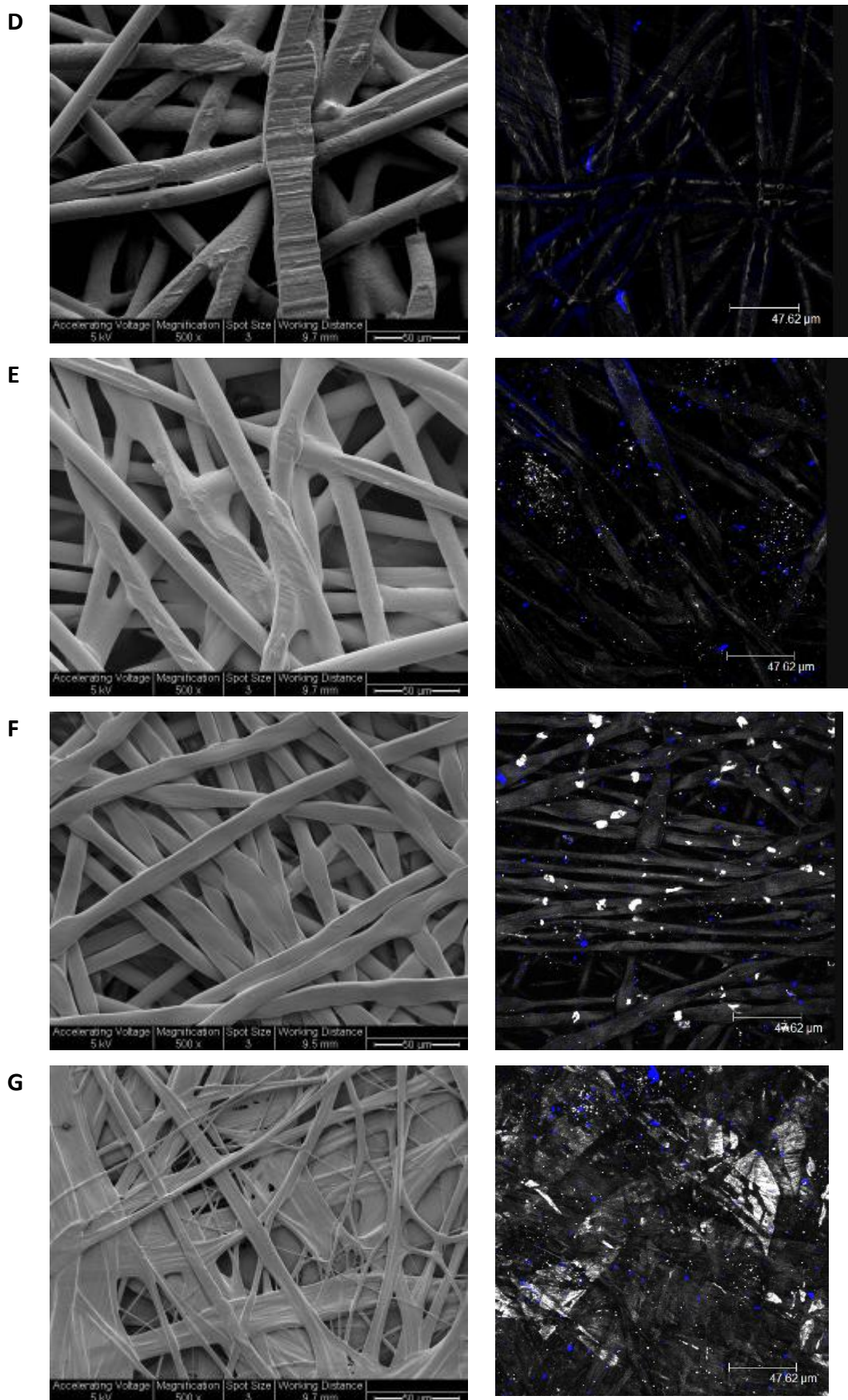
A

B

C

Figure 10.3: SEM and confocal microcope pictures of the membrane separators: Rhinohide (A), Tyvek (G), Scimat 700/70 (B), 700/77 (C), 700/30k (D), 700/40k (E), 850/61 (F).